

---

Electronic Thesis and Dissertation Repository

---

10-27-2016 12:00 AM

## Electrospinning of poly (ester amide) fibres for mesenchymal progenitor cell differentiation

Sarah Kiros  
*The University of Western Ontario*

Supervisor  
Dr. Kibret Mequanint  
*The University of Western Ontario*

Graduate Program in Biomedical Engineering  
A thesis submitted in partial fulfillment of the requirements for the degree in Master of Engineering Science  
© Sarah Kiros 2016

Follow this and additional works at: <https://ir.lib.uwo.ca/etd>



Part of the [Molecular, Cellular, and Tissue Engineering Commons](#)

---

### Recommended Citation

Kiros, Sarah, "Electrospinning of poly (ester amide) fibres for mesenchymal progenitor cell differentiation" (2016). *Electronic Thesis and Dissertation Repository*. 4205.  
<https://ir.lib.uwo.ca/etd/4205>

This Dissertation/Thesis is brought to you for free and open access by Scholarship@Western. It has been accepted for inclusion in Electronic Thesis and Dissertation Repository by an authorized administrator of Scholarship@Western. For more information, please contact [wlsadmin@uwo.ca](mailto:wlsadmin@uwo.ca).

## **Abstract**

The *in vitro* vascular tissue engineering paradigm seeks to produce biologically responsive vascular substitutes using cells, biodegradable scaffolds, and bioreactors to mature the tissue for the potential treatment of vascular occlusions and to create 3D tissue models for pre-clinical testing. In this work, a poly (ester amide) (PEA) derived from L-phenylalanine, sebacoyl chloride and 1,4 butanediol was synthesized and electrospun to form both 3D fibrous mats and tubular constructs. Both the polymer solution concentration and mandrel rotation speed were optimized to fabricate bead-free fibres. Cytocompatibility and proliferation studies using mesenchymal progenitor 10T1/2 cells showed PEA fibres were not cytotoxic and were able to support proliferation for 14 days. 10T1/2 cells demonstrated increased attachment and spreading for up to 7 days on fibrous mats but perfusion bioreactor studies on tubular scaffolds did not demonstrate sufficient cell infiltration. 10T1/2 cell differentiation studies using qPCR and Western blot showed a TGF $\beta$ 1 induced upregulation in both the gene and protein expression of vascular smooth muscle cell (VSMC) specific markers smooth muscle alpha-actin (SM- $\alpha$ -actin) and smooth muscle myosin heavy chain (SM-MHC) on PEA fibres, with the differentiation further confirmed using immunofluorescence staining. Overall, this *in vitro* model of 10T1/2 cell differentiation may serve as a potential platform to fabricate small-diameter tissue engineered vascular grafts.

## **Keywords**

poly (ester amide), 10T1/2 cells, differentiation, electrospinning, vascular smooth muscle cells, TGF $\beta$ 1

## **Acknowledgments**

I would like to express my sincerest gratitude to my supervisor, Dr. Kibret Mequanint for his guidance and support during my graduate studies. I would also like to thank my lab group members for their help and words of encouragement, particularly Dr. Somiraa Said for assisting me with polymer synthesis and electrospinning and Dr. Shigang Lin for his help and insight with the cell culture studies.

I would additionally like to thank the Biotron staff members for their assistance and training with the scanning electron microscope.

I wish to acknowledge the Western Graduate Research Scholarship (WGRS) for providing me with financial support. Last but certainly not least, I wish to extend my heartfelt appreciation to my family for their patience, love and ongoing support.

## Table of Contents

|                                                                               |     |
|-------------------------------------------------------------------------------|-----|
| Abstract.....                                                                 | i   |
| Acknowledgments.....                                                          | ii  |
| Table of Contents.....                                                        | iii |
| List of Tables.....                                                           | vi  |
| List of Figures.....                                                          | vii |
| List of Abbreviations.....                                                    | x   |
| Chapter 1.....                                                                | 1   |
| 1 Introduction.....                                                           | 1   |
| 1.1 Scope.....                                                                | 1   |
| 1.2 Thesis outline.....                                                       | 3   |
| Chapter 2.....                                                                | 4   |
| 2 Literature review.....                                                      | 4   |
| 2.1 Paradigms of tissue engineering.....                                      | 4   |
| 2.2 Functional requirements of tissue engineered vascular grafts (TEVGs)..... | 7   |
| 2.3 Why <i>in vitro</i> Vascular Tissue Engineering?.....                     | 8   |
| 2.3.1 Clinical motivation: Cardiovascular Disease.....                        | 8   |
| 2.3.2 Diagnostic applications: 3D tissue model.....                           | 15  |
| 2.4 Vascular tissue engineering components.....                               | 17  |
| 2.4.1 Cell source.....                                                        | 17  |
| 2.4.2 Scaffolds.....                                                          | 20  |
| 2.4.3 Ideal scaffold characteristics.....                                     | 21  |
| 2.4.4 Scaffold materials.....                                                 | 21  |
| 2.4.5 Scaffold fabrication methods.....                                       | 25  |

|                                                                               |    |
|-------------------------------------------------------------------------------|----|
| 2.5 Bioreactors .....                                                         | 28 |
| 2.6 Stem cell-based vascular tissue engineering: relevant studies.....        | 29 |
| 2.6.1 Pluripotent stem cells.....                                             | 30 |
| 2.6.2 Multipotent stem cells.....                                             | 34 |
| 2.7 Motivation and Objectives .....                                           | 40 |
| Chapter 3.....                                                                | 42 |
| 3 Materials and Methods.....                                                  | 42 |
| 3.1 Materials .....                                                           | 42 |
| 3.2 Methods.....                                                              | 42 |
| 3.2.1 Monomer synthesis .....                                                 | 42 |
| 3.2.2 Polymer synthesis (8-Phe-4).....                                        | 43 |
| 3.2.3 Spectroscopic analysis: <sup>1</sup> H-NMR .....                        | 43 |
| 3.2.4 Gel permeation chromatography (GPC).....                                | 43 |
| 3.3 Scaffold fabrication.....                                                 | 44 |
| 3.3.1 Electrospinning of 3D fibrous mat.....                                  | 44 |
| 3.3.2 Electrospinning of tubular scaffold.....                                | 44 |
| 3.3.3 Scanning electron microscopy (SEM) .....                                | 44 |
| 3.4 Cell studies.....                                                         | 45 |
| 3.4.1 Cytotoxicity and cell proliferation assays.....                         | 45 |
| 3.4.2 Bioreactor and dual-pump perfusion system design.....                   | 46 |
| 3.4.3 C3H10T1/2 cell seeding on tubular scaffold .....                        | 47 |
| 3.5 Immunofluorescence staining and laser scanning confocal microscopy .....  | 48 |
| 3.6 Smooth muscle phenotype marker expression: qPCR and Western blot analyses | 49 |
| Chapter 4.....                                                                | 52 |
| 4 Results and Discussion.....                                                 | 52 |
| 4.1 PEA synthesis and characterization .....                                  | 52 |

|       |                                                                                                |     |
|-------|------------------------------------------------------------------------------------------------|-----|
| 4.2   | Electrospinning .....                                                                          | 55  |
| 4.2.1 | Electrospun 3D fibrous mats.....                                                               | 55  |
| 4.2.2 | Effect of solution concentration on fibre morphology.....                                      | 58  |
| 4.2.3 | Electrospun 3D tubular scaffold fabrication.....                                               | 60  |
| 4.2.4 | Effect of mandrel rotation speed on fibre orientation.....                                     | 62  |
| 4.3   | Cell viability, interaction, and differentiation studies.....                                  | 68  |
| 4.3.1 | 10T1/2 cell viability and proliferation studies.....                                           | 68  |
| 4.3.2 | 10T1/2 cell interactions with electrospun PEA fibre mats.....                                  | 72  |
| 4.3.3 | 10T1/2 cell interactions with electrospun tubular PEA scaffolds.....                           | 74  |
| 4.3.4 | Effect of TGF $\beta$ 1 on VSMC differentiation of 10T1/2 cells on electrospun PEA fibres..... | 78  |
| 5     | Conclusion and future work.....                                                                | 83  |
| 5.1   | Conclusion .....                                                                               | 83  |
| 5.2   | Strengths and limitations.....                                                                 | 84  |
| 5.3   | Future work.....                                                                               | 85  |
| 5.4   | Significance.....                                                                              | 85  |
| 6     | References.....                                                                                | 86  |
| 7     | Copyright permissions .....                                                                    | 103 |
| 8     | Curriculum Vitae.....                                                                          | 106 |

## List of Tables

|                                                                                                        |    |
|--------------------------------------------------------------------------------------------------------|----|
| Table 4.1 Summary of electrospinning parameters used for 3D electrospun mats and tubular scaffold..... | 57 |
|--------------------------------------------------------------------------------------------------------|----|

## List of Figures

|                                                                                                                                                                                                                                                                                                                                                                                             |    |
|---------------------------------------------------------------------------------------------------------------------------------------------------------------------------------------------------------------------------------------------------------------------------------------------------------------------------------------------------------------------------------------------|----|
| Figure 2.1 <i>in vitro</i> tissue engineering paradigm .....                                                                                                                                                                                                                                                                                                                                | 6  |
| Figure 2.2 Blood vessel anatomy. Reprinted with permission from Waterhouse, A., Wise, S. G., Ng, M. K. C. & Weiss, A. S. Elastin as a nonthrombogenic biomaterial. <i>Tissue Eng. Part B. Rev.</i> 17, 93–99 (2011). <sup>160</sup> Copyright © 2010, Mary Ann Liebert, Inc. ....                                                                                                           | 9  |
| Figure 2.3 TEVG as an extracardiac total cavopulmonary connection in the Fontan operation. <sup>38</sup> Reprinted from Patterson, J. T. <i>et al.</i> Tissue-engineered vascular grafts for use in the treatment of congenital heart disease: from the bench to the clinic and back again. <i>Regen. Med.</i> 7, 409–419 (2012). Copyright (2012) with permission from Future Medicine. 13 | 13 |
| Figure 2.4 Schematic drawing of the electrospinning process. <sup>161</sup> Reprinted from Sill, T. J. & von Recum, H. A. Electrospinning: Applications in drug delivery and tissue engineering. <i>Biomaterials</i> 29, 1989–2006 (2008). Copyright (2008) with permission from Elsevier.....                                                                                              | 28 |
| Figure 4.1 Synthesis scheme for 8-Phe-4 derived from L-phenylalanine, 1,4 butanediol and sebacyl chloride by interfacial polymerization .....                                                                                                                                                                                                                                               | 52 |
| Figure 4.2 <sup>1</sup> H-NMR spectra of PEA from L-phenylalanine, 1,8-butanediol and sebacyl chloride (8-Phe-4) .....                                                                                                                                                                                                                                                                      | 53 |
| Figure 4.3 GPC trace of 8-Phe-4 derived from L-phenylalanine, 1,4-buanediol and sebacyl chloride by interfacial polymerization .....                                                                                                                                                                                                                                                        | 55 |
| Figure 4.4 SEM images of 6% and 7% w/w PEA fibres and respective fibre diameter distributions. Scale bar represents 2 µm. Bin size for histogram is 20 µm.....                                                                                                                                                                                                                              | 59 |
| Figure 4.5 A) Digital image of PEA tubular scaffold B) Cross-section SEM image of PEA tubular scaffold at 300× magnification, (L) indicates the lumen of the structure. Scaffold wall thickness is 113 µm C) PEA nanofibres at 5000× magnification. Purple circles indicate bundling of the nanofibres. Scale bar in B and C represent 50 µm and 2 µm, respectively ...                     | 61 |



|                                                                                                                                                                                                                                                                                                                                                                                                                                                                   |    |
|-------------------------------------------------------------------------------------------------------------------------------------------------------------------------------------------------------------------------------------------------------------------------------------------------------------------------------------------------------------------------------------------------------------------------------------------------------------------|----|
| Figure 4.6 Representative SEM images of PEA fibres electrospun onto small diameter tubular scaffold at 150, 1000, and 2000 RPM using three magnifications. Scale bars represent for A-C =10 $\mu\text{m}$ , D-F = 5 $\mu\text{m}$ and G-I = 2 $\mu\text{m}$ , respectively. ....                                                                                                                                                                                  | 63 |
| Figure 4.7 The effect of mandrel rotation speed on fibre diameter distribution for 150, 1000 and 2000 RPM .....                                                                                                                                                                                                                                                                                                                                                   | 64 |
| Figure 4.8 Fibre orientation histograms for PEA fibres spun at 150, 1000 and 2000 RPM on a rotating mandrel .....                                                                                                                                                                                                                                                                                                                                                 | 65 |
| Figure 4.9 10T1/2 metabolic activity on PEA fibres and TCPS positive control. Scaffolds were seeded with a cell density of 10000 cells/scaffold on 96 well plates and cultured for 3, 7 and 14 days before MTT treatment. Data represents mean $\pm$ SD for three independent experiments conducted in triplicate. Two-way ANOVA and post-hoc Tukey comparative tests were used. Solid line coupled with * indicates $p < 0.05$ , ** represents $p < 0.01$ . .... | 70 |
| Figure 4.10 10T1/2 cell proliferation on electrospun PEA fibres. Scaffolds were seeded with a cell density of 2000 cells/cm <sup>2</sup> and cultured for 3, 7 and 14 days before performing CyQUANT cell proliferation assay (n=6). One-way ANOVA and post-hoc Tukey comparative tests were used. Solid line coupled with ** represents $p < 0.01$ . Absorbance was measured at 480 nm excitation/520 nm emission wavelengths. ....                              | 71 |
| Figure 4.11 Representative confocal image of 10T1/2 cells cultured on glass coverslips (A,B) and electrospun PEA fibres (C, D). Red represents F-actin (phalloidin) and blue represents nuclei (DAPI). Scale bar represents 50 $\mu\text{m}$ .....                                                                                                                                                                                                                | 73 |
| Figure 4.12 Dual-pump flow perfusion bioreactor design for 10T1/2 cell interaction and infiltration study (Lin and Mequanint, unpublished work) <sup>163</sup> .....                                                                                                                                                                                                                                                                                              | 75 |
| Figure 4.13 Representative confocal microscopy images of 10T1/2 cells cultured on tubular scaffolds in static conditions for 7 days (A, C) and static culture for 3 days followed by dynamic culture for 4 days (B, D). Green represents F-actin (phalloidin) and blue represents nuclei (DAPI) . White arrows indicate cellular infiltration. Scale bar represents 20 $\mu\text{m}$ .....                                                                        | 77 |

Figure 4.14 Quantitative real-time polymerase chain reaction (qPCR) demonstrating 10T1/2 cell expression of smooth muscle  $\alpha$ -actin (SM- $\alpha$ -actin) and smooth muscle myosin heavy chain (SM-MHC) genes on PEA fibres treated with 2 ng/mL and 4 ng/mL of TGF $\beta$ 1, respectively after 3 days. Results were normalized to GAPDH expression. Statistical significance was analyzed using student's *t* test ( \* indicates  $p < 0.05$ , \*\* indicates  $p < 0.01$ ) ..... 79

Figure 4.15 Western blot demonstrating 10T1/2 expression of smooth muscle-  $\alpha$ -actin (SM- $\alpha$ -actin) and myosin heavy chain (SM-MHC) proteins on PEA fibres after 7 days. 10T1/2 cells were treated with with 2 ng/mL and 4 ng/mL of TGF $\beta$ 1, respectively. GAPDH was used as a loading control..... 80

Figure 4.16 Representative confocal microscopy image of 10T1/2 cells treated with 4 ng/mL TGF $\beta$ 1 and cultured for 7 days. Green represents F-actin, blue represents nuclei and red represents SM-MHC. Scale bar represents 50  $\mu$ m..... 81

## List of Abbreviations

|                   |                                                                                           |
|-------------------|-------------------------------------------------------------------------------------------|
| 8-Phe-4           | L-phenylalanine, sebacoyl chloride and 1,4-bis(2-hydroxyethyl)terephthalate based polymer |
| 10T1/2            | C3H10T1/2 cells (murine mesenchymal progenitor models)                                    |
| ASC               | Adipose stem cells                                                                        |
| BM-MNC            | Bone marrow mononuclear cells                                                             |
| BM-MSC            | Bone marrow mesenchymal stem cells                                                        |
| CABG              | Coronary artery bypass graft                                                              |
| CCA               | Common carotid artery                                                                     |
| CHCl <sub>3</sub> | Chloroform                                                                                |
| DES               | Drug eluting stents                                                                       |
| DMSO              | Dimethyl sulfoxide                                                                        |
| EC                | Endothelial cells                                                                         |
| EBs               | Embryoid body                                                                             |
| ECM               | Extracellular matrix                                                                      |
| ePTFE             | Expanded poly(tetrafluoroethylene)                                                        |
| FACS              | Fluorescence activated cell sorting                                                       |
| FBS               | Fetal bovine serum                                                                        |

|           |                                                                                |
|-----------|--------------------------------------------------------------------------------|
| HCASMC    | Human coronary artery smooth muscle cells                                      |
| HSC       | Hematopoietic stem cells                                                       |
| HUMANITY® | Humacyte's investigational tissue-engineered vascular conduit for hemodialysis |
| IH        | Intimal hyperplasia                                                            |
| PCL       | Poly- $\epsilon$ -caprolactone                                                 |
| PCI       | Percutaneous coronary intervention                                             |
| PDGF-BB   | Platelet derived growth factor-BB                                              |
| PET®      | Poly (ethylene terephthalate)                                                  |
| PGA       | Polyglycolic acid                                                              |
| PLA       | Poly(lactic acid)                                                              |
| PLCL      | Poly(L-lactide-co-caprolactone) copolymer                                      |
| PLGA      | Poly(lactic-co-glycolic acid)                                                  |
| PLLA      | Poly(L-lactic acid)                                                            |
| PEA       | Poly(ester amide)                                                              |
| qPCR      | Real-time polymerase chain reaction                                            |
| RA        | All-trans retinoic acid                                                        |

|                     |                                                              |
|---------------------|--------------------------------------------------------------|
| R&D                 | Research and development                                     |
| H&E                 | Hematoxylin and eosin                                        |
| HSC                 | Hematopoietic stem cells                                     |
| SM- $\alpha$ -actin | Smooth muscle- $\alpha$ –actin                               |
| MyoCD               | Myocardin                                                    |
| MMP                 | Matrix metalloproteinases                                    |
| MSC                 | Mesenchymal stem cells                                       |
| MTT                 | 3-(4,5-dimethylthiazol-2-yl)-2,5-diphenyltetrazolium bromide |
| SCID                | Severe combined immunodeficiency                             |
| SPC                 | Sphingosylphosphorylcholine                                  |
| SMIM                | Smooth muscle inductive medium                               |
| TCPC                | Total cavopulmonary connection                               |
| TEVG                | Tissue engineered vascular graft                             |
| TEVA                | Tissue engineered vascular adventitia                        |

|        |                                        |
|--------|----------------------------------------|
| TIMP   | Tissue inhibitor of metalloproteinases |
| TCPS   | Tissue culture polystyrene             |
| SM-MHC | Smooth muscle myosin heavy chain       |
| VSMC   | Vascular smooth muscle cells           |

# Chapter 1

## 1 Introduction

### 1.1 Scope

Diseases of the cardiovascular system are the second leading cause of death in Canada, with coronary artery disease (CAD) being the most prevalent vascular condition.<sup>1</sup> Notwithstanding improved outcomes for percutaneous coronary interventions (PCI) and autologous coronary artery bypass grafts (CABG) using saphenous veins (SV) or internal mammary arteries (IMA), elderly patients with pre-existing vascular disorders such as varicose veins or previous vessel harvest may not have suitable grafts for this procedure.<sup>2</sup> Synthetic grafts composed of Poly (ethylene terephthalate) (PET<sup>®</sup>, Dacron) and expanded poly(tetrafluoroethylene) (ePTFE, Gore-Tex<sup>®</sup>) can be used as an alternative, however they exhibit reduced patency rates and an increased risk for intimal hyperplasia (IH) due to mechanical mismatch with the native coronary artery.<sup>3</sup> Moreover, their lack of biodegradability renders these grafts unable to support tissue remodeling and regeneration, thus limiting their use for pediatric patients who require grafts which can grow and remodel during normal development.<sup>4</sup>

The shortcomings of these interventions led to active and prolific research in the field of vascular tissue engineering. The intent is to produce biologically and mechanically responsive vascular substitutes that can mimic the properties of the native vessel. In the most frequently utilized tissue engineering paradigm, cells are seeded onto a biodegradable scaffold, mimicking the native extracellular matrix (ECM) environment and matured in a

bioreactor.<sup>5</sup> The scaffold acts as a temporary support structure for the cells to infiltrate the porous three dimensional (3D) scaffold, while secreting and assembling their own ECM proteins. In a bioreactor that simulates the hemodynamic environment, the construct matures into a functional tissue.<sup>5</sup> The use of adult stem cells is a promising alternative to primary vascular smooth muscle cells (VSMC) and endothelial cells (ECs) due to their increased proliferative capacity compared to differentiated primary cells, their ability to differentiate into VSMC and EC lineages with the addition of soluble growth factors,<sup>6</sup> and their ability to circumvent the ethical concerns surrounding the use of embryonic stem cells. Tissue engineered vascular graft (TEVG) studies using bone marrow mononuclear cells (BM-MNC), bone marrow mesenchymal stem cells (BM-MS) and synthetic polymers such polyglycolic acids (PGA), polylactic acid (PLA), and their hybrids have been widely reported,<sup>7,8,9</sup> however, their degradation products include acidic by-products that may be cytotoxic and have been shown to negatively affect vascular smooth muscle phenotype.<sup>10</sup> Poly (ester amide)s (PEAs), are a class of synthetic biomaterials which contain both acidic and basic degradation products, providing a buffering effect and limiting the downward pH drift.<sup>11</sup> PEAs derived from naturally occurring  $\alpha$ -amino acids have been investigated for vascular tissue engineering and gene and drug delivery applications<sup>12,13</sup>; however, the majority of these studies have used differentiated vascular cells.<sup>11,14</sup> C3H10T1/2 cells, commonly referred to as 10T1/2 cells, are a clonal cell line derived from 14-17 day old mouse embryos, and are commonly used as an *in vitro* model for VSMC differentiation studies due to their undemanding culture conditions and their ability to differentiate to VSMC in 2D culture using only one growth factor, TGF $\beta$ 1.<sup>15</sup>



Thus, the objective of this work is to study the cell-material interactions of 10T1/2 cells on nanofibrous PEA scaffolds as well as their differentiation into a vascular smooth muscle lineage and to study cell infiltration in 3D tubular electrospun scaffolds, towards fabricating a small diameter vascular graft.

## **1.2 Thesis outline**

This thesis consists of 5 chapters. Chapter 1 provides a brief introduction to the work. Chapter 2 introduces discusses the importance of vascular tissue engineering, scaffold fabrication methods and relevant stem cell differentiation studies for vascular tissue engineering applications, with specific objectives of this work provided at the end of Chapter 2. Chapter 3 details the experimental procedures, while Chapter 4 presents the results and discusses the results of this study. Finally, a summary of the important findings, the strengths and limitations of the study, and future directions are summarized in Chapter 5.

## Chapter 2

### 2 Literature review

#### 2.1 Paradigms of tissue engineering

Tissue engineering is an interdisciplinary field which combines engineering principles and life sciences to construct biological substitutes that can repair, replace, or regenerate damaged tissues.<sup>5</sup> The four most commonly adopted approaches in this field are cell transplantation, scaffold transplantation, cell-loaded scaffold implantation, and *in vitro* tissue engineering.<sup>5</sup>

Cell transplantation is a minimally invasive approach in which cells are introduced directly into the host tissue without the use of a scaffold or a bioreactor. For instance, in myocardial tissue engineering, cardiomyocytes (mature contracting heart cells) or adult mesenchymal stem cells (MSCs) can be injected to repair the damaged myocardium following a myocardial infarction, or heart attack.<sup>5</sup> Though this is the simplest and least invasive of the four paradigms, the primary drawback of this procedure is host immune rejection, if the patient's cells are not used for this procedure. Additionally, it is difficult to ensure that cells alone will regenerate a functional tissue, as the cells need to integrate into the damaged tissue and secrete extracellular matrix proteins.

Immunosuppressant drugs are often utilized in conjunction with this procedure to overcome host immune rejection<sup>16</sup> however these drugs severely deplete immune function and may leave the patient highly vulnerable to infection.

Other techniques such as the use of immune suppressing molecules to protect human embryonic stem cells (hESCs) from immune rejection,<sup>17</sup> and induced pluripotent stem cells (iPSCs), derived from the patient's own cells<sup>18</sup> are being investigated to eliminate the use of immunosuppressant drugs.

Scaffold transplantation relies on recruiting endogenous cells to the implanted material in order to regenerate damaged tissue. As an example, decellularized porcine pulmonary heart valves have been used as structural templates in which cells populate and remodel the scaffold to form a functional heart valve.<sup>19</sup> The decellularization process involves the use of detergents to remove cellular material from a given tissue to isolate the connective tissue matrix, forming a 3D structure that can facilitate host cell recruitment and ingrowth.<sup>5</sup> Additionally, some heart valve regeneration strategies rely on the use of a resorbable matrix derived from natural or synthetic polymers to degrade and undergo *in vivo* remodeling to facilitate neotissue formation.<sup>20</sup> Though these studies rely on the patient's cells to populate the valve, implantation of a scaffold does not ensure cell recruitment,<sup>21</sup> and failure to recruit cells to populate the valve results in graft failure. Synthetic vascular grafts are another example of scaffold transplantation,<sup>21</sup> however these conduits are biostable and therefore unable to remodel *in vivo*, which may hinder their use in pediatric patients.

Cell-seeded scaffold transplantation has been used to address some of the limitations of scaffold transplantation alone. Here, cells are seeded onto a scaffold, and implanted into the host omitting the *in vitro* bioreactor maturation step.<sup>5</sup> Endothelial cell seeded vascular grafts are one example of this technique. These scaffolds are typically surface treated with proteins, such as fibronectin which will further promote cell attachment and maturation of the construct *in vivo*.<sup>22</sup> Typical synthetic grafts for small-diameter blood vessels, such as

Dacron<sup>®</sup> and ePTFE, have reduced patency rates compared to saphenous vein and internal mammary artery grafts caused in part by a lack of endothelial cell (EC) lining. The EC lining exhibits vasoprotective properties such as the ability to secrete heparan sulfate, which acts as a cofactor in the activation of antithrombin, an enzyme which inhibits thrombosis.<sup>22</sup>

Finally, the most commonly utilized paradigm is *in vitro* tissue engineering (Figure 2.1). Cells are seeded on a synthetic or naturally derived polymeric scaffold, and the construct is matured *in vitro* in a bioreactor simulating physiological conditions.<sup>5</sup> The scaffold supports the cells while they proliferate, infiltrate, and synthesize their ECM proteins at which point the scaffold may degrade. The tissue is then implanted into the patient where further *in vivo* remodeling occurs as the construct integrates into the existing structure.

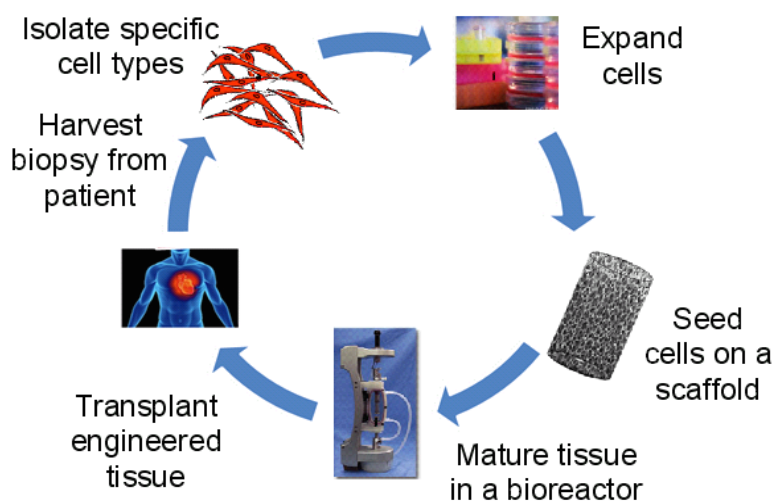


**Figure 2.1 *in vitro* tissue engineering paradigm**

One of the first major breakthroughs in vascular tissue engineering was constructed by Weinberg and Bell in 1986 and utilized bovine smooth muscle cells cultured in gelatin.<sup>23</sup> The outer surface was seeded with bovine smooth muscle cells and the inner layer was seeded with bovine endothelial cells to replicate the tunica adventitia and the tunica media, respectively.<sup>23</sup> Though these grafts were able to exhibit the morphological properties of native arteries, they eventually required reinforcement with Dacron<sup>®</sup> sleeves as their mechanical properties (i.e. burst pressure, mechanical strength) were unable to maintain the physiological burst pressure conditions that would be encountered post-implantation. The burst pressure reached 323 mmHg, which is not suitable to withstand the hemodynamic environment, thus emphasizing the primary limitation of natural biomaterials in the fabrication of tissue engineered vascular grafts. Despite this drawback, the results from this seminal work were encouraging and gave impetus to the vascular tissue engineering field.

## **2.2 Functional requirements of tissue engineered vascular grafts (TEVGs)**

In order to fabricate suitable grafts which can mimic the native tissue, TEVGs should have a burst pressure greater than 1,700 mmHg, which is equivalent to saphenous vein, the graft primarily used in CABG. Further, the graft must be physiologically compliant and be capable of withstanding hemodynamic stresses.<sup>24</sup> The mechanical properties of the vessel are largely derived from two critical ECM proteins: collagen and elastin. Collagen maintains the structural integrity of the vessel, due to its high tensile strength. Elastin acts as a recoil protein and contributes to vascular compliance, and prevents vessel stenosis.<sup>25</sup> Collagen synthesis has been observed in several TEVGs,<sup>26,27</sup> however promoting sufficient elastogenesis within tissue engineered vascular

substitutes has been one of the most challenging obstacles to overcome in vascular tissue engineering research.<sup>28,29</sup> TEVGs must also be nonthrombogenic, nonimmunogenic and easily suturable.<sup>30</sup> Additionally, in order to scale up tissue fabrication, the fabrication process must be consistent, with negligible variation in compositional and mechanical properties.<sup>31</sup>

### **2.3 Why *in vitro* Vascular Tissue Engineering?**

The emergence of the vascular tissue engineering field has been primarily motivated by two factors: (i) the high incidence of cardiovascular diseases and the increasing need for bypass graft surgeries with the aging population and (ii) the increasing need for *in vitro* preclinical models for drug screening and studying physiological processes.

#### **2.3.1 Clinical motivation: Cardiovascular Disease**

Cardiovascular diseases (CVDs), a term describing the disorders affecting the heart muscle, heart valves and systemic blood vessels, are the second leading cause of death in Canada and accounted for 20 percent of all deaths in 2011.<sup>1</sup> It is estimated that 1.3 million Canadians are living with cardiovascular diseases, and more than 300,000 Canadians are hospitalized each year due to CVD incidents.<sup>32</sup> In addition to its devastating effects, CVDs represent a major economic burden, with an estimated cost of 20.9 billion per year in hospital costs, lost wages, and decreased productivity.<sup>32</sup>

Of all CVDs, coronary artery disease (CAD) is one of the most common and causes significant morbidity and mortality.<sup>1</sup> The coronary artery is composed of three layers (Figure 2.2): (i) the tunica intima, which consists of a layer of endothelial cells (EC) that

form a barrier between blood and the vessel wall, and provide an anti-thrombogenic surface by secreting nitric oxide, a potent vasodilator.<sup>28</sup> (ii) The tunica media, which is adjacent to the intimal layer and comprises of a densely packed layer of concentrically oriented vascular smooth muscle cells (VSMCs) and elastic fibres, and is separated from the intimal layer by elastic lamina. The tunica media is thicker in more contractile and elastic vessels such as the coronary artery, which need to maintain vascular tone to regulate blood pressure in response to hemodynamic stresses, therefore recapitulating the properties of this layer is of utmost importance in the design of TEVGs.<sup>28</sup> (iii) The tunica adventitia layer, which consists of fibroblasts, fibrous connective tissues such as collagen, nerves, and capillaries.

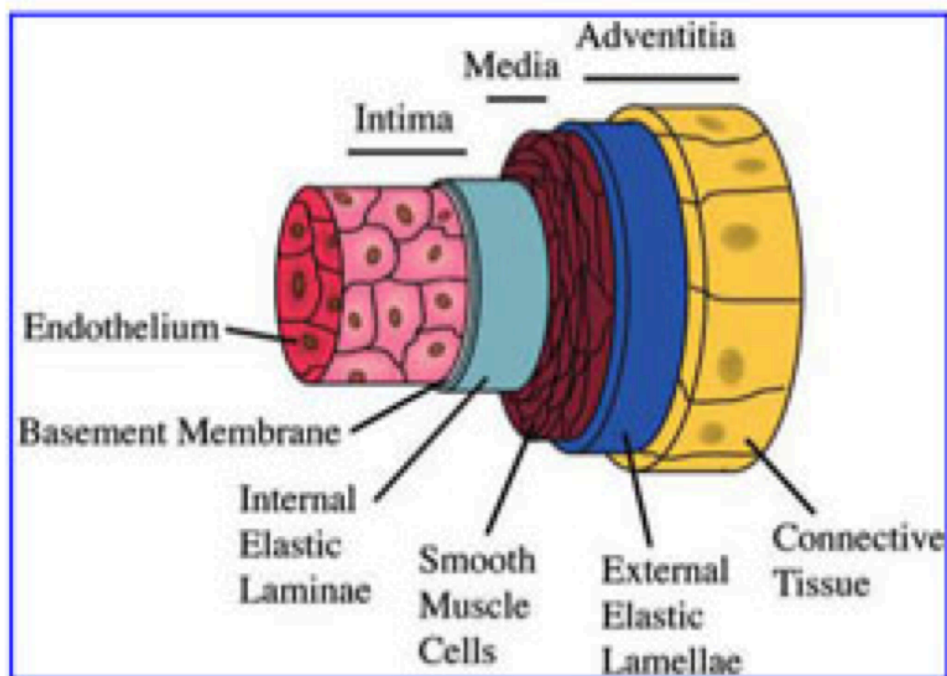


**Figure 2.2 Blood vessel anatomy. Reprinted with permission from Waterhouse, A., Wise, S. G., Ng, M. K. C. & Weiss, A. S. Elastin as a nonthrombogenic biomaterial. *Tissue Eng. Part B. Rev.* 17, 93–99 (2011).<sup>160</sup> Copyright © 2010, Mary Ann Liebert, Inc.**

The primary cause of coronary artery occlusions is atherosclerosis, a condition in which plasma lipids, inflammatory cells and connective tissue aggregate to form plaque. The plaque initiates a progressive narrowing of the artery, resulting in insufficient blood flow to and from the heart. If a complete blockage forms in one or more of the coronary arteries, this portion of the heart tissue becomes deprived of oxygen, or ischemic, which leads to the death of cardiomyocytes. If blood flow is not restored, irreversible tissue death (necrosis) will occur, eventually causing a myocardial infarction, otherwise known as a heart attack.

The two most common treatments for CAD consist of preventative measures and clinical interventions. Lifestyle changes such as increased physical activity and dietary changes are recommended by healthcare professionals to mitigate the risk factors of cardiovascular disease, such as blood pressure, diabetes and high cholesterol.<sup>33</sup> Aside from lifestyle changes, the two primary clinical interventions used to treat coronary artery disease are percutaneous coronary intervention (PCI) and coronary artery bypass grafts (CABG).<sup>34</sup>

In PCI, a balloon is attached to a catheter and guided to the blocked coronary artery using X-ray fluoroscopy. The balloon is inflated at the blockage site, first, pushing the plaque aside to improve blood flow, then deploying a stent to prevent the arterial wall from collapsing.<sup>33</sup> Anticoagulant medications are often prescribed in conjunction with this procedure, as the stent may scratch the intimal lining of the artery, causing vessel damage, which induces excessive blood clot formation.<sup>33</sup> Additionally, stents can produce an immunogenic reaction causing inflammatory cells to proliferate, which can occur in a condition known as intimal hyperplasia (IH), the thickening of the intimal layer of the blood vessel, eventually causing vessel restenosis (narrowing). In order to overcome this



limitation, drug eluting stents (DES) coated with polymers have been developed, to slowly release drugs that prevent the formation of scar tissue in the arterial lining.<sup>35</sup>

Vascular smooth muscle phenotypic modulation can also lead to IH. VSMCs can exist along a continuum from their quiescent state, known as the contractile phenotype to a synthetic phenotype, characterized by proliferation, migration and ECM deposition. In response to vascular injury, such as the scratching of the endothelial layer of the blood vessel by a stent, the cells may suppress contractile genes and upregulate synthetic gene markers, to increase cell proliferation and migration to the injured site. Once the injury has been repaired, the cells can downregulate synthetic markers to return to the quiescent phenotype, however if the phenotypic switching process is left uncontrolled, excessive proliferation and ECM deposition can lead to IH, causing stenosis, or narrowing, of the artery, which if left uncontrolled, could cause a complete blockage.<sup>36</sup> In view of this, controlling phenotypic plasticity to co-ordinate a proliferative phase to populate and remodel the construct, and a contractile phase, is crucial in the design of TEVGs.

In bypass grafts, the synthetic graft or autologous saphenous vein or mammary artery is sutured to the artery to bypass the ischemic portion and provide new path for oxygen-rich blood to flow. The autologous grafts prevent the immunogenic response, however the vein graft is not able to withstand the high arterial pressures, resulting in graft failure and repeat revascularization. Additionally, this procedure requires two sites of injury: one to extract the graft and one to revascularize the ischemic tissue, increasing the morbidity of the procedure. Moreover, due to co-morbidities such as diabetes and hypertension, some older patients may not have suitable autologous grafts for the procedure.

Synthetic grafts such as Dacron and ePTFE may be used due their high burst pressures, particularly for larger arterial grafts (>6 mm internal diameter), however the mismatch in compliance at the anastomotic site between the native tissue and synthetic grafts causes turbulent blood flow, and increase the chance for restenosis in smaller diameter constructs (<6 mm internal diameter).

Synthetic grafts are the standard treatment used in Fontan operations for pediatric patients with congenital heart defects, shown in Figure 2.3, whereby the inferior vena cava is connected directly to the pulmonary artery to bypass the malfunctioning right ventricle and supply venous return directly to the pulmonary system for oxygenation. Unfortunately, these constructs lack growth potential, which is an inconvenience to children who would need multiple procedures throughout their lifetime.

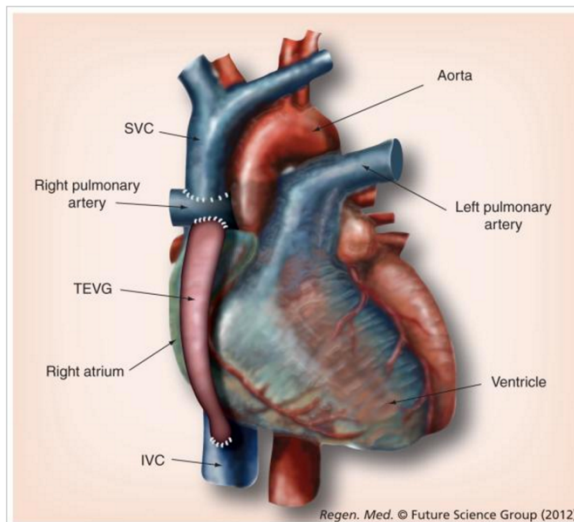


**Figure 2.3** TEVG as an extracardiac total cavopulmonary connection in the Fontan operation.<sup>38</sup> Reprinted from Patterson, J. T. *et al.* Tissue-engineered vascular grafts for use in the treatment of congenital heart disease: from the bench to the clinic and back again. *Regen. Med.* 7, 409–419 (2012). Copyright (2012) with permission from Future Medicine

The first clinically used TEVG was reported in 2001 by Shinoka and colleagues.<sup>37</sup> In this study, a 4-year-old girl received pulmonary artery reconstruction surgery, utilizing engineered vascular tissue fabricated from a tubular biodegradable poly(L-lactide-co-caprolactone) (PLCL) copolymer scaffolds reinforced with PGA mesh and the patient's own venous cells seeded on the scaffold *in vitro* prior to implantation. No evidence of graft occlusion was observed after 7 months.

Following this report, three pediatric patients underwent the same procedure.<sup>38</sup> One of the primary drawbacks of the procedure was the cell source, which required time consuming cell culture (8 to 12 weeks) prior to seeding and the use of xenoserum due to the presence of fetal bovine serum (FBS) in cell culture media, to prevent cellular dedifferentiation or host immunogenic response.

In 2001, this research group began to use autologous bone marrow mononuclear cells (BM-MNC) from the anterior superior spine, which were available on the day of surgery. TEVGs were implanted in 25 pediatric patients from ages 1 to 24 as extracardiac total cavopulmonary connections (Figure 2.3).<sup>39</sup> Two follow ups were performed after surgery at 16.7 months<sup>39</sup> and 5.8 years<sup>40</sup> (mean follow up time) respectively, with no evidence of aneurysm formation, graft rupture, or graft infection at either time point. One patient was treated with anticoagulant medication for mural thrombosis and percutaneous angioplasty was performed on three patients experiencing graft stenosis. Additionally, the graft's diameters increased with time ( $110\% \pm 7\%$  of the implanted size), indicating the growth potential of the engineered tissue,<sup>39</sup> and late term results of the procedure showed that 40% of patients remained free of any daily medications. Sadly, four patients died, with none of the deaths graft-related.<sup>40</sup> It is also important to note that these grafts were sutured into the pulmonary circulation which has a much lower systolic pressure compared to coronary arteries (20 to 30 mmHg during systole), which is less demanding than the higher-pressure environment of the coronary artery (100 to 140 mm Hg during systole).<sup>24</sup> The first US clinical trial was approved in 2011 at Yale University, where six patients received TEVGs, with the first patient in the US receiving a TEVG in August 2011.<sup>41</sup>

Other research and development (R&D) companies, notably Cytograft<sup>®</sup> and Humacyte<sup>®</sup> have emerged since Shinoka's publication in 2001.<sup>39</sup> Cytograft<sup>®</sup> uses the TEBV blueprint fabricated by L'Heureux *et al.*<sup>42</sup> with autologous human fibroblasts producing sheets of tissue that were then rolled onto a stainless steel mandrel. The construction of the TEBV took 6–9 months and yielded robust vessels with burst strengths greater than 3,000 mmHg.

These grafts were utilized in clinical trials in Argentina and Poland as arteriovenous shunts for ten patients with end-stage renal disease, delivering promising results including graft patency over six months.<sup>43</sup> Humacyte<sup>®</sup> founded by Niklason and colleagues is a cell-based therapeutics company fabricating TEVGs for applications such as end-stage renal disease, using biodegradable grafts made with human allogenic or canine VSMCs grown on tubular PGA scaffolds. The constructs are then decellularized, to prevent immunogenic response, which maintains the newly synthesized ECM,<sup>44</sup> with the newly formed construct named the human acellular vessel (HAV). Humacyte<sup>®</sup> recently commenced Phase III of their HUMANITY<sup>®</sup> study in the U.S, Europe and Israel with 350 evaluable subjects, making it the largest study of any engineered vascular tissue to date.<sup>45</sup>

Both of these are exciting breakthroughs in vascular tissue engineering and have the potential to be adapted to fabricate tissue engineered grafts for CAD patients, with Humacyte's technique showing success in the canine CAD model.<sup>44</sup>

### **2.3.2 Diagnostic applications: 3D tissue model**

Although the clinical need for engineered vascular substitutes for patients with CVDs is the primary motivation for vascular tissue engineering, the majority of the constructs are not ready for clinical translation due to several regulatory factors which hinder the progress of tissue engineered constructs into the clinic. These factors include safe harvesting of living cells from patients, cell survival and differentiation in the patient, cost, and reproducible cell production.<sup>46</sup>

Notwithstanding these barriers to clinical translation, a need has been identified in the research community and the pharmaceutical industry for *in vitro* biomimetic vascular

substitutes for drug screening,<sup>47</sup> as well as vascular disease models, as these constructs can more accurately mimic the *in vivo* tissue microenvironment and the cell-cell and cell-matrix interactions compared to conventionally used 2D tissue culture polystyrene plates (TCPS).<sup>47</sup> Additionally, unlike 2D culture, TEVGs are often cultured in environments simulating hemodynamic conditions (i.e. cyclic mechanical strain, pulsatile flow), which are known to have a significant impact on vascular cell response, including, but not limited to, cell proliferation, and the regulation of vascular smooth muscle phenotype.<sup>48</sup>

Although 2D flow-based endothelial cell models exist to overcome this limitation, the tubular geometry of the graft more accurately recapitulates the native structure of the vessel, which allows for assessment of intravascular devices, such as stents, and drug delivery models,<sup>47</sup> and the ability to construct physiologically relevant models of vascular diseases. While human vascular tissue is the most ideal model to study vascular therapeutics, this process is hindered by donor heterogeneity, tissue availability<sup>49</sup> and the inability to test directly on human subjects. Indeed, bovine and porcine vascular tissues are frequently used as models in pharmacological research, however species variability may limit the ability to extrapolate the results of intravascular or pharmacological studies to humans.<sup>50</sup> Tissue engineered models of the medial and adventitial arterial layers were designed and investigated by L'Heureux *et al.* and LaFlamme *et al.*, respectively.

L'Heureux *et al.*<sup>51</sup> fabricated tissue engineered vascular media (TEVM) using human vascular smooth muscle cells (VSMC), and tested the efficacy of known vasoactive agents on the contractility of their construct, which was exhibited by an increase in cytosolic  $\text{Ca}^{2+}$  concentration in response to these agents. LaFlamme *et al.*<sup>49</sup> constructed a tissue engineered vascular adventitia (TEVA) and studied its effect in the regulation of vascular

tone. TEVGs comprised of vascular cells and ECM proteins, although simplified compared to the complex *in vivo* environment in which native blood vessels reside, can still provide a physiologically relevant, reproducible and high throughput construct that can be used to model vascular pathologies, such as atherosclerosis, and investigate disease progression and therapeutic outcomes.<sup>52</sup>

## **2.4 Vascular tissue engineering components**

As mentioned previously, the key components of *in vitro* tissue engineering are the cells, the scaffold and the bioreactor. This section highlights the specific scaffold, bioreactor and cell source characteristics that are required to construct tissue engineered vascular grafts (TEVG), lists the specific components that can be utilized, and discusses the advantages and drawbacks of these elements.

### **2.4.1 Cell source**

As mentioned previously, the cell sources that are traditionally employed in vascular tissue engineered constructs are differentiated primary cells. Differentiated primary cells are lineage-committed cells extracted from an animal (xenogenic source), a donor (allogenic source) or the patient (autologous source) and grown *in vitro* prior to implantation.

The differentiated primary cell sources under consideration in vascular tissue engineering are endothelial cells (ECs), VSMCs and fibroblasts as these are the cells that line the intimal, medial and adventitial layers, respectively. Several TEVGs have been fabricated using these cells, with the most notable constructs fabricated by L'Heureux and Niklason's groups respectively, and are highlighted in section 2.3.1.

The culture time for fabricating tissue-engineered vascular constructs is typically 6-9 weeks. The long cell culture duration, is to ensure that the cells can generate sufficient ECM to mimic native arterial mechanical properties.<sup>25</sup> VSMCs are required to undergo approximately 45-60 population doublings (PDs) to generate an adequate amount of ECM,<sup>26</sup> however VSMCs can only proliferate for 10–30 PDs before undergoing senescence.<sup>25</sup> VSMC senescence results in a decrease in cell proliferation and ECM deposition.<sup>25</sup> Overall, the inability to harvest a sufficient cell population using primary cells is a limiting step in the tissue engineering paradigm.

Stem cells have emerged as an alternative cell source to address this limitation.<sup>53</sup> Stem cells are undifferentiated cells which have the capacity to self-renew and differentiate into daughter cells with specialized functions, with most stem cell populations categorized as pluripotent or multipotent. Pluripotent stem cell populations, such as embryonic stem cells (ESCs) and induced pluripotent stem cells (iPSCs) are self-renewing and can differentiate into almost any cell and form all three germ lineages. ESCs, derived from the inner cell mass of the blastocyst, have the highest degree of plasticity and differentiation potential, however limitations such as ethical considerations and the potential for immune rejection due to allogenic cell sourcing often preclude their use.

Induced pluripotent stem cells (iPSCs), developed by Yamanaka and colleagues<sup>54</sup> are a new and exciting stem cell source that have the potential to circumvent both the ethical and allogenic sourcing limitations. iPSCs are derived from terminally differentiated cells which have been reprogrammed into pluripotent stem cells by including four specific transcription factors using viral vectors to force expression of genes that are responsible



for maintaining pluripotency in embryos, namely Oct3/4, Sox2, Klf4, and c-Myc. Moreover, both cell sources have been utilized for vascular tissue engineering applications, by differentiating into VSMCs *in vitro* prior to culturing on 3-D nanofibrous PLGA/PLA scaffolds,<sup>55</sup> PLLA scaffolds,<sup>56</sup> and fibrin scaffolds,<sup>57</sup> respectively. Despite these outstanding benefits, ethical considerations often inhibit the use of ESCs. Moreover, both ESCs and iPSCs bear the risk of forming germ cell tumours, or teratomas *in vivo*, which may exacerbate the problem rather than alleviate it. The efficiency of iPSCs is usually quite low (0.01-10% of primary cells used respond to forced gene expression) and the viral vectors used may transfect the genes anywhere in the genome, which could potentially silence the expression of a gene regulating cell division, potentially cause uncontrollable cell division resulting in cancer.<sup>58</sup>

Multipotent stem cells (or adult stem cells) are an autologous stem cell source and have a more limited differentiating potential than pluripotent stem cells.<sup>59</sup> The main function of adult stem cells is to maintain tissue homeostasis and replenish dying cells.<sup>59</sup> Two types of adult stem cells exist: hematopoietic stem cells (HSCs) and mesenchymal stem cells (MSCs). HSCs are found in the bone marrow and differentiate into blood and lymphatic cells.<sup>60</sup> MSCs differentiate into mesodermal layer tissues (ex. bone, cartilage, fat and muscle) and are of primary interest in vascular tissue engineering.

The most common types of MSCs are bone marrow MSCs (BM-MSCs) and adipose stem cells (ASCs). BM-MSCs acquired by bone marrow aspiration are relatively rare, with 1 in 10 000 cells from bone marrow aspirate are stem cells.<sup>60</sup> ASCs, acquired from adipose tissue by lipoaspiration are approximately 5000 times more abundant than BM-MSCs and have been explored as a cell source for vascular smooth muscle cells in TEVGs.<sup>61</sup>

Before stem cells acquire their fully differentiated state, they develop an intermediate, partially differentiated cell type commonly referred to as precursor or progenitor cells.<sup>59</sup> Progenitor cells are described as oligopotent or unipotent. Examples of these cell types include satellite cells, which play a role in muscle cell differentiation and response to injury<sup>60</sup> and endothelial progenitor cells (EPCs), derived from bone marrow, which play a role in regenerating the endothelial lining of blood vessels, with the addition of specific growth factors. Additionally, immortalized progenitor cell lines such as A19 cells and mesenchymal progenitor C3H10T1/2 (10T1/2 cells) are frequently used for smooth muscle differentiation analysis. Studies using immortalized and human stem cells for vascular tissue engineering will be further discussed in section 2.6.

#### **2.4.2 Scaffolds**

Tissue engineered scaffolds are 3D structures fabricated from natural or synthetic biomaterials which mimic the topography of the ECM. Scaffolds act as a structural template for cells to synthesize their matrix proteins, thereby remodeling the construct and facilitating neo-tissue formation.<sup>62</sup>

One of the most important and challenging factors influencing the success of TEVGs is the ability of the cells to remodel the tissue engineered construct, therefore understanding the characteristics of a suitable scaffold, the materials which can be used and the scaffold fabrication methods available are of vital importance.<sup>63</sup>

### 2.4.3 Ideal scaffold characteristics

In order to design an optimal tissue engineered scaffold, a number of considerations need to be made, regardless of the specific tissue application. Firstly, and most importantly, the scaffold material must be biocompatible in order to support cell adhesion, migration and proliferation, and should be biodegradable to allow the cells to synthesize their own ECM and the degradation rate of the scaffold should occur at the same as tissue formation. The degradation by-products should be non-toxic have no adverse effects on cell behavior. In addition to biocompatibility, scaffolds should ideally be porous and interconnected structures to allow for cell ingrowth and nutrient diffusion, while maintaining mechanical properties specific to the native vascular environment.<sup>63,64</sup> Many of these properties are highly dependent on the material used and the fabrication method chosen, which will be described in subsequent sections.

### 2.4.4 Scaffold materials

Scaffolds can be fabricated from naturally occurring or synthetic materials. Natural polymers such as collagen<sup>65</sup>, fibrin,<sup>66,24</sup> and elastin,<sup>67</sup> among others, are integral ECM proteins and have been extensively studied as scaffold materials for vascular tissue engineered constructs.

These polymers are found in the human body, and therefore are highly biocompatible, have very low toxicity, and a decreased probability of immune rejection.<sup>68</sup> Biological scaffolds contain adhesive Arg-Gly-Asp (RGD) peptides which bind to integrin receptors on the cell surface, facilitating cell adhesion and interaction with the scaffold material.<sup>69</sup> The primary limitation of natural materials is their rapid degradation *in vivo* following implantation due,

in part, to the difficulty in modifying their chemical structure in order to incorporate functionality and mechanical strength.<sup>70</sup> Chemical crosslinking has been used to address this limitation, however the use of harsh solvents such as glutaraldehyde may increase the toxicity of the scaffold.<sup>71</sup>

Decellularized scaffolds are another type of naturally derived scaffold. As described in Section 2.1, decellularization involves the removal of cellular material from an allogenic or xenogenic vascular conduits using detergents, removing potentially immunogenic cells and leaving behind the native extracellular matrix environment. The matrix can then be recellularized and implanted directly into the host or placed in a bioreactor until maturation. Providing cells with their tissue-specific matrix is advantageous, as it has been shown to play a crucial role in controlling stem cell fate,<sup>72</sup> however this technique does pose limitations as well, such as disease transmission due to xenogenic sourcing<sup>73</sup> and the potential removal of proteoglycans.<sup>74</sup>

Synthetic scaffolds have been extensively studied for vascular tissue engineering applications due to their superior mechanical properties, wide availability and potential for scale-up production.<sup>75</sup> Polyurethanes and biodegradable aliphatic polyesters composed of PLA, PGA, poly-L-lactic acid (PLLA), poly- $\epsilon$ -caprolactone (PCL), and their copolymers, are the most frequently utilized materials. PGAs have been used as sutures,<sup>76</sup> vascular tissue engineering scaffolds,<sup>77</sup> and neo-urinary conduits<sup>78</sup> among other clinical applications. Indeed, the first clinically utilized vascular graft was fabricated using a poly-L-lactic acid/poly- $\epsilon$ -caprolactone (PLCL) copolymer.<sup>37</sup>

Notwithstanding their superior mechanical properties and biocompatibility, synthetic materials are not bioactive and cannot provide the complex biochemical cell-ECM interactions required for cell proliferation and tissue remodeling long-term. In order to address this, methods to adsorb cell adhesion peptides to scaffold surfaces<sup>79</sup> and to fabricate biomimetic scaffolds, by functionalizing synthetic polyesters in order to incorporate peptides and growth factors into the polymer backbone have been developed.<sup>80,81,14</sup>

In addition to synthetic scaffolds' inherent lack of bioactivity, PGA, PLA and their copolymers have been shown to produce acidic degradation products that create localized regions of low pH, which are cytotoxic and may contribute to an unmitigated phenotype switching of vascular smooth muscle cells from a functional, contractile phenotype to a proliferative, synthetic phenotype<sup>10</sup> which if uncontrolled, could lead to vessel narrowing and intimal hyperplasia *in vivo*.<sup>82</sup> Moreover, due to their synthesis from one monomer, polyesters do not possess tunable degradation characteristics. Copolymerization of polymers or blending is often adopted to make these materials more tunable, however these methods are not always successful.<sup>83</sup>

Poly(ester amide)s (PEAs) derived from  $\alpha$ -amino acids are a newer class of synthetic copolymers being considered for vascular tissue engineering<sup>11,84</sup> to overcome the limitations of aliphatic polyesters. The PEAs used in this work consist of an amino acid, an alcohol and a diacid, and bear ester and amide repeat units. As these units can be introduced using a variety of starting materials, the term PEA is more generic rather than specific. PEAs can be degraded both hydrolytically and enzymatically<sup>84</sup> and their degradation products contain both acidic and basic by-products, in addition to  $\alpha$ -amino acids which are found in the body limiting both the toxicity and the downward pH drift

exhibited in aliphatic polyesters.<sup>85</sup> PEAs have been shown to exhibit a surface degradation mechanism, meaning that the mass loss kinetics are linear and the molecular weight remains unchanged over time.<sup>11</sup> This linear degradation rate will facilitate tissue remodeling and regeneration by allowing enough time for the cells to synthesize their matrix proteins and remodel the scaffold, while the constant molecular weight and linear mass loss indicates that the mechanical properties of the scaffold will not be dramatically altered during the degradation process.<sup>11</sup>

As previously mentioned, PEAs derived from naturally occurring  $\alpha$ -amino acids have been investigated for vascular tissue engineering applications.<sup>13</sup> Karimi *et al.*<sup>86</sup> developed a class of PEAs derived from 1,4-butanediol, 1,6-hexanediol, and sebacic acid by interfacial polymerization using, L-phenylalanine and L-methionine as  $\alpha$ -amino acids. Vascular smooth muscle cells cultured on the PEA films exhibited a well-spread morphology, and the scaffolds fabricated using 1,6 hexanediol and L-methionine, and 1,4 butanediol demonstrated high porosity and interconnectivity, indicating the potential for PEAs to be viable scaffold biomaterials for vascular tissue engineering. Following this, PEA films functionalized with amine and carboxylic groups were investigated by Horwitz *et al.*<sup>84</sup> for endothelial cell biocompatibility, proliferation and inflammatory response. They concluded that the PEA films were noncytotoxic over 72 hours and noninflammatory after culture for 48 hours and that amine functionalized PEAs best supported cell spreading and proliferation. Srinath *et al.*<sup>11</sup> investigated human coronary artery smooth muscle cells (HCASMC) cultured on PEA discs and PEA/PCL blended scaffolds with varying PEA:PCL ratios and assessed the suitability of PEA material properties for vascular tissue engineering and the ability of the fibrous scaffolds to induce elastin synthesis.

Cytocompatibility analyses following 7 days of cell culture showed that PEA/ PCL fibrous mats had significantly higher viability compared to PCL fibre mats. Protein synthesis was observed using Western blotting demonstrated an upregulation of elastin on 3D PEA/PCL blended scaffolds compared to PEA films and PCL scaffold controls, indicating that elastin synthesis was influenced by the composition of the fibres and the 3D topography.

Previous works have shown that in addition to their the role of scaffolds as structural supports, the 3D scaffold topography and stiffness can provide complex signaling cues which can instruct cells on adhesion, proliferation, migration, differentiation and ECM protein synthesis.<sup>87</sup>

Additionally, Lin *et al.*<sup>88</sup> showed that the porous 3D environment of poly(carbonate) urethane (PCU) scaffolds alone, without the use of exogenous growth factors, increased elastin expression two-fold after 4 days of culture compared to its 2D counterpart. These findings suggest that vascular smooth muscle interaction with fibrous ECM-mimicking structures may play an important role in vascular cell behavior.

#### **2.4.5 Scaffold fabrication methods**

Scaffold morphology and architecture can be tailored depending on the intended application using a variety of fabrication methods. The techniques most often utilized are freeze-drying, solvent casting/particulate leaching and electrospinning. Freeze-drying is accomplished by first dissolving the polymer in water. The solution is then frozen at a pressure below the triple-point pressure. The environmental pressure imposed on the scaffold is then reduced to sublime the ice crystals, leaving behind a highly porous structure which can be modified by controlling the freezing rate.<sup>79</sup> The unfrozen water in the material

is removed by desorption in a secondary drying process.<sup>90</sup> Freeze drying is typically used for natural polymers that are soluble in water such as collagen. Although freeze drying allows for the fabrication of porous and interconnected scaffolds, it is a difficult technique to use for materials that are soluble in organic solvents as these materials have a much lower freezing temperature than water.

Solvent casting/particulate leaching is another technique used to fabricate highly porous and interconnected scaffolds. Here, the polymer of interest is typically dissolved in an organic solvent and poured into a mold containing porogens. After solvent evaporation, the porogen is leached out, thus forming a porous polymer scaffold. It is important to note that in order for this process to be successful, the solvent dissolving the polymer should not dissolve the porogen and the solvent used to dissolve the porogen in the final step must not affect the polymer. Solvent casting is a relatively simple procedure and the pore size can be tuned according to the size and type of porogen used, both of which are advantageous when designing tissue engineering scaffolds.<sup>91</sup>

Despite these benefits, there are some disadvantages to this technique. The scaffold fabrication time is long, with the leaching step alone lasting up to two days,<sup>91</sup> and as this technique employs toxic solvents there is the possibility of residual solvents affecting the cytocompatibility of the scaffold. The differences in densities between the salt and polymer solutions, contributes to a heterogeneous pore distribution, resulting in uneven cell spreading.<sup>92</sup> The uneven pore distribution means that some of the porogen may not be completely removed during the leaching step if the scaffold is too thick.<sup>92</sup>



Electrospinning is a highly versatile scaffold fabrication method that can create fibres in the nanoscale and microscale range, and mimic the dynamic ECM microenvironment.<sup>64</sup> In this technique, shown in Figure 2.4, a high voltage source is connected to a syringe containing a polymer solution. The solution becomes charged, and as the electric forces overcome the surface tension, a charged solution of polymer is ejected, forming a Taylor cone. The solution undergoes a whipping instability as it exits the needle tip, increasing the path length and travel time, thus allowing the solvent to evaporate before the fibres are deposited onto a grounded collector.<sup>4</sup> The versatility is owed to the user's ability to vary process parameters (i.e. flow rate and the distance from the needle tip to the collector, geometry of the collector) as well as solution parameters (i.e. polymer concentration, solvent) and is very advantageous for vascular tissue engineering applications. For instance, the geometry of the collector can be adapted to a cylindrical collector to create a tubular multilayered scaffold, which can be used to mimic the coronary artery,<sup>94</sup> or a flat collector, to form a fibrous mat to be used as a vehicle for drug delivery. Moreover, the fibre morphology can be modified by increasing the solute concentration, creating fibers with larger diameters and increased pore size.<sup>95</sup>

The ability to precisely tune the fibre characteristics using processing and solution parameters allows for simple modification of crucial mechanical properties such as tensile strength and burst pressure. Despite the overwhelming advantages of this technique, the primary challenge associated with electrospun scaffolds is inadequate cell infiltration due to the the dense packing of fibres, and small pore sizes.<sup>95</sup>

Aside from increasing fibre diameter, several post-processing approaches are being investigated to improve cell infiltration such as leaching sacrificial layers,<sup>96</sup> and cryogenic electrospinning, which involves the simultaneous deposition of fibres and ice crystals on a collector followed by the lyophilization of ice crystals to create uniform pores.<sup>95</sup>

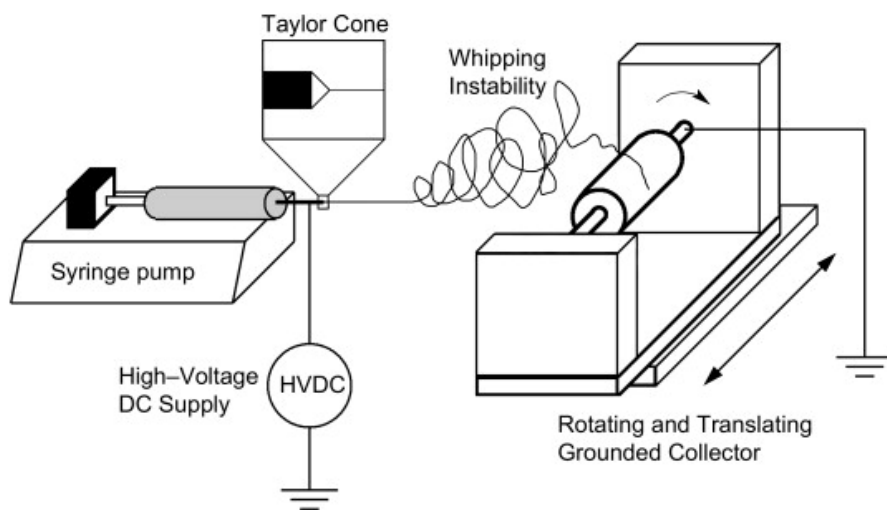


**Figure 2.4 Schematic drawing of the electrospinning process.**<sup>161</sup> Reprinted from Sill, T. J. & von Recum, H. A. *Electrospinning: Applications in drug delivery and tissue engineering. Biomaterials* 29, 1989–2006 (2008). Copyright (2008) with permission from Elsevier

## 2.5 Bioreactors

Bioreactors are systems which recreate tissue-specific physiological forces in a controlled *in vitro* environment and provide nutrient and oxygen delivery to the engineered tissue,<sup>97</sup> and as such are very important tools in the maturation of TEVGs. Three typical hemodynamic forces induced by pulsatile blood flow in vascular conduits *in vivo* are (1) shear stresses, which are frictional tangential forces that act directly on the endothelial cell layer (2) luminal pressure, a cyclic normal force attributed to blood pressure, and (3) circumferential mechanical stretch caused by blood pressure<sup>24</sup> These forces have been

shown to modulate vascular smooth muscle cell phenotype, cell proliferation and vascular differentiation<sup>98</sup> Pulsatile perfusion bioreactors are among the most utilized systems for designing vascular tissue engineered constructs.

The primary components of these systems are a sterile culture chamber containing the engineered construct, a motor driven pump to drive pulsatile perfusion, a medium circulating system to provide continuous flow of culture medium through the chamber, and a reservoir to feed culture medium into the system.<sup>99</sup> Several studies have utilized both human and animal vascular smooth cells<sup>99,100</sup> in order to elucidate biochemical pathways involved in phenotype modulation, however there are few studies using 3D stem cell cultures in a bioreactor setting for vascular tissue engineering applications, with the majority focusing on the role of shear stress mediated endothelial cell differentiation.<sup>101</sup> As stem cells have an increased proliferative capacity and growth potential, exploring the role of pulsatile flow on VSMC differentiation on coronary artery-mimicking scaffolds as opposed to 2D cultures could have important implications in vascular tissue engineering.

## **2.6 Stem cell-based vascular tissue engineering: relevant studies**

As previously mentioned, stem cells have emerged as viable candidates to address the cell source limitation issue due to their proliferative and self-renewal capabilities.<sup>6</sup> The following section will highlight relevant studies utilizing stem cells as sources for vascular cells as well as the important insights which can be gained by exploring stem cell interactions with tissue engineered scaffolds.

## 2.6.1 Pluripotent stem cells

### 2.6.1.1 Embryonic stem cells (ESCs)

As mentioned in section 2.4.1, embryonic stem cells (ESCs) are the most expansive stem cell source and can differentiate into somatic cells from all three germ lineages, increasing the possibility of obtaining the large number of specialized cells required for vascular tissue engineering applications.<sup>102</sup> Levenberg *et al.*<sup>55</sup> cultured human ESCs on porous salt-leached PLGA scaffolds using two methods: (i) suspending the hESC cell culture in Matrigel and (ii) coating the scaffold with fibronectin to increase cell attachment and explored the ability of the 3D microenvironment combined with TGF $\beta$ 1 and retinoic acid (RA) growth factor stimulation to facilitate 3D vessel-like formation. They observed, using immunostaining, CD34<sup>+</sup>/CD31<sup>+</sup> capillary networks when treated with control medium and medium supplemented with insulin growth factor (IGF). Interestingly, samples treated with RA did not form CD34<sup>+</sup>/CD31<sup>+</sup> capillary networks or express the genes. This study also demonstrated liver and neural crest and hepatic cell differentiation with a cocktail of growth factors, suggesting that cellular transdifferentiation may occur. Control of differentiation has been one of the persistent barriers precluding the use of ESCs.<sup>6,55</sup> Sundaram *et al.*<sup>102</sup> sought to control ESC differentiation and improve the proliferative capacity of MSCs by utilizing a specialized culture medium to differentiate highly proliferative hESCs into MSCs as an intermediary step. Following this, hESC-derived MSCs were either cultured on PGA mesh in a bioreactor for 8 weeks to assess cell infiltration and matrix protein deposition, or the MSCs were differentiated into VSMCs using TGF $\beta$ 1 and varying serum concentrations prior to seeding on the PGA mesh

scaffolds. H&E staining indicated cell growth throughout the construct, and Masson's trichrome stain showed collagen deposition, however elastin was not detected.

VSMC differentiation was verified by immunostaining with smooth muscle- $\alpha$ -actin (SM- $\alpha$ -actin) and calponin after TGF $\beta$ 1 and serum treatments, however chondrogenic, and osteogenic markers were also observed after 14 days of culture in a customized bioreactor, indicating transdifferentiation and further highlighting the difficulty in controlling ESC plasticity.

#### **2.6.1.2 Induced pluripotent stem cells (iPSCs)**

Human iPSCs provide an autologous source of pluripotent cells, circumventing the ethical and immunological concerns that limit the use of ESCs, making them a new and attractive cell source to be explored in vascular tissue engineering.<sup>103</sup> Since its discovery<sup>54</sup> several studies have emerged using human iPSCs in vascular tissue engineering. Sundaram *et al.*<sup>102</sup> generated MSCs from human iPSCs, in a manner similar to their work with ESCs, using specialized differentiation media. The pure MSC population was isolated using flow cytometry with cell surface markers CD73<sup>+</sup>, CD90<sup>+</sup>, and CD105<sup>+</sup> and CD45<sup>-</sup>. After culture for 8 weeks in a bioreactor, TEVGs exhibited burst pressure and suture retention strength that measured approximately half of saphenous veins.

Additional karyotyping studies also showed that TEVGs containing cells with chromosomal abnormalities and shortened telomeres exhibited positive Von Kossa staining for mineral deposition and calcification, which is associated with atherosclerosis,<sup>104</sup> and could contribute to vessel hardening if the construct is implanted *in*

*vivo*.<sup>105</sup> This may be attributed to osteogenic differentiation, or cell senescence, among other biological events,<sup>105</sup> however further studies need to be performed to understand the underlying mechanisms involved.

In another study, Xie *et al.*<sup>56</sup> utilized viral vectors for Oct4, KLF4, Sox2 and c-Myc to generate murine iPSCs from mouse embryonic fibroblasts and treated the cells with  $10^{-5}$  M of all-trans RA for 5 days to differentiate them to a VSMC phenotype prior to seeding onto porous freeze-dried PLLA scaffolds. Gene expression analysis using qPCR indicated RA treatment suppressed the expression of pluripotent markers and increased expression of late VSMC markers myocardin (MyoCD), and smooth muscle myosin heavy chain (SM-MHC) over 2 weeks compared to the spontaneous differentiation control treated with dimethyl sulfoxide (DMSO), suggesting late-term differentiation to an VSMC phenotype, however subcutaneous TEVG implantation in severe combined immunodeficient (SCID) mice for 14 days showed no significant difference in expression of late term markers smoothelin and SM-MHC gene expression in both the treatment and the pluripotent control group suggesting cellular dedifferentiation and some pluripotent cell retention. Further studies employed a more clinically relevant source of human aortic fibroblasts to generate human iPSCs, and an optimized VSMC differentiation protocol utilizing DMEM with 10% FBS and SmGM2 growth media at pre-determined time points.<sup>106</sup>

qPCR results indicated upregulation of  $\alpha$ -SMA, CNN1 (calponin) and SM22 $\alpha$  and contractile response was assessed using carbachol, demonstrating the functionality of iPSC derived VSMCs. Subcutaneous TEVG implantation into nude SCID was consistent, showing collagen deposition and positive staining for SM-  $\alpha$ -actin, CNN1 and SM22 $\alpha$ .

Though these results are very promising steps towards the fabrication of patient-specific TEVGs, the process of generating VSMCs from iPSCs is very long, requiring approximately 42 days and the robustness of the VSMC population derived from iPSCs is not known.<sup>106</sup>

Improvements to the iPSC derived VSMC efficiency were recently reported by Dash *et al.*<sup>107</sup> whereby iPSCs were generated from adult fibroblasts using Yamanaka factors and differentiated to VSMCs in 21 days. Using FACS analysis, they demonstrated that over 90% of human iPSC-VSMCs were positive for SM-22 $\alpha$  and calponin. Additionally, when switched to a maturation medium containing SmGM-2, 0.5% (FBS) and 1 ng/ml TGF $\beta$ 1 for 10 days, gene expression analysis indicated that SM-MHC and elastin in hiPSC-VSMCs increased from 3.86%  $\pm$  1.80% and 17.32%  $\pm$  2.30%, to 87.45%  $\pm$  7.10% and 74.65%  $\pm$  4.60%, respectively. The VSMCs were injected into an agarose mold to fabricate scaffold-free vascular rings, forming tissue after 1 day of seeding and demonstrating a robust cell population, VSMC marker expression, and collagen deposition. VSMCs were utilized to engineer a 3D model of supravalvular aortic stenosis (SVAS).<sup>108</sup> The SVAS disease model tissue rings exhibited a significant decreased contractility and an increased proliferative cell count compared to the control group exhibited by the carbachol assay and staining for ki67 positive cells, respectively. Overall, this is the first study to generate a robust VSMC population from iPSCs, and presents an innovative way to design tissue models to study vascular disease pathogenesis.<sup>107</sup>

## 2.6.2 Multipotent stem cells

### 2.6.2.1 Bone marrow mononuclear cells

The bone marrow is a soft connective tissue composed of a highly diverse cell population including multipotent hematopoietic stem cells (HSCs), endothelial cells, monocytes and MSCs among other cell types.<sup>6</sup> This cell population, termed bone marrow mononuclear cells (BM-MNC) can be harvested directly from bone marrow by centrifugation. BM-MNCs are available the same day and do not require time consuming cell culture. BM-MNCs were among the first stem cell source investigated for vascular tissue engineering applications.<sup>109</sup> Shinoka's group seeded canine BM-MNCs onto tubular PLCL scaffolds and implanted it into the inferior vena cava of a dog, and were able to construct vessels composed of both VSMCs and ECs which remained patent for up to 2 years.<sup>109</sup>

Cho *et al.*<sup>110</sup> designed a similar study, instead differentiating BM-MNCs into a VSMC population using Medium 199 supplemented with 10% FBS and penicillin/streptomycin prior to seeding onto decellularized porcine abdominal aorta and found matrix metalloproteinases (MMP) and tissue inhibitor of matrix metalloproteinase (TIMP) expression in the TEVGs and native abdominal aortas at 18 weeks, suggesting the occurrence of vascular remodeling, which is a crucial step in the tissue engineering paradigm.

To study this effect, Roh *et al.*<sup>111</sup> seeded human BM-MNC onto biodegradable PLCL and implanted them as venous interposition grafts, however the BM-MNCs were no longer



detectable within a few days of implantation. Instead, scaffolds were initially repopulated by mouse monocytes and subsequently repopulated by mouse SMCs and ECs. They proposed a mechanism for vascular remodeling, whereby, BM-MNCs secrete a factor called monocyte chemoattractant-1 (MCP-1) to recruit monocytes to the scaffold via paracrine signaling which will proceed to release angiogenic cytokines and growth factors to cause vascular remodeling within the scaffold. Though BM-MNCs provide a rich heterogeneous cell population, the cell extraction process is difficult and the proliferative capacity of the cells decreases with donor age and cell passage number, meaning that older patients who are most in need of TEVG therapeutics may not have a suitable autologous source. These limitations have led to investigations into alternative stem cell sources.

#### **2.6.2.2 Bone marrow mesenchymal stem cells**

Mesenchymal stem cells (MSCs) are adult progenitor cells which can differentiate into adipocytes, chondrocytes, osteocytes and other mesoderm-derived tissues.<sup>6</sup> MSCs are the most widely used stem cell source in cell-based therapies for three reasons: (1) unlike ESCs, there are no ethical considerations that preclude their use, (2) MSCs are less likely than ESCs and iPSCs to undergo spontaneous differentiation, and (3) they do not express the major histocompatibility complex (MHC) II largely responsible for immunorejection, which allows for allogenic cell sourcing.<sup>112</sup>

MSCs derived from skeletal muscle<sup>113</sup> and hair follicles<sup>114</sup> among other sources, have been studied for their ability to differentiate into VSMCs and their suitability as cell sources for TEVGs, however the two most commonly utilized MSCs in vascular tissue engineering are adipose stem cells (ASCs) and bone marrow mesenchymal stem cells (BM-MSCs).

BM-MSCs represent a small fraction of the heterogeneous bone marrow cell population, and have been shown to differentiate into VSMCs using TGF $\beta$ 1 and platelet derived growth factor-BB (PDGF<sub>BB</sub>), two growth factors which were initially investigated for their roles in murine mesenchymal progenitor 10T1/2 cell differentiation by Hirschi *et al.*<sup>115</sup> Building upon this work, Gong *et al.*<sup>77</sup> utilized human BM-MSCs and PGA tubular scaffolds and cultured the cell-scaffold construct in a bioreactor for 8 weeks in an optimized culture medium to create small diameter blood vessels and examined the effects of cyclic mechanical strain and growth factor addition on VSMC differentiation. Their findings demonstrated expression of the early and mid markers SM- $\alpha$ -actin and calponin, respectively using immunofluorescence staining and Western blot after 14 days in the presence of 1 ng/mL of TGF $\beta$ 1. Interestingly, the late marker SM-MHC was not observed, suggesting that the cells were still at an early myofibroblast-like differentiation stage, possibly due to the acidic degradation products of the PGA scaffold. The tubular scaffolds consisted of 22% collagen by dry weight, which is about half that of native vessels and had burst pressures of over 200 mmHg, however elastin was not observed.

Zhao *et al.*<sup>116</sup> studied VSMCs and ECs derived from ovine bone marrow MSCs seeded to decellularized vein scaffolds. VSMCs were differentiated using DMEM, serum, insulin, antibiotics and TGF $\beta$ 1, and implanted into a sheep model.

The early VSMC marker SM- $\alpha$ -actin was observed using immunostaining, however mid and late-term markers such as calponin and SM-MHC were not shown, which may suggest the cells have not fully differentiated into contractile VSMCs. Nonetheless, the grafts demonstrated mechanical stability for 5 months, suitable burst pressure and suture retention, as well as the presence of collagen and 2 and 5 months. *In vivo* studies using

human BM-MSCs have also been used to investigate antithrombogenicity by Hashi *et al.*,<sup>117</sup> whereby BM-MSCs were seeded on aligned nanofibrous scaffolds and rolled around a mandrel to mimic collagen fibril organization and implanted into a rat common carotid artery. Confluent layers of ECs and VSMCs were observed in the constructs. Additionally, when comparing the graft to an acellular control, they found that acellular grafts had significant intimal thickening after 60 days, whereas BM-MSC-seeded vascular grafts showed little intimal thickening, which suggests that MSCs may assist in reducing inflammatory responses induced by the foreign scaffold material.

### **2.6.2.3 Adipose stem cells (ASCs)**

Adipose stem cells (ASCs) were first characterized by Zuk *et al.*<sup>118</sup> in 2001, as a multipotent MSC source. ASCs are an attractive cell source due to their high proliferative capacity, relative ease in acquisition and *ex vivo* expansion, and high frequency of acquisition. ASCs are commonly derived from lipoaspirates obtained by cannular suction under local anesthesia. Self-renewing bone marrow mesenchymal stem cells (BM-MSC), are obtained by invasive drilling, which increases both the morbidity and risk of the procedure. Furthermore, BM-MSCs only comprise 0.01% of bone marrow, whereas ASCs are 500 times more abundant per equivalent volume of adipose tissue.<sup>119</sup>

It is important to note, however, that direct comparisons between BM-MSCs and ASCs as cell-based therapies are difficult to ascertain due to the donor variability of the stem cell samples.<sup>119,120</sup> Rodriguez *et al.*<sup>121</sup> were the first to demonstrate the VSMC and EC differentiation capabilities of ASCs using SMIM, FBS serum and heparin by induction of

VSMC markers SM- $\alpha$  –actin, calponin, and SM-MHC using both reverse-transcriptase polymerase chain reaction and Western blotting.

Wang *et al.*<sup>122</sup> designed small diameter vascular grafts, first by deriving VSMCs from human ASCs using TGF $\beta$ 1 and bone morphogenic protein-4 (BMP4) and using those cells on a biodegradable PGA tubular scaffold. Mechanical stimulation increased collagen content in the PGA construct to 50  $\mu$ g/g, corresponding to approximately 70% of human saphenous vein, which was used as the positive control. Further, vessel mechanical properties such as burst pressure and tensile strength were significantly increased in pulsatile conditions compared to their static counterparts. Similarly, Harris *et al.*<sup>123</sup> obtained lipoaspirates from 10 patients and studied ASC differentiation using angiotensin, TGF $\beta$ 1 and sphingosylphosphorylcholine (SPC). Gene expression studies using qPCR and Western blot suggested that the extent of differentiation varied across patient lines, which they suggested may have been due to cell harvesting from older patients (mean age 65 years), the majority of whom had co-morbidities. Previous work by this group<sup>124</sup> indicated that ASC extraction efficiency was unaffected by donor age, obesity or comorbidities although diabetes did appear to diminish the number of ASCs extracted from lipoaspirates. Contrary to this finding, Madonna *et al.* reported a decline in ASC availability with increasing patient age<sup>125</sup> although neither study tested their differentiation capacity.<sup>124,126</sup> Krawiec *et al.*<sup>127</sup> tested the differentiation capacity of ASCs from diabetic and elderly patients and determined that the ability of ASCs from diabetic and elderly patients to differentiate into VSMCs under angiotensin II stimulation decreased and that ASC derived VSMCs from elderly donors did not promote SMC migration.

Building upon this study, ASCs from healthy and diabetic donors were used to fabricate TEVGs and implanted them as aortic interposition grafts in a rat model, and found that TEVGs fabricating using ASCs from diabetic patients had a higher incidence of thrombosis<sup>128</sup> further demonstrating that donor variability and health status are limiting factors that must be taken into consideration when using ASCs for vascular tissue engineering.<sup>127</sup>

#### **2.6.2.4 Immortalized progenitor cells**

Autologous and allogenic stem cell sources are an exciting cell source and have abundant potential for the fabrication of TEVGs, however they have a small optimal passage range before losing their functionality, proliferation capacity and differentiation potential. Moreover, some stem cell sources, particularly ESCs and iPSCs, can undergo spontaneous differentiation, rendering the use of these cell sources difficult when conducting preliminary analyses of stem cell behavior, and the effect of growth factors on differentiation and cellular response.

Due to these limitations, immortalized stem and progenitor cells are used as *in vitro* models to study the cellular and molecular mechanisms controlling vascular smooth muscle differentiation.<sup>15</sup>

Immortalized cells, are stem cells which have been genetically reprogrammed to divide and proliferate almost indefinitely in cell culture, meaning the cell population can be expanded for a longer period of time, and derive a larger number of cells which is an asset when conducting extensive biological analyses. Cell lines frequently used for smooth

muscle differentiation analysis include A19 cell and C3H10T1/2 (10T1/2 cells). Hirschi *et al.*<sup>115</sup> studied if and how ECs recruit mural cell progenitor 10T1/2 cells and induce their differentiation during neovessel formation. Using immunohistochemistry and Western blot, their findings showed that 10T1/2 cells increased their expression of contractile smooth muscle markers calponin, SM-MHC and SM22 $\alpha$  when co-cultured with ECs and with the addition of TGF $\beta$ 1. Moreover, using, EC-10T1/2 co-culture under agarose gel, they demonstrated the role of PDGF-BB in inducing 10T1/2 migration towards ECs. This was one of the first studies determining the role of cell-cell interactions and paracrine signaling on the recruitment and differentiation potential of mural progenitor cells and the formation of blood vessels. In addition to cytokine addition and paracrine signaling mechanical stimulation has been shown to have a significant impact on cell proliferation, migration and differentiation, serving as a springboard for further studies investigating the potential of stem and progenitor cells as novel cell sources for vascular tissue engineering.<sup>77</sup>

## 2.7 Motivation and Objectives

Current synthetic materials used to support stem cell differentiation in vascular tissue engineering applications such as PGA and PLA produce acidic degradation products, which can lead to a cytotoxic environment and may be adversely affecting differentiation<sup>77</sup> and their degradation rates are difficult to control.<sup>129</sup>

Poly (ester amides) containing  $\alpha$ - amino acids produce both acidic and basic by-products, thus limiting the downward pH drift. Moreover, as the material is a copolymer, the degradation rate and mechanical properties can be tuned depending on the starting

materials used. PEAs have been studied as novel biomaterials for vascular tissue engineering,<sup>11, 85, 86</sup> however studies thus far have used primary cells, and the ability of this material to support vascular differentiation has yet to be explored.

10T1/2 cells were chosen for this study because they have a robust proliferative capacity, are less likely to undergo spontaneous differentiation and are able to maintain stable phenotype in culture.<sup>15</sup>

Moreover, 10T1/2 cells are able to differentiate to VSMCs using TGF $\beta$ 1. This cell source will be used to determine the ability of our PEA material to support VSMC differentiation and the feasibility of fabricating a small diameter vascular tissue to be used as a preclinical testing model.

The objectives of this thesis work are therefore the following:

- (i) Fabricate a 3-D fibrous mat and tubular scaffold using electrospinning
- (ii) Study 10T1/2 cell-material interactions with the mat and tubular scaffold, by assessing cell attachment, spreading and infiltration
- (iii) Differentiate 10T1/2 cells to a VSMC lineage using TGF $\beta$ 1 examining both gene and protein expression

## Chapter 3

### 3 Materials and Methods

#### 3.1 Materials

*p*-toluenesulfonic acid salt crystals was purchased from JT Baker (Phillipsburg, NJ). All other chemicals, including L-phenylalanine were obtained from Sigma Aldrich (Milwaukee, WI). All solvents were acquired from Caledon (Georgetown, ON).

#### 3.2 Methods

##### 3.2.1 Monomer synthesis

The poly (ester amide) was synthesized as previously reported.<sup>85</sup> Briefly, the di-*p*-toluenesulfonic acid salt monomer was synthesized by acid-catalysed condensation. A mixture of L-phenylalanine (60.8 mM, 2.2 equivalents), *p*-toluenesulfonic acid monohydrate (66.3 mM, 2.4 equivalent), and 1,4-butanediol (27.6 mM, 1 equivalent) in toluene (100 mL) was heated to 140°C while stirring in a flask equipped with a Dean-Stark apparatus. The solution was refluxed for 48 h, and then the solvent was removed under vacuum. The resulting product was filtered and washed with toluene. The monomer was purified by dissolving in boiling deionized water (300 mL) followed by hot filtration, and the solution was left to recrystallize overnight at 4°C. The purification step was repeated; the monomer crystals were then filtered and dried under vacuum.



### 3.2.2 Polymer synthesis (8-Phe-4)

To synthesize the polymer, sebacoyl chloride (5 mM, 1 equivalent) was dissolved in glass distilled anhydrous dichloromethane (15 mL) and the solution was added dropwise to an aqueous solution (15 mL) containing di-p-toluenesulfonic acid salt monomer (5.0 mM, 1 equivalent) and sodium carbonate (10 mM, 2 equivalents), and allowed to react for 16 h. The solution was rotovapped once the reaction was complete in order to remove residual dichloromethane. The polymer was then washed with deionized water prior to purification via Soxhlet extraction with ethyl acetate for 48 h, followed by drying under vacuum for 72 h.<sup>85</sup>

### 3.2.3 Spectroscopic analysis: <sup>1</sup>H-NMR

<sup>1</sup>H-NMR (400 MHz) spectra were obtained on a Varian Inova 400 spectrometer (Varian Canada Inc., Mississauga, ON). Chemical shifts are reported in parts per million (ppm) and are calibrated against residual solvent signals of chloroform (CHCl<sub>3</sub>, δ 7.2 ppm).

### 3.2.4 Gel permeation chromatography (GPC)

Gel Permeation Chromatography (GPC) data was obtained using a Waters 2695 Separations Module that was equipped with a Waters 2414 Refractive Index Detector (Waters Limited, Mississauga, ON) and two PLgel 5 μm mixed-D (300nm × 7.5mm) columns connected in series (Varian Canada Inc., Mississauga, ON). Samples (5 mg/mL) dissolved in DMF with 10 mM lithium bromide and 1 % (v/v) triethylamine were injected (100 μL) at a flow rate of 1 mL/min.<sup>130</sup>

### **3.3 Scaffold fabrication**

#### **3.3.1 Electrospinning of 3D fibrous mat**

The electrospinning setup consists of a high voltage DC Power Supply (ES30P, Gamma high voltage, USA), a glass syringe (Becton, Dickinson and Co., 0.5 mL, NJ, USA) with a blunt-tip stainless steel needle controlled by a syringe pump (KD101, KD scientific, USA), and a stainless steel rotating mandrel (25 mm diameter) covered with aluminum foil. The concentrations of the polymer used were 5, 6 and 7 % w/w, in order to obtain bead-free fibers with uniform fiber diameter distribution.<sup>130</sup>

#### **3.3.2 Electrospinning of tubular scaffold**

In order to fabricate tubular PEA scaffolds, the electrospinning setup was modified to include a 4 mm diameter stainless steel rotating mandrel. The rotating mandrel was coated with Span<sup>®</sup> 80 (Sigma-Aldrich, Milwaukee, WI), prior to electrospinning, to facilitate the removal of the fibres and preserve its tubular structure. Formulation parameters were kept constant at 6% w/w while the rotation speed (150, 1000, and 2000 RPM) was varied to obtain bead-free fibres with uniform fibre diameter distribution.

#### **3.3.3 Scanning electron microscopy (SEM)**

The morphology of the PEA fibres was visualized using SEM, (S-2600N, Hitachi, Japan); fibrous mats and tubular scaffolds were cut into square mats to facilitate the imaging of the fibrous structure. Samples were mounted on carbon-taped aluminum stubs and sputtered with gold/palladium (K550X, sputter coater, Emitech Ltd., UK) at 15 mA for 3 to 5 minutes prior to analysis.

Samples were scanned at a working distance of 9 mm and an accelerating voltage of 5 kV. Fibre diameter distributions were assessed using ImageJ software (NIH, Bethesda, MD, USA), where a sample size of 100 fibres from three separate images were measured for each fibre diameter distribution, and the ImageJ directionality plugin was utilized to determine the preferred fibre orientation.<sup>131</sup> Fibre diameter distribution and fibre orientation histograms were computed using GraphPad Prism 6.

### **3.4 Cell studies**

#### **3.4.1 Cytotoxicity and cell proliferation assays**

Circular samples (4 mm in diameter) of electrospun mats on aluminum foil were punched and affixed to a 96-well cell culture plate (BD Falcon™, Franklin Lakes, NJ) using silicone grease, and sterilized by immersion in 70% ethanol (100 µL) for 30 min, before conditioning overnight in Hank's balanced salt solution (HBSS, 100 µL; Invitrogen Canada, Burlington, ON).

For cytotoxicity, 3-(4,5-dimethylthiazol-2-yl)-2,5-diphenyltetrazolium bromide (MTT) assay was performed following the manufacturer's protocol (Vybrant<sup>®</sup>, Invitrogen, Burlington, ON, Canada). First, cells were seeded onto electrospun PEA mats at 10,000 cells/scaffold which were then cultured in DMEM supplemented with 1% penicillin/streptomycin (P/S) solution and 5% FBS for 3, 7 and 14 days, respectively. Medium was refreshed (100 µL) every 3 to 4 days. At the pre-determined time points, 12 mM MTT solution was added to each well and then incubated at 37 °C for 4 h. Afterwards, 100 µL 10% (w/v) SDS was added to solubilize the formazan, and further incubated at 37 °C for 18 h.

Lastly, the absorbance of the coloured product was recorded at 562 nm by a microplate reader in a 96-well plate. Negative control experiments were conducted by adding MTT to the culture medium only and were subtracted from the samples to obtain the final reading.

DNA quantification was assessed using the CyQUANT cell proliferation assay (ThermoFisher Scientific, Burlington, ON). Briefly, the cell-seeded PEA scaffolds were removed from the incubator at 3, 7 and 14 days, washed three times with  $1 \times$  PBS, placed in microcentrifuge tubes, and frozen at  $-80^{\circ}\text{C}$  until assayed. The cells were thawed at room temperature, and  $100 \mu\text{L}$  of CyQUANT GR dye/cell lysis buffer was added to each microcentrifuge tube to release the DNA from the constructs. The constructs were covered in aluminum foil and incubated for 5 min at room temperature in the dark, at which point the supernatant was collected and the fluorescence intensity was measured on an M1000 Infinite Pro microplate (Tecan US, Inc. Morrisville, NC) at an excitation wavelength of 480 nm and an emission wavelength of 520 nm.

### **3.4.2 Bioreactor and dual-pump perfusion system design**

The ElectroForce<sup>®</sup> bioreactor system from BOSE (Eden Prairie, MN, USA) with customized modifications to simulate the hemodynamic environment was used for this work. The bioreactor consists of four parts: a sterilisable BioDynamic<sup>®</sup> chamber, a pulsatile pump coordinating with pulsatile manifold to induce luminal pulsation, a peristaltic pump (MasterFlex<sup>®</sup>, Coleparmer, Canada) providing global circulation of culture medium, and a reservoir with tubing to feed culture medium into the system.

In order to culture the constructs dynamically, culture medium contained in a media reservoir was peristaltically pumped into the chamber generating a chamber circulation, at a flow rate of 4.8 mL/min.

In the meantime, medium in the chamber was also rhythmically pumped into scaffold lumen driven by a pulsatile pump at a frequency of 1 Hz, generating a pulsatile perfusion at a flow rate of 40 mL/min (Level 1) and 8 mL/min (Level 2) corresponding to 63 drops/min. WinTest<sup>®</sup> software (version 4.0) was used to provide data acquisition and instrument control. The bioreactor system was maintained in a humidified incubator at 37 °C containing 5% CO<sub>2</sub>. (Lin and Mequanint., unpublished work)<sup>163</sup>

### **3.4.3 C3H10T1/2 cell seeding on tubular scaffold**

10T1/2 cells were maintained in high glucose DMEM with 5% FBS and 1% P/S, and incubated at 37 °C and 5% CO<sub>2</sub>. The cells were passaged just prior to reaching confluence. Tubular scaffolds were pre-conditioned in HBSS overnight, then sectioned into 1 cm segments and fully submerged in 70% ethanol to sterilize for 30 minutes. Following sterilization, the scaffolds were washed three times with HBSS, and then changed to normal culture medium for equilibration. Scaffolds were placed back into a sterilized glass chamber, with similar dimensions to the rotating mandrel, with a stainless steel rod placed in the lumen of scaffolds. The scaffolds were seeded at high density with approximately  $5 \times 10^6$  cells. First, the cell pellet was quickly resuspended in 120  $\mu$ L of DMEM culture medium containing 2 mg/mL of rat tail collagen type 1 (Corning Inc., USA), 90  $\mu$ g/mL of human fibronectin (Biomedical Technologies Inc., Stoughton, MA), and 1.58  $\mu$ L of 1N NaOH to maintain pH at 7.4. The cell suspension was pipetted into the scaffold (120  $\mu$ L/1

cm segment) and the central mandrel was gently stirred to ensure even spreading of cell suspension on the scaffold. The cell-collagen gel was allowed to polymerize at 37 °C in the incubator for 30 minutes to ensure cell adhesion had occurred and was subsequently transferred into a tissue culture flask for static pre-culture.

After 3 days of static pre-culture, the static culture control was kept in the flask for 4 days, and the sample for dynamic culture was transferred into the bioreactor for 4 days. (Lin and Mequanint., unpublished work)<sup>163</sup>

### **3.5 Immunofluorescence staining and laser scanning confocal microscopy**

Cell attachment, spreading and infiltration were assessed for electrospun PEA fibre mats and tubular scaffolds using confocal microscopy. For the fibre mats, 10T1/2 cells were seeded onto control glass coverslips and PEA fibers, for three and seven days. Cells were washed with pre-warmed PBS immediately prior to fixing at 4 °C for 15 min in 4% formaldehyde solution (1 mL; EMD Chemicals) in divalent cation-free PBS. Following three washes in PBS, 10T1/2 cells were permeabilized with 0.1% Triton X-100 (0.5 mL; VWR International, Mississauga, ON) in PBS for 5 min and again washed three times with PBS. The cells were incubated with 1% BSA in PBS (0.5 mL; Sigma-Aldrich, Oakville, ON) for 30 min at room temperature prior to their incubation with Alexa<sup>TM</sup> Fluor 568-conjugated phalloidin (1:50 dilution; Invitrogen Canada, Burlington, ON) in the dark for 1 h at room temperature followed by another three washes with PBS. The cells were then counterstained with 4'-6-diamidino-2-phenylindole dihydrochloride (DAPI, 300 nM in PBS, 0.5 mL; Invitrogen Canada, Burlington, ON) for 5 min to label the nuclei and again washed three times with PBS. No.1 coverslips were mounted on microscope slides with

Trevigen® Fluorescence Mounting Medium (Trevigen INC., Gaithersburg, MD) and sealed with clear nail enamel. Samples were analyzed with a Zeiss LSM 5 Duo confocal microscope with nine laser lines and appropriate filters (Carl Zeiss, Toronto, ON, Canada).

For tubular scaffolds, a similar methodology was employed, whereby the constructs were fixed in 4% (w/v) paraformaldehyde (EMD Chemicals Inc. Gibbstown, NJ) and embedded in optimal cutting temperature (OCT) compound (VWR, Canada), and cut into 30-50 µm sections with a Leica CM3050 S Cryostat (Leica Microsystems Inc., Canada) prior to imaging, using DAPI and Alexa<sup>TM</sup> Fluor 468-conjugated phalloidin (green).<sup>132</sup>

The late-term VSMC marker SM-MHC was identified using immunofluorescence staining of OCT-embedded sections with rabbit anti-SM-MHC IgG (1:50; BT Inc.). Primary antibody binding was detected using Alexa Fluor<sup>®</sup> 555-conjugated goat anti-rabbit IgG as a secondary antibody (1:500; Life Technologies, Burlington, ON). 4',6-Diamidino-2-phenylindole (DAPI; 300 nmol in PBS) was used to visualize cell nuclei and F-actin was observed with Alexa<sup>TM</sup> Fluor 594-conjugated phalloidin (1:100; Life Technologies). Images were taken with a Zeiss LSM 510 confocal microscope (Zeiss, Canada) with nine lasers and appropriate filters.

### **3.6 Smooth muscle phenotype marker expression: qPCR and Western blot analyses**

10T1/2 cells were seeded at a density of  $2.5\text{--}5.0 \times 10^5$  cells per scaffold on 12-well plates (circular specimens 1.9 cm in diameter), and the samples were extracted at day 3 and day 7 for qPCR and Western blot analysis, respectively. qPCR was used to quantify messenger RNA (mRNA) expression of SM- $\alpha$ -actin and SM-MHC in 10T1/2 cells grown on PEA

fibres. First, total RNA was extracted using Trizol reagent (Life Technologies) following the manufacturer's instructions.

Complementary DNA (cDNA) was synthesized using 1 µg of total RNA primed with random primers as described in Promega™ Random Hexamers protocol (Fisher Scientific, Canada). qPCR was conducted in 10 µl of reaction volumes, using a CFX96™ Real-Time System (C1000 Touch Thermal Cycler; Bio-Rad, Canada) and gene expression of glyceraldehyde-3-phosphate dehydrogenase (GAPDH), SM- $\alpha$ -actin, and SM-MHC were determined with iQ™ SYBR® Green Supermix (Bio-Rad) according to the recommended protocol of the manufacturer. The sequences of primers were designed using Primer3Web. SM- $\alpha$ -actin forward primer 5'-GGG CTA TAT AAC CCT TCA GCG-3', reverse primer: 3'-GCT GTC TTC CTC TTC ACA CAT-5'. GAPDH forward primer 5'-GGT GGT CTC CTC TGA CTT CAA CA -3' reverse primer 3'-GTT GCT GTA GCC AAA TTC GTT GT-5'. SM-MHC forward primer 5'-CTG GTT ACA TTG TAG GTG CCA-3', reverse primer 3'-GCG AGC AGG TAG TAG AA GAT G-5'. The results were analyzed with the comparative threshold cycle method and normalized with GAPDH as an endogenous reference. (Lin and Mequanint, unpublished work)<sup>163</sup>

Western blotting was performed to evaluate the expression levels of VSMC phenotypic marker proteins. At day 7, cells were washed three times with ice-cold PBS and whole cell lysates were obtained by harvesting cells in 100 mL of sodium dodecylsulfate electrophoresis sample buffer containing 5% (v/v)  $\beta$ -mercaptoethanol. Lysates were sonicated, microcentrifuged, and the protein concentrations were determined by 660 nm Protein Assay (Thermo Scientific, Ottawa, Canada). Protein samples (30 µg) were



separated by 10% sodium dodecylsulfate-polyacrylamide gel electrophoresis (SDS-PAGE) and transferred at 90 V for 1 h at 4 °C to a nitrocellulose membrane in a Tris-glycine buffer.

Transfer efficiency was assessed by Ponceau red stain. Nitrocellulose membranes were blocked with 5% nonfat dry milk in PBS and incubated overnight at 4 °C with primary antibodies (anti SM- $\alpha$ -actin 1:1000; anti-GAPDH (1:5000, Millipore); anti-SM-MHC IgG (1:500; Biomedical Technologies Inc). Membranes were again washed three times, and then incubated for 5 min in SuperSignal West Pico Chemiluminescent substrate (Thermo Fisher Scientific, Rockford, IL) and examined with a Molecular Imager ChemiDoc™ XRS+ system (Bio-Rad Laboratories (Canada) Ltd., Mississauga, ON).

## Chapter 4

### 4 Results and Discussion

#### 4.1 PEA synthesis and characterization

In this work, PEA synthesis using L-phenylalanine, 1,8 butanediol and sebacyl chloride was obtained using the interfacial polymerization technique, and the results were consistent with previous reports (Figs 4.1 and 4.2).<sup>85</sup> Interfacial polymerization, a technique in which two reactive monomers in an aqueous and organic layer form a polymer film near the interface, was preferred over the conventional solution polycondensation technique for two reasons: Firstly, the polymerization times are shorter compared to the solution polycondensation technique. Secondly, the synthesis can be performed at room temperature, which yields fewer side products and impurities as the majority of these are unreactive at room temperature, which may allow for the production of linear polymers with higher molecular weight.<sup>85,133</sup>

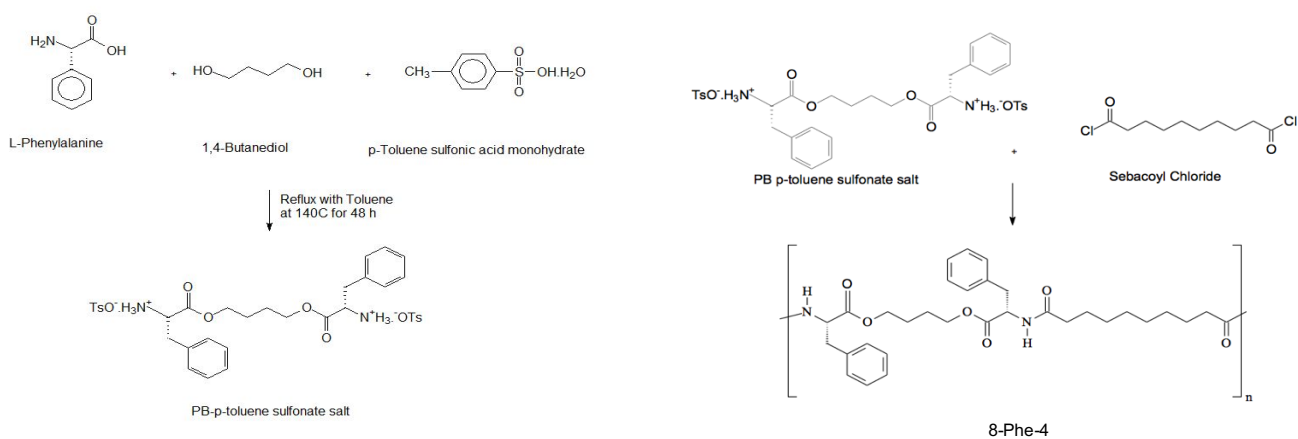


**Figure 4.1** Synthesis scheme for 8-Phe-4 derived from L-phenylalanine, 1,4 butanediol and sebacyl chloride by interfacial polymerization

$^1\text{H-NMR}$  was used to confirm the structure of 8-Phe-4. All the anticipated peaks were detected as shown in Figure 4.2 confirming the purity of the product. The  $\text{CDCl}_3$  solvent peak appears at a chemical shift of 7.2 ppm.

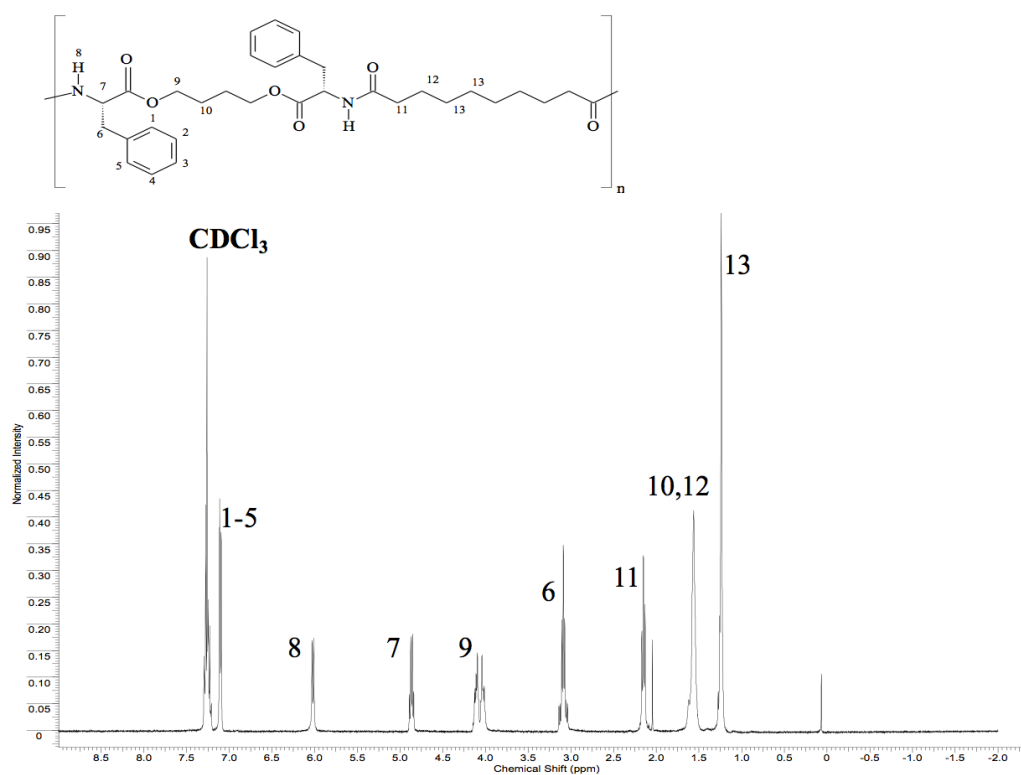


**Figure 4.2**  $^1\text{H-NMR}$  spectra of PEA from L-phenylalanine, 1,8-butanediol and sebacoyl chloride (8-Phe-4)

The 8-Phe-4 polymer was subsequently characterized using gel permeation chromatography (GPC), a technique which separates molecules based on their effective size in order to determine molecular weight distribution. Molecular weight is a very

important parameter as it plays a role in polymer characteristics such as mechanical properties, degradation rate, and glass transition temperature ( $T_g$ ), which are all essential components to consider when assessing the suitability of a material for vascular tissue engineering applications.

Figure 4.3 demonstrates the GPC trace for 8-Phe-4, demonstrating the elution time of the 8-Phe-4 polymer, which was compared to a polystyrene standard in order to determine the molecular weight. An average molecular weight of 55 kDa and a polydispersity index (PDI) of 2.01 were obtained. The PDI is the ratio of the weight average molecular weight, ( $M_w$ ) to the number average molecular weight ( $M_n$ ) and measures the non-uniformity of the polymer chains which is inherent in condensation polymerization. PDI values approaching 1 indicate more uniform molecular weight distributions. The 8-Phe-4 yield was 80%, and molecular weights were kept consistent between 55 and 60 kDa for the different batches prepared. In the following sections, the generic name PEA will be used in place of 8-Phe-4 for simplicity.

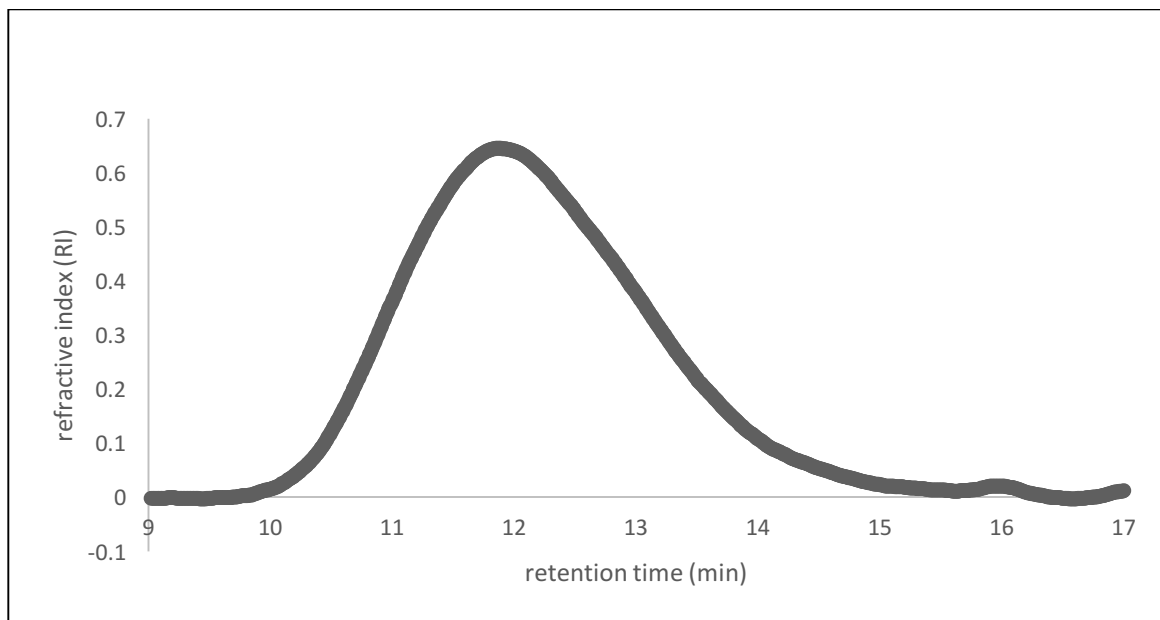


**Figure 4.3 GPC trace of 8-Phe-4 derived from L-phenylalanine, 1,4-buanediol and sebacoyl chloride by interfacial polymerization**

## 4.2 Electrospinning

### 4.2.1 Electrospun 3D fibrous mats

After successfully synthesizing the PEA, and obtaining batches with consistent molecular weights (between 55 and 60 kDa), the material was electrospun to fabricate 3D fibrous mats for subsequent mesenchymal progenitor 10T1/2 cell interaction and vascular differentiation studies. As mentioned in the literature review, electrospinning is a highly modular and versatile technique, that is often utilized in tissue engineering strategies to fabricate nanofibres which can mimic the ECM microenvironment.<sup>64</sup> The increased surface area to volume ratio allows for improved cell adhesion, and the ability to easily tune the mechanical and biological properties of the fibres by varying solution parameters (e.g.

polymer concentration and solvent) and process parameters (rotation speed, geometry of the collector, and needle tip to collector distance) is a significant advantage that is difficult to achieve in other scaffold fabrication methods.<sup>95</sup> Table 4.1 summarizes the electrospinning parameters that were studied in this work. The PEA was electrospun with a co-solvent mixture of 9:1 chloroform ( $\text{CHCl}_3$ ) and DMSO and a flow rate of 0.1 mL/h previously optimized in our laboratory.<sup>130</sup> The DMSO was added, as its high dielectric constant increases the conductivity of the polymer solution, which is a phenomenon known to favor bead-free fibre formation.<sup>134</sup> The processing parameters (i.e. solution volume, rotation speed and mandrel geometry) were investigated in subsequent studies using the 3D electrospun tubular scaffold.

| <b>Parameters</b>                | <b>PEA fibre mat</b>                       | <b>PEA tubular scaffold</b>               |
|----------------------------------|--------------------------------------------|-------------------------------------------|
| <b>Concentration</b>             | 5, 6, and 7% w/w                           | 6% w/w                                    |
| Voltage                          | 20 kV                                      |                                           |
| Flow rate                        | 0.1 mL/h                                   |                                           |
| Spinneret diameter               | 22 gauge                                   |                                           |
| Solvent                          | 9:1 w/w CHCl <sub>3</sub> : DMSO           |                                           |
| Needle tip to collector distance | 8 cm                                       |                                           |
| <b>Volume spun</b>               | 0.5 mL                                     | 1.5 mL                                    |
| <b>Rotation speed</b>            | 1000 RPM                                   | 125, 1000, and 2000 RPM                   |
| <b>Mandrel geometry and size</b> | Large cylindrical rotating mandrel (25 mm) | Small cylindrical rotating mandrel (4 mm) |

**Table 4.1 Summary of electrospinning parameters used for 3D electrospun mats and tubular scaffold**

#### 4.2.2 Effect of solution concentration on fibre morphology

For the 3D electrospun mats, the primary objective was to fabricate scaffolds with uniform fibre diameter and defect-free fibres. As previous studies have demonstrated polymer solution concentration is one of the most important determinants of fibre morphology and bead formation,<sup>135,136</sup> solution concentrations of 5, 6 and 7% w/w were electrospun to study the effect of polymer concentration on fibre morphology in this work. These concentrations were adapted from previous studies using PEA fibres, which determined that working concentrations above 7% w/w were highly concentrated and too viscous and resulted in polymer drying at the needle tip, due to the high volatility of chloroform (Boiling Point = 61°C).<sup>130</sup> PEA solutions electrospun at 5% w/w were not viscous enough for electrospinning and resulted in the formation of a electrospayed thin layer of polymer film (data not shown), as such, studies were continued using working concentrations of 6% and 7% w/w.

Figure 4.4 demonstrates SEM images of 3D fibrous mats spun at these concentrations. Morphologically, the 3D electrospun mats at 6% w/w and 7% w/w showed uniform fibres and exhibited random orientation. One hundred fibre diameters were measured randomly from three images using ImageJ, and a histogram was plotted order to determine which concentration had the most uniform fibre diameter distribution. The average fibre diameters were  $134 \pm 35$  nm for 6% and  $161 \pm 74$  nm for 7%. Although there was no significant difference between the mean fibre diameters at 6% and 7% solution concentrations, the fibres spun using 6% w/w PEA solution demonstrated a more uniform fibre diameter distribution, observed in Figure 4.4C, by the smaller standard deviation and



the narrower Gaussian distribution curve. Uniform fibres have been shown to improve cell adhesion and F-actin distribution and spreading, the latter of which, is a crucial element in cell migration and proliferation.<sup>137</sup> For this reason, 6% w/w solution concentration was utilized for subsequent tubular scaffold fabrication and cell-scaffold interaction studies.

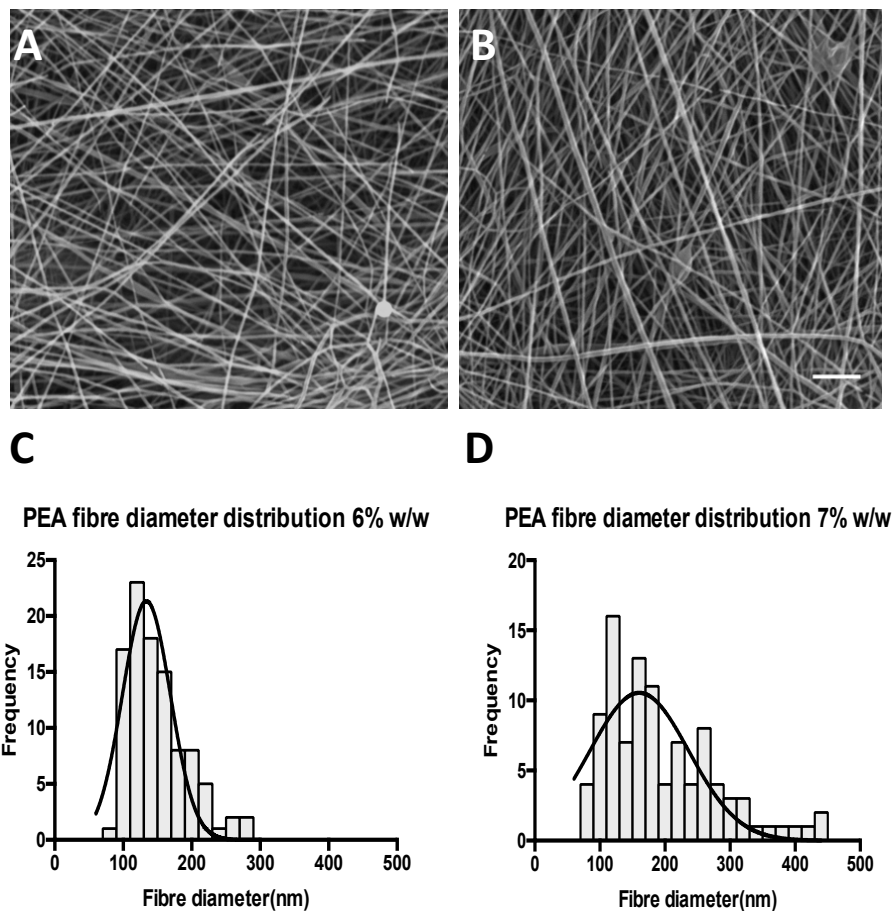


**Figure 4.4 SEM images of 6% and 7% w/w PEA fibres and respective fibre diameter distributions. Scale bar represents 2  $\mu\text{m}$ . Bin size for histogram is 20  $\mu\text{m}$**

### **4.2.3 Electrospun 3D tubular scaffold fabrication**

Once the solution parameters which produced uniform and bead-free fibres were established, the PEA was electrospun onto a small-diameter rotating mandrel in order to mimic the dimensions of the coronary artery as opposed to the 3D electrospun mats which were spun onto aluminum foil. The volume of electrospun PEA solution increased to obtain a construct with a wall thickness of 113  $\mu\text{m}$ . Following the electrospinning process, the scaffold adhered tightly to the mandrel, which made removal of the sample difficult, without compromising the integrity of the nanofibres. Initially, soaking the scaffolds in water for 72 h was considered to facilitate the removal of the tubular scaffold from the mandrel, however this resulted in excessive fibre fusion and swelling. In order to address this, Span-80, a nonionic surfactant was used to lubricate the surface of the mandrel prior to electrospinning. This method, combined with cutting the constructs into small segments with a blade and careful removal from the mandrel with tweezers, resulted in intact tubular constructs shown in Figures 4.5 A-C.

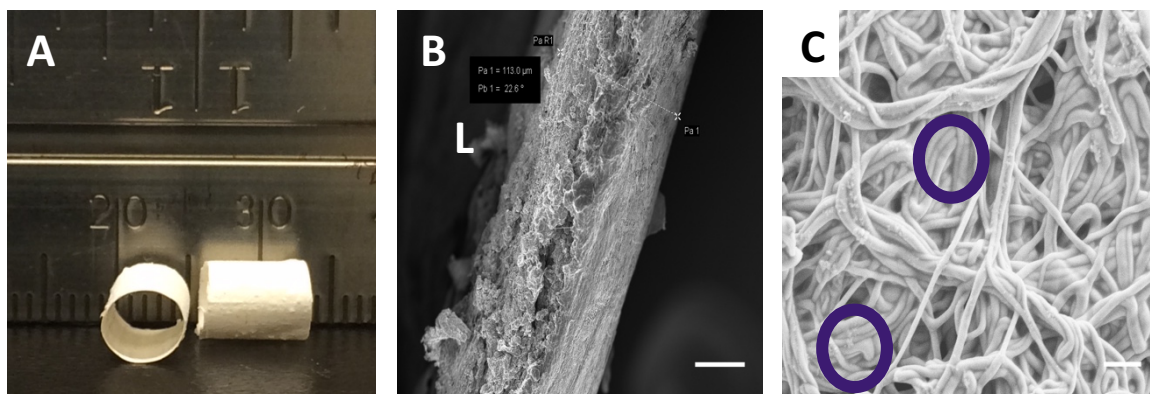


**Figure 4.5 A) Digital image of PEA tubular scaffold B) Cross-section SEM image of PEA tubular scaffold at 300× magnification, (L) indicates the lumen of the structure. Scaffold wall thickness is 113 μm C) PEA nanofibres at 5000× magnification. Purple circles indicate bundling of the nanofibres. Scale bar in B and C represent 50 μm and 2 μm, respectively**

Figure 4.5A demonstrates a macroscopic image of two tubular scaffolds, with the first image showing a dimensionally stable tubular scaffold, which is approximately 4 mm in internal diameter, consistent with luminal diameter studies conducted by Dodge Jr. *et al.*<sup>138</sup> which found the internal left anterior descending coronary artery diameter to be  $3.7 \pm 0.4$  mm. The SEM images in Figures 4.5 B&C show the tubular scaffold cross-section, and fibre morphology, respectively. In Figure 4.5B, the wall thickness was measured at 113 μm. In Figure 4.5C, significant fibre bundling was observed.

#### **4.2.4 Effect of mandrel rotation speed on fibre orientation**

Previous studies suggested that the orientation of the nanofibres is affected by the rotation speed of the mandrel,<sup>139,140</sup> whereby an increase in rotation speed will favour parallel fibre orientation. In this study, the effect of rotation speed on possible fibre alignment was explored by varying the number of revolutions per minute (RPM) of the rotating mandrel to 150 RPM, 1000 RPM (the rotation speed used in the previous section), and 2000 RPM. To visualize this effect on fiber morphology, SEM images were taken at 1500×, 3500× and 10000×, and are shown in Figure 4.6.

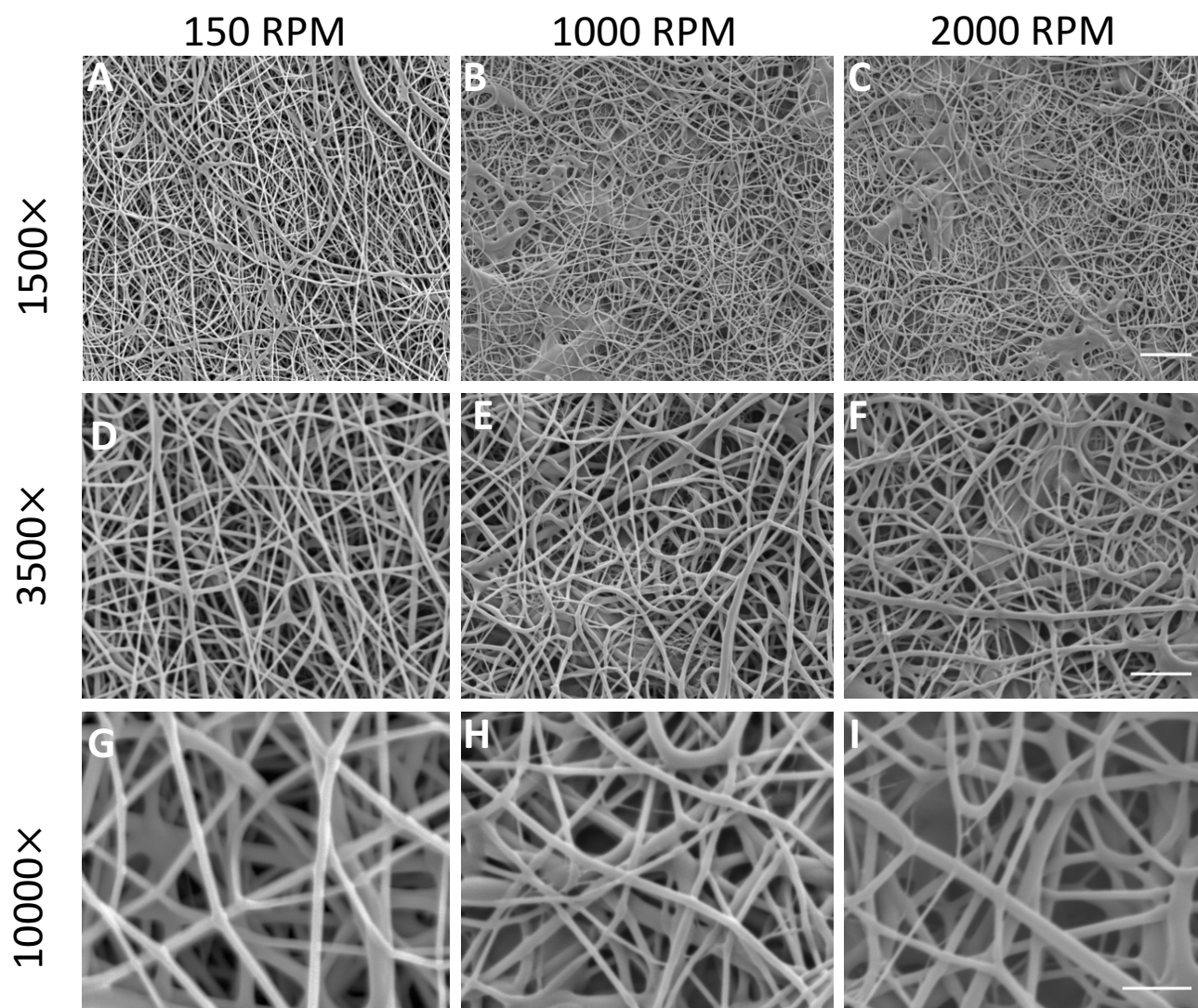


**Figure 4.6** Representative SEM images of PEA fibres electrospun onto small diameter tubular scaffold at 150, 1000, and 2000 RPM using three magnifications. Scale bars represent for A-C =10  $\mu\text{m}$ , D-F = 5  $\mu\text{m}$  and G-I = 2  $\mu\text{m}$ , respectively.

In Figure 4.6 (G-I), little morphological variation was observed between the rotation speeds, however some fibre fusion was observed in Figures 4.6B & C using 1000 and 2000 RPM, which is undesired as it may indicate the presence of residual solvent,<sup>141</sup> which could potentially affect the cytocompatibility of the PEA fibres. Mean fibre diameter distributions shown in Figure 4.7 were  $289 \pm 85$  nm,  $276 \pm 107$  nm, and  $289 \pm 113$  nm for 150, 1000 and 2000 RPM, respectively, confirming that varying the rotation speed of the mandrel had no significant impact on fibre diameter in this study.

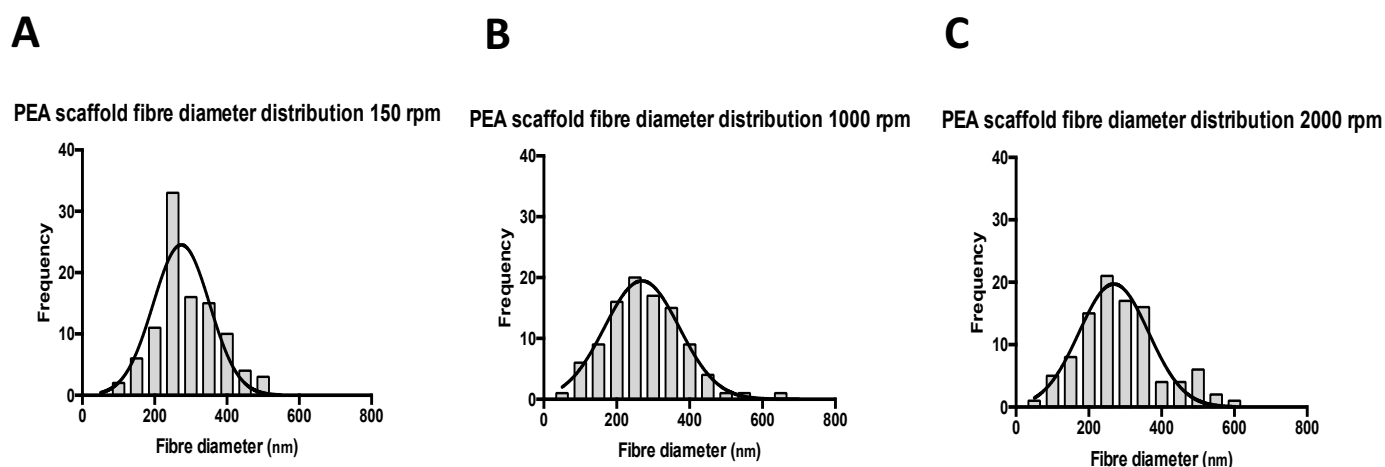


**Figure 4.7** The effect of mandrel rotation speed on fibre diameter distribution for 150, 1000 and 2000 RPM.

Once the effect of mandrel rotation speed on fiber morphology and diameter distribution was studied, and qualitative differences were not observed, the degree of orientation of the fibres was determined quantitatively using the computerized ImageJ directionality plugin.

The directionality plugin computes the preferred orientation of the fibres in the SEM image, between  $-90^{\circ}$  and  $90^{\circ}$ , from a pre-determined reference, and plots a histogram demonstrating the proportion of fibres oriented around a given angle.<sup>131</sup>

The directionality plugin was utilized for three SEM images at each rotation speed, with the data from one representative SEM image at each RPM collected, and plotted on GraphPad using non-linear regression analysis and shown in Figure 4.8. SEM images with non-oriented fibres give a flat histogram, while fibres that have a preferred orientation will give histograms with a Gaussian distribution.<sup>131</sup>

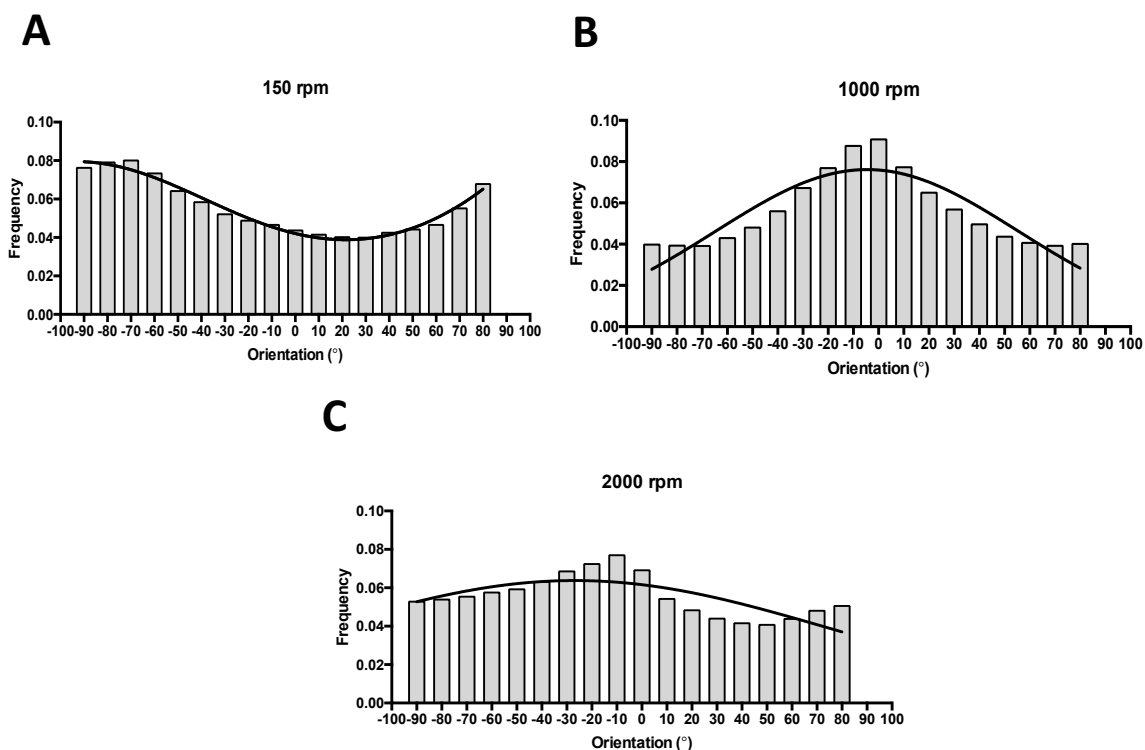


**Figure 4.8 Fibre orientation histograms for PEA fibres spun at 150, 1000 and 2000 RPM on a rotating mandrel**

In Figure 4.8A, which shows the fibre orientation frequency distribution for the PEA fibres spun at 150 RPM, the frequency distribution was analyzed using the sum of two Gaussians instead of the typically used Gaussian distribution. This suggests that there are two normally distributed fibre orientations within the image, at approximately  $+80^\circ$  and  $-80^\circ$ , and that the fibres have more than one preferred orientation. In Figure 4.8B, it can be seen from the Gaussian distribution curve, that increasing the rotation speed to 1000 RPM caused the preferential orientation of the PEA fibres at  $-5^\circ$ , and 25 percent of the PEA fibres were oriented between  $-10^\circ$  and  $10^\circ$  with respect to the reference. Although the Gaussian distribution curve was not as narrow, the fibre orientation histogram obtained using 2000 RPM exhibited a similar distribution profile to Figure 4.12B, with a preferred orientation at  $-20^\circ$ , and 25 percent of fibres oriented between  $-40^\circ$  and  $-10^\circ$ , with respect to the reference. Taken together, the results of this study suggest that increasing the mandrel rotational speed above 150 RPM supports increased fibre directionality and preferential fibre orientation around one angle.

Overall, the results of this work were consistent with previous studies which concluded that an increase in mandrel rotation speed increases fibre directionality, and favours the formation of aligned fibres.<sup>142,143</sup> Indeed, the ability to easily tune fibre orientation during the fabrication of electrospun scaffolds using rotation speed, is a characteristic that can be tailored to several applications in the tissue engineering field. For instance, in skeletal muscle tissue engineering, an aligned ECM provides topological cues which influence cytoskeletal organization, promoting myoblast orientation in parallel and providing contact guidance for myoblast contraction and differentiation. In a study by Aviss *et al.*,<sup>142</sup> aligned



electrospun PLGA scaffolds were fabricated by increasing the rotation speed from 300 RPM to 1500 RPM. Additionally, immunofluorescence staining demonstrated a significant increase in staining for myoblast differentiation marker fast myosin heavy chain in aligned scaffolds compared to their randomly orientated counterparts. Similarly, other tissue engineering strategies have utilize aligned scaffolds for intervertebral disk regeneration<sup>144</sup> and tendon regeneration. In a previous study conducted by Yin *et al.*<sup>145</sup> which sought to determine the role of matrix orientation on the differentiation of tendon stem cells, it was found that increasing the rotation speed to 4000 RPM during the electrospinning process resulted in fully aligned fibres, and an upregulation of tendon-specific genes was observed on aligned fibres compared to their randomly-oriented counterparts.

For the work in this thesis, which focuses on the fabrication of *in vitro* vascular tissue engineered constructs, random fibre orientation is desired as it may increase pore size, allowing improved 10T1/2 cell interaction, infiltration and diffusion of metabolic waste, and the subsequent remodeling of the construct, and as such 150 RPM was chosen as the mandrel rotation speed for the following *in vitro* bioreactor maturation studies.

### **4.3 Cell viability, interaction, and differentiation studies**

#### **4.3.1 10T1/2 cell viability and proliferation studies**

As previously mentioned, the three primary constituents in the tissue engineering paradigm are scaffolds, cells, and bioreactors. Scaffolds mimic the native ECM microenvironment and provide a porous 3D environment for cellular ingrowth. In view of this, once the scaffold fabrication parameters have been refined, the next step was to ensure that the electrospun scaffolds are cytocompatible and can support cell attachment and proliferation. Therefore, in order to evaluate 10T1/2 cell viability and proliferation, two biological assays were used. For cytocompatibility, MTT assays were performed using 4 mm PEA fibres which were hole-punched and affixed to 96-well plates using silicon grease, and standard TCPS wells used as a positive control. The MTT assay is a colorimetric assay evaluating metabolic activity, whereby viable cells with an active metabolism reduce the yellow MTT tetrazole salts into purple formazan crystals. The formazan crystals were solubilized using 10% sodium dodecyl sulfate (SDS), and the fluorescence reading was recorded at 562 nm using a microplate reader. As the conversion relies on the activity of mitochondrial oxidoreductase enzymes, it can be directly related to metabolic activity and indirectly related to the number of viable cells.

Figure 4.9 shows the results of the MTT assay recorded at day 3, day 7 and day 14. Although the TCPS control did seem to promote a slight increase in metabolic activity compared to the PEA fibres at day 3 and day 7, this observation may be attributed to reduced cell retention on the PEA fibres at this time point compared to the tissue culture plate, which is chemically treated with positive charges to induce electrostatic interactions

with the negatively charged cell membrane, thereby maximizing the number of cells which initially attach to its surface. Additionally, the absorbance levels between TCPS and PEA are similar at day 14, suggesting that the cells retained on the scaffold are continuing to grow in a similar manner. Overall, there was no statistical difference in terms of metabolic activity between the TCPS control and the PEA fibres at all time points. Statistical significance was observed at day 7 and day 14 on PEA fibres and TCPS compared to day 3 ( $p < 0.05$  and  $p < 0.01$ , respectively).

A slight increase in metabolic activity was observed between day 7 and day 14 for both the PEA fibres and the TCPS control, although the difference was not statistically significant. At this point, the cells may be reaching confluency, due to the small growth area ( $0.32 \text{ cm}^2$ ), the high initial seeding density (10000 cells/scaffold) and the fast doubling time of the 10T1/2 cells (16 hours). The combination of these factors may have decreased the metabolic activity of the 10T1/2 cells. Overall, this study suggests that the PEA scaffolds are not cytotoxic and, based on previous studies,<sup>11</sup> that their degradation products may not be affecting 10T1/2 cell metabolic activity.

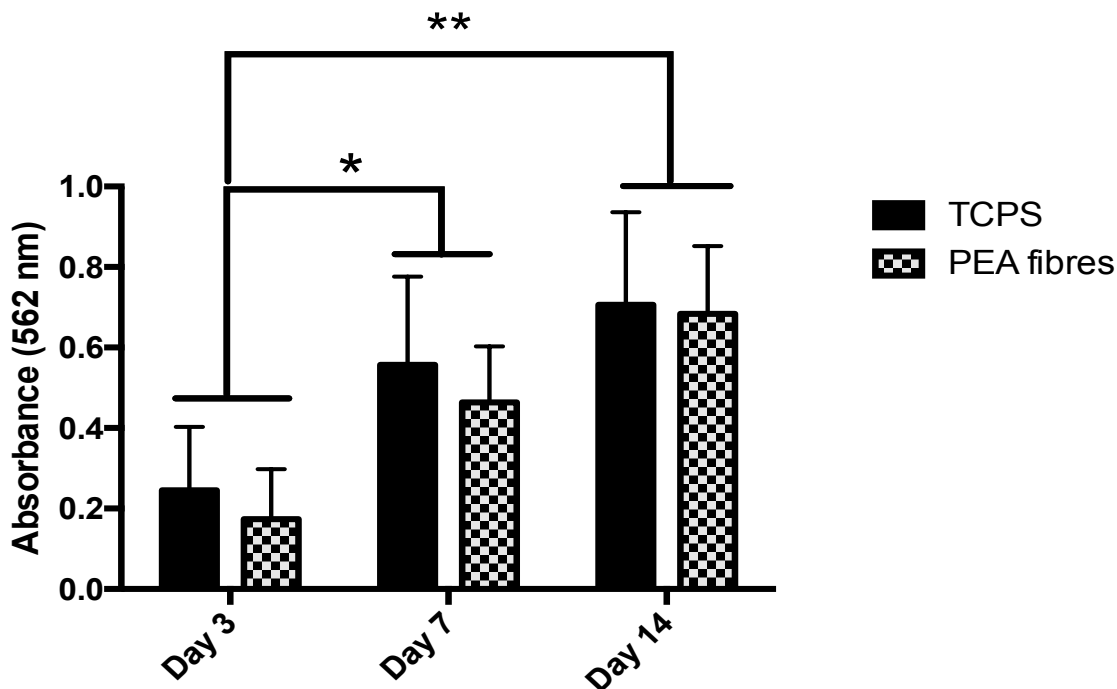


**Figure 4.9** 10T1/2 metabolic activity on PEA fibres and TCPS positive control. Scaffolds were seeded with a cell density of 10000 cells/scaffold on 96 well plates and cultured for 3, 7 and 14 days before MTT treatment. Data represents mean  $\pm$  SD for three independent experiments conducted in triplicate. Two-way ANOVA and post-hoc Tukey comparative tests were used. Solid line coupled with \* indicates  $p < 0.05$ , \*\* represents  $p < 0.01$ .

Although MTT assays are a relatively quick, inexpensive and well-established assay to determine cytocompatibility in 2D cell cultures, they rely on an indirect reading of cell viability using mitochondrial activity, and therefore do not provide a direct measurement of cell proliferation.<sup>146</sup> Furthermore, studies have suggested that results are inconsistent when translating these studies to 3D cell cultures, as cell metabolism is significantly different in 2D environments compared to 3D environments,<sup>146,87</sup> and that the diffusivity of reagents in 3D is more difficult due to the longer concentration gradient.<sup>146</sup> DNA

quantification provides a more accurate representation of cell number, and was therefore utilized to ascertain the results from the metabolic activity assay observed in Figure 4.9.

Here, 10T1/2 cells were seeded on electrospun PEA scaffolds affixed to 24-well plates for 3, 7 and 14 days and fluorescence intensity was recorded following the CyQUANT cell proliferation assay. Previous metabolic and proliferation assays using PEA scaffolds used short-term cell culture times for their studies (up to 7 days),<sup>11,14</sup> and the statistically significant increase in fluorescence between day 3 and day 14 ( $p < 0.01$ ) suggest that electrospun PEA scaffolds maintain 10T1/2 cell proliferation over 14 days, further confirming that PEA scaffolds support 10T1/2 metabolic activity and proliferation over 14 days.

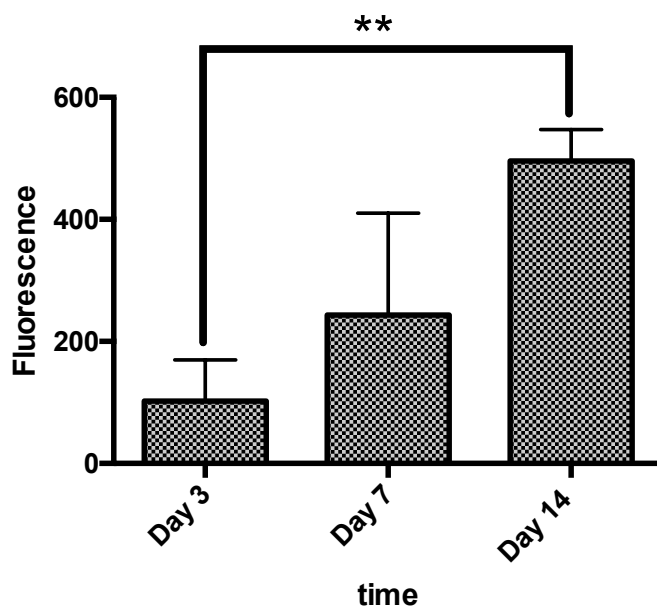


**Figure 4.10** 10T1/2 cell proliferation on electrospun PEA fibres. Scaffolds were seeded with a cell density of 2000 cells/cm<sup>2</sup> and cultured for 3, 7 and 14 days before performing CyQUANT cell proliferation assay (n=6). One-way ANOVA and post-hoc Tukey comparative tests were used. Solid line coupled with \*\* represents  $p < 0.01$ . Absorbance was measured at 480 nm excitation/520 nm emission wavelengths.

### 4.3.2 10T1/2 cell interactions with electrospun PEA fibre mats

In addition to facilitating cell viability and proliferation, PEA fibres must support cell attachment, spreading and infiltration to allow for cellular ingrowth, remodeling and eventual formation of *in vitro* vascular tissue engineered constructs. Given the ability of PEA fibres to support 10T1/2 cell viability and proliferation, as observed by the MTT and CyQUANT cell proliferation assays, 10T1/2 cell-material interactions were assessed using confocal microscopy to understand the influence of the 3D environment on cell attachment, spreading and infiltration over 7 days. Here, cells were directly seeded onto glass coverslips as well as PEA fibers affixed to a 3 cm dish, and stained for F-actin cytoskeleton using phalloidin (red) and nuclei using 4',6-diamidino-2-phenylindole (DAPI) (blue) at day 3 and day 7.

Comparing the two materials at day 3 in Figure 4.11 A & B, 10T1/2 cells seeded on both the glass coverslip and the PEA fibres adopted a fibroblast-like morphology with abundant F-actin filaments, and promoted similar attachment, spreading and distribution of F-actin filaments, confirming previous MTT data which determined no significant difference in cell viability between the two surfaces.

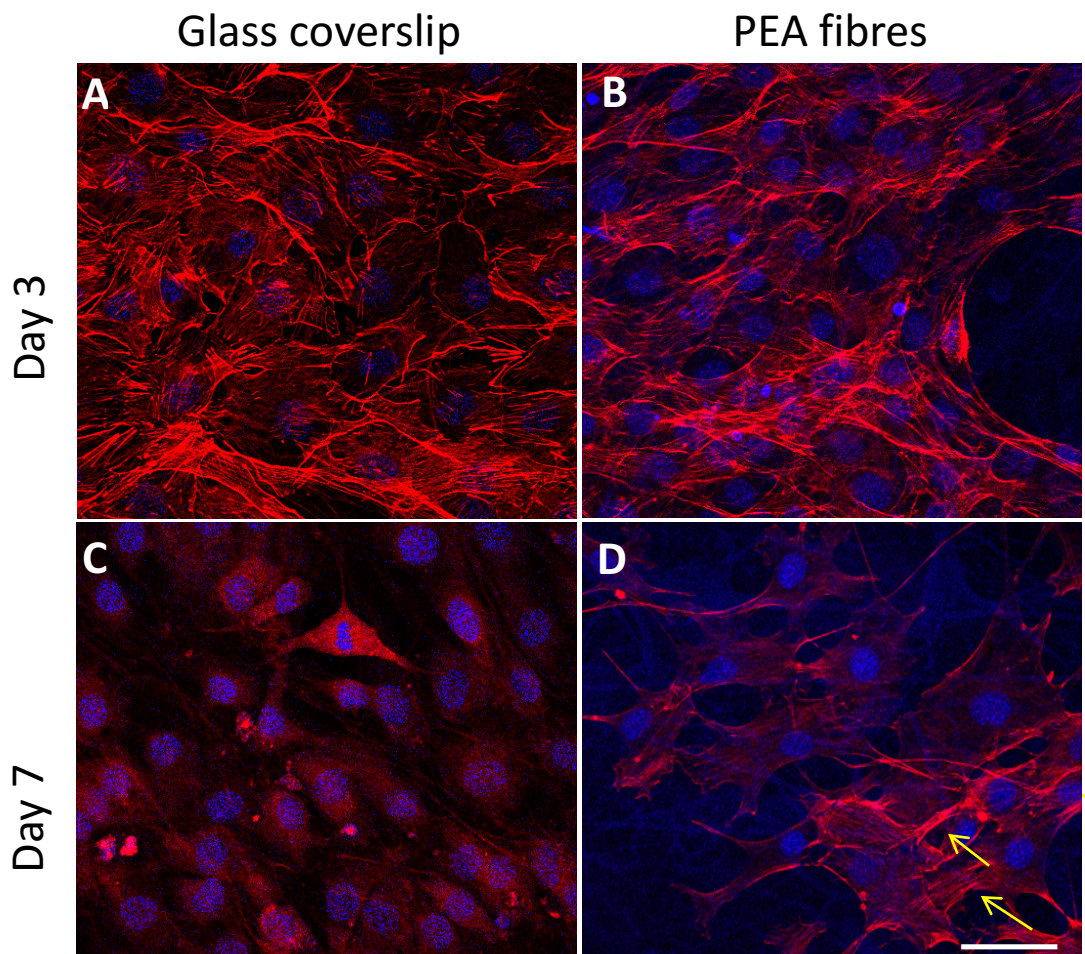


**Figure 4.11** Representative confocal image of 10T1/2 cells cultured on glass coverslips (A,B) and electrospun PEA fibres (C, D). Red represents F-actin (phalloidin) and blue represents nuclei (DAPI). Scale bar represents 50  $\mu\text{m}$

In Figure 4.11C & D, changes in F-actin distribution patterns and overall 10T1/2 cell morphology were observed. 10T1/2 cells typically reach confluency between 5 and 7 days, therefore, the lack of available growth area may be contributing to the morphological changes observed. In Figure D, the PEA scaffolds are seen by the autofluorescence in the blue channel, and the 10T1/2 cells are displaying increased interaction and infiltration with

the PEA fibres at 7 days. Although the overall spatial F-actin distribution and 10T1/2 cell morphology is similar to the cells on the glass coverslip, some 10T1/2 cells, indicated by yellow arrows, have maintained the fibroblast-like morphology observed in Figures 4.11 A and B, as demonstrated by their aligned F-actin distribution, indicating that PEA scaffolds may be able to support 10T1/2 cell proliferation for up to 7 days. This observation may be due to the increased surface area of the PEA fibres compared to the glass coverslips, and the ability of the cells to infiltrate the PEA scaffold. This data is consistent with previous studies reporting HCAMSC focal adhesion formation,<sup>14</sup> and 10T1/2 cell infiltration<sup>130</sup> on PEA fibres. Taken together, this data suggests that electrospun PEA fibre mats are able to support cell attachment, spreading and increased infiltration for up to 7 days.

### **4.3.3 10T1/2 cell interactions with electrospun tubular PEA scaffolds**

The favorable 10T1/2 cell interactions with electrospun PEA fibre mats combined with the successful electrospinning of randomly oriented fibrous tubular scaffolds enabled the preliminary study of 10T1/2 cell interactions with electrospun tubular PEA scaffolds. Sterilized 1 cm PEA tubular scaffold segments were placed into a cylindrical glass chamber with a stainless steel mandrel placed in the lumen of the scaffold.

10T1/2 cells were resuspended in media containing collagen I prior to seeding on the abluminal side of the scaffold, and placed in the incubator at 37 °C to allow for cell attachment. The scaffolds were then transferred to a tissue culture flask for 3 days of static pre-culture. The 3 day static culture was either transferred to the bioreactor for 4 days of dynamic culture (dynamic) or 4 days of static culture in the incubator both at 37 °C.



The bioreactor setup shown in Figure 4.12 was utilized to conduct dynamic culture studies. It consisted of four main parts: a chamber, a pulsatile pump to generate pulsatile flow through the lumen, a peristaltic pump to provide global circulation of cell culture medium, and a reservoir with tubing to feed the cell culture medium into the system. The luminal pulsatile and abluminal perfusion flow were utilized to recapitulate shear forces and pressures experienced by coronary artery vessels *in vivo*.

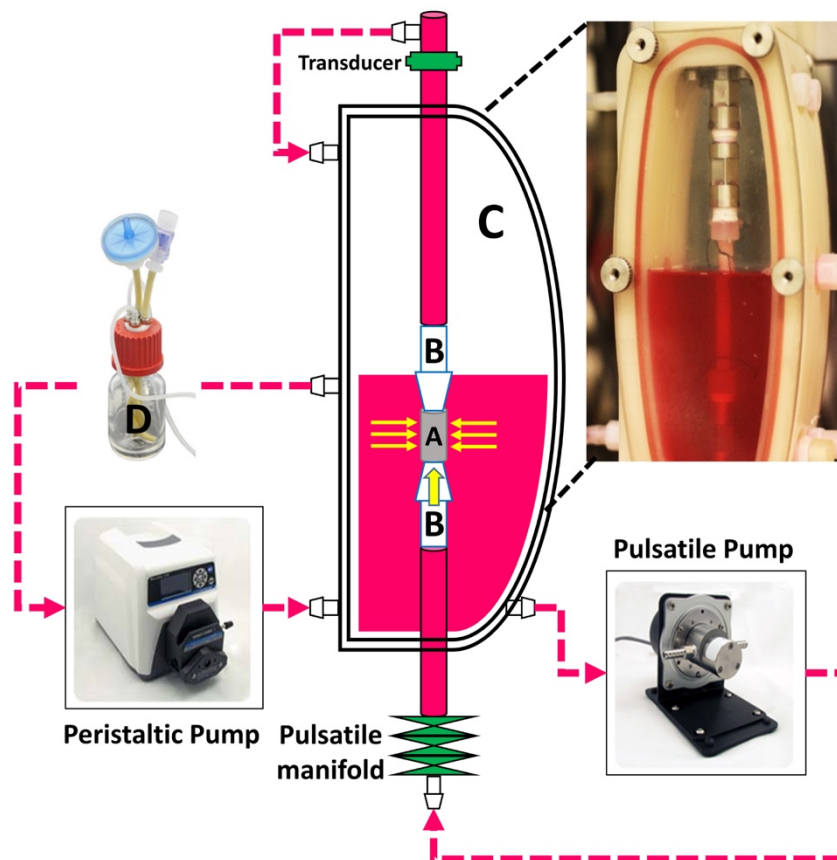


**Figure 4.12 Dual-pump flow perfusion bioreactor design for 10T1/2 cell interaction and infiltration study (Lin and Mequanint, unpublished work)<sup>163</sup>**

10T1/2 seeded constructs subjected to dual-pump bioreactor dynamic conditions shown in Figures 4.13 B and D, formed a dense layer of 10T1/2 cells on the abluminal surface. Some positive DAPI staining below the scaffold surface indicate some cellular infiltration had occurred, indicated by white arrows, however it was not sufficient to populate the thicker tubular scaffold cross-section.

Overall, this suggests that though the scaffold porosity combined with coronary artery-mimicking static and hemodynamic forces was not sufficient to allow for homogenous cell distribution throughout the construct, the *in vitro* bioreactor conditions, particularly the perfusion of cell culture medium supported increased cell proliferation and expansion potential compared to their static counterparts. Previous studies have shown that continuous perfusion increases oxygen transport and nutrient diffusion,<sup>147,148</sup> with one study by Zhao *et al.*<sup>148</sup> investigating perfusion flow on MSC-seeded on PET fibrous mats, showing an increase in MSC cell density over 40 days.

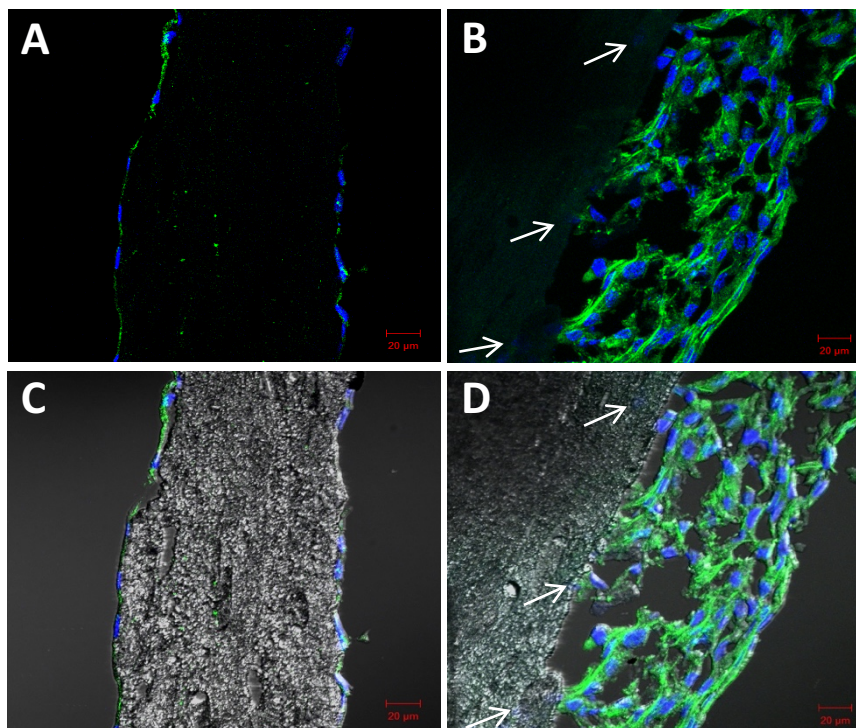


**Figure 4.13** Representative confocal microscopy images of 10T1/2 cells cultured on tubular scaffolds in static conditions for 7 days (A, C) and static culture for 3 days followed by dynamic culture for 4 days (B, D). Green represents F-actin (phalloidin) and blue represents nuclei (DAPI). White arrows indicate cellular infiltration. Scale bar represents 20  $\mu\text{m}$

As previously mentioned, cell infiltration in electrospun scaffolds is one primary limitation that is being actively addressed using post-processing methods such as salt leaching,<sup>149</sup> and sacrificial polymers,<sup>150</sup> both of which are being currently investigated using electrospun PEA fibres in our laboratory. This, in conjunction with the processing methods used in this work, which produced randomly oriented fibres post-processing should be optimized to improve cell infiltration and promote the formation of a three-dimensional *in vitro* vascular construct.

#### 4.3.4 Effect of TGF $\beta$ 1 on VSMC differentiation of 10T1/2 cells on electrospun PEA fibres

Given their ability to support 10T1/2 cell attachment, spreading and infiltration, the capacity of electrospun PEA fibres to support VSMC differentiation using TGF $\beta$ 1 was assessed using qPCR and Western blot analyses for SM- $\alpha$ -actin and SM-MHC - two important VSMC-specific markers which represent early and late stage differentiation, respectively. TGF $\beta$ 1 is a potent cytokine that has been shown to differentiate 10T1/2 cells to VSMC in 2D cell cultures.<sup>115</sup> TGF $\beta$ 1 has been shown to modulate the phenotype of VSMC cells in 3D culture,<sup>88</sup> however, to our knowledge, the *in vitro* vascular differentiation potential of 10T1/2 cells on electrospun 3D scaffolds has not been investigated.

In order to assess the effect of TGF $\beta$ 1 concentration on VSMC marker gene expression, PEA fibres were affixed to 12-well plates, and seeded with 10T1/2 cells, with exogenous TGF $\beta$ 1 growth factor added on day 1. qPCR was conducted after 3 days of cell culture. The qPCR data shown in Figure 4.14 demonstrated a significant increase in SM- $\alpha$ -actin expression with the addition of 2 ng/mL ( $p < 0.05$ ) and 4 ng/mL TGF $\beta$ 1 ( $p < 0.01$ ). Late term differentiation marker SM-MHC expression reached significant levels only with the addition of 4 ng/mL of TGF $\beta$ 1 ( $p < 0.05$ ). This study has shown that exogenous TGF $\beta$ 1 treatment supported an increase in gene expression of VSMC differentiation markers SM- $\alpha$ -actin and SM-MHC in 10T1/2 cells, with 4 ng/mL significantly increasing expression of both markers.

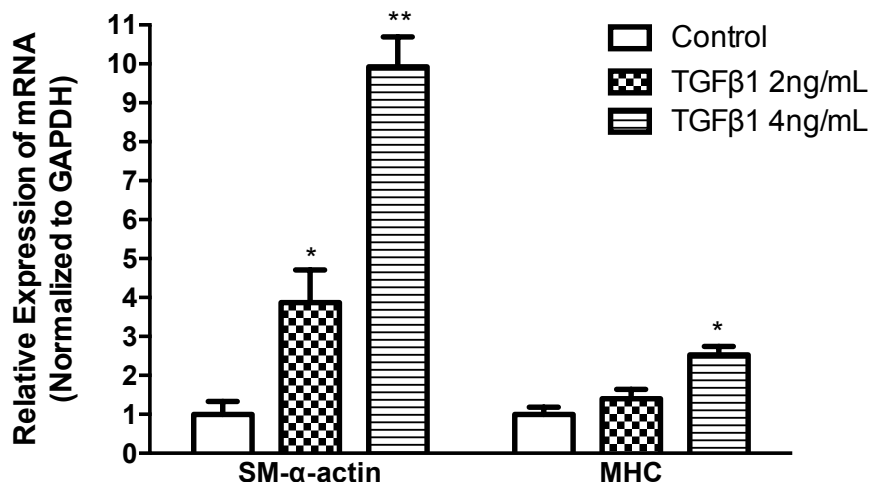


**Figure 4.14** Quantitative real-time polymerase chain reaction (qPCR) demonstrating 10T1/2 cell expression of smooth muscle  $\alpha$ -actin (SM- $\alpha$ -actin) and smooth muscle myosin heavy chain (SM-MHC) genes on PEA fibres treated with 2 ng/mL and 4 ng/mL of TGF $\beta$ 1, respectively after 3 days. Results were normalized to GAPDH expression. Statistical significance was analyzed using student's *t* test ( \* indicates  $p < 0.05$ , \*\* indicates  $p < 0.01$ )

In order to determine if the successful transcription of VSMC markers can lead to translation and subsequent protein expression of early and late markers SM- $\alpha$ -actin and SM-MHC, Western blot analysis was carried out after 7 days of cell culture, with TGF $\beta$ 1 added on day 1 and day 4, and displayed in Figure 4.15. In terms of growth factor addition, TGF $\beta$ 1 did not have any significant effect on SM- $\alpha$ -actin expression, while SM-MHC protein expression was upregulated with the addition of 2 ng/mL of TGF $\beta$ 1.

Increasing the TGF $\beta$ 1 concentration to 4 ng/mL did not appear to have an effect on SM-MHC expression, however, the efficiency of additional growth factor may have been attenuated by the potential presence of TGF $\beta$ 1 in the FBS growth serum in this particular study.<sup>151</sup> Although the data is limited to draw a comprehensive conclusion from this study,

the increase in SM-MHC expression observed suggests that treatment with 2 ng/mL of TGF $\beta$ 1 was sufficient to induce the differentiation of 10T1/2 cells to VSMCs on electrospun PEA fibres.

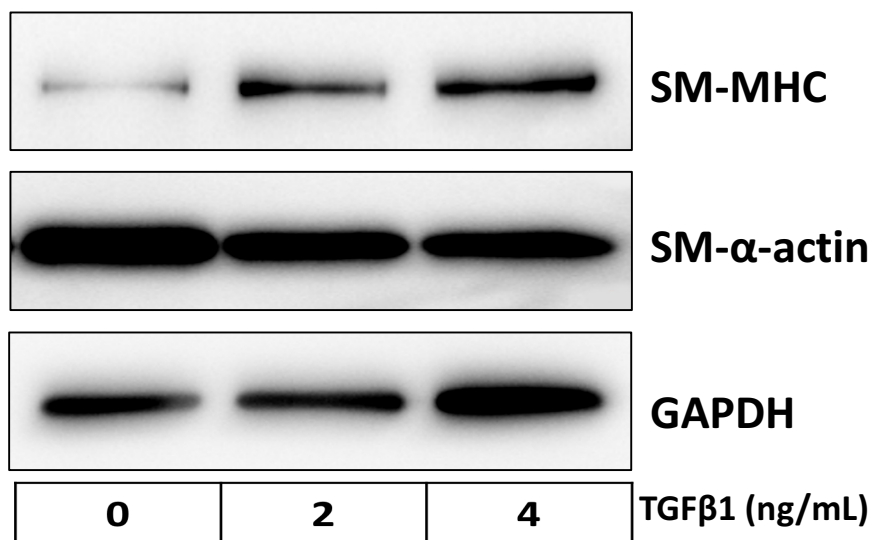


**Figure 4.15** Western blot demonstrating 10T1/2 expression of smooth muscle-  $\alpha$ -actin (SM- $\alpha$ -actin) and myosin heavy chain (SM-MHC) proteins on PEA fibres after 7 days. 10T1/2 cells were treated with with 2 ng/mL and 4 ng/mL of TGF $\beta$ 1, respectively. GAPDH was used as a loading control.

To further confirm 10T1/2 differentiation towards a vascular smooth muscle lineage, immunofluorescent staining was performed on 10T1/2 cells cultured on PEA fibres for 7 days, and pre-treated with 4 ng/mL of TGF $\beta$ 1. Figure 4.16 presents the staining for SM-MHC, F-actin and DAPI, where an increase in positive staining for SM-MHC can be observed between the control and the TGF $\beta$ 1 treated scaffold as indicated by the yellow arrows, demonstrating the occurrence of VSMC differentiation on TGF $\beta$ 1-treated PEA

fibres, consistent with the Western blot and qPCR data. Additionally, the increasing number of cells maintaining a fibroblast-like morphology, on TGF $\beta$ 1-treated scaffolds at day 7, suggests that TGF $\beta$ 1 has may have increased the ability of 10T1/2 cells to maintain their proliferative capacity over 7 days.

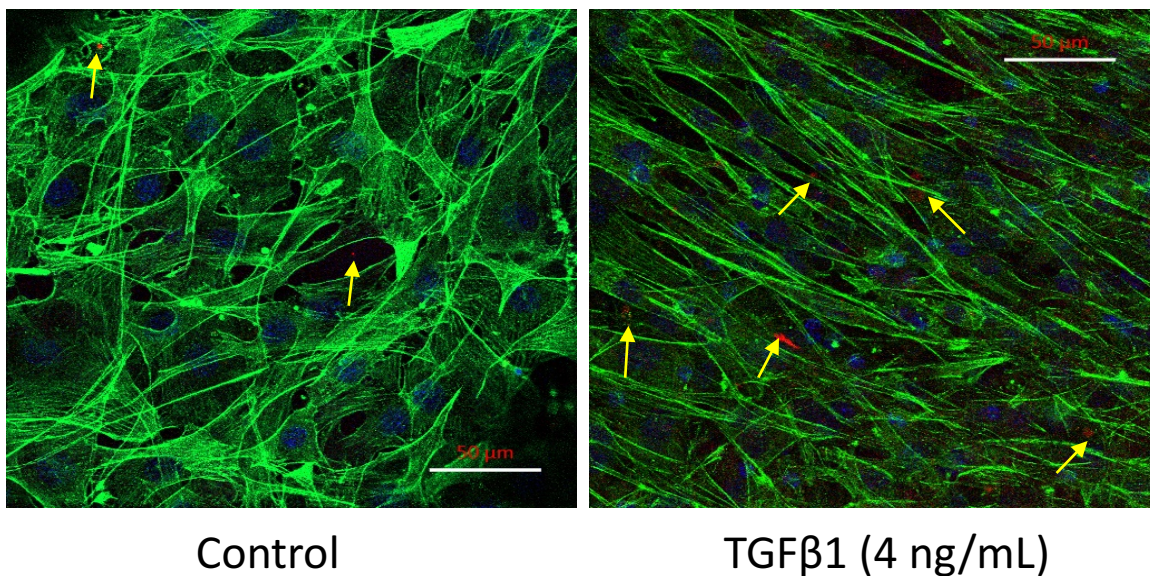


**Figure 4.16** Representative confocal microscopy image of 10T1/2 cells treated with 4 ng/mL TGF $\beta$ 1 and cultured for 7 days. Green represents F-actin, blue represents nuclei and red represents SM-MHC. Scale bar represents 50  $\mu$ m.

TGF $\beta$ 1 has been shown to regulate mesenchymal progenitor 10T1/2 cell differentiation in 2D cell cultures,<sup>152</sup> and is one of many useful models to study *in vitro* VSMC differentiation.<sup>15</sup> Though there have been some inconsistencies in SM-MHC expression in 2D cell cultures,<sup>153</sup> the 3D *in vitro* model using 10T1/2 cells and electrospun PEA fibres demonstrated a TGF $\beta$ 1-induced increase in SM- $\alpha$ -actin and SM-MHC gene expression, using qPCR, and SM-MHC protein expression indicated by Western blot and immunostaining.

Taken together, the results obtained using multiple methodologies, suggested that 10T1/2 cells treated with TGF $\beta$ 1 on electrospun PEA fibres were able to support 10T1/2 cell differentiation into a vascular smooth muscle lineage, making electrospun PEA scaffolds a potential model to fabricate small diameter vascular tissues substitutes for use in preclinical testing.



## Chapter 5

### 5 Conclusion and future work

#### 5.1 Conclusion

In this study, electrospun PEA scaffolds were investigated for their ability to support 10T1/2 differentiation to VSMC and for the fabrication of vascular constructs. First, the PEA biomaterial derived from L-phenylalanine, 1,4 butanediol and sebacoyl chloride was synthesized, and the structure was confirmed by <sup>1</sup>H-NMR and GPC. Once synthesized, the PEA was electrospun to form 3D fibrous mats and tubular scaffolds. The effect of solution concentration was explored for 3D fibrous mats, using three different concentrations, with fibres spun at 6% w/w providing a uniform and bead-free fibrous structure. For tubular scaffolds, an increase in rotation speed above 150 RPM was found to increase fibre directionality, fibre fusion and preferential fibre orientation around one angle, therefore the rotation speed of the mandrel was adjusted to 150 RPM to obtain randomly oriented fibres. Cytotoxicity and cell proliferation studies indicated that the scaffolds were not cytotoxic and supported proliferation over 14 days, while 10T1/2 cell interactions on 3D electrospun PEA fibre mats demonstrated cell attachment, spreading and infiltration for up to 7 days. The *in vitro* perfusion bioreactor study showed that although cell infiltration may not have been sufficient, the perfusion of cell culture medium supported increased cell proliferation and expansion potential compared to tubular constructs cultured under static conditions.

Finally, VSMC studies using qPCR, Western blot analysis and immunofluorescent staining confirmed the gene and protein expression of early and late VSMC markers SM- $\alpha$ -actin and MHC using TGF $\beta$ 1, suggesting that PEA scaffolds support *in vitro* VSMC differentiation. Overall, the results of this study suggested a potential model to fabricate small diameter vascular substitutes for use in preclinical testing.

## **5.2 Strengths and limitations**

To our knowledge, this study was the first to investigate 10T1/2 cell differentiation using PEAs, which up until now, have largely been investigated using endothelial cells<sup>84</sup> and HCASMC.<sup>14,11</sup> Additionally, the PEA biomaterial supported favorable interactions between PEA fibres and 10T1/2 cells, and facilitated TGF $\beta$ 1-induced differentiation of 10T1/2 cells to VSMCs as observed by the increased VSMC gene and protein expression.

Although some studies have investigated the use of PEAs as biomaterials for vascular tissue engineering, the studies utilized 2D polymer films<sup>154</sup> and electrospun mats<sup>14,11</sup> and this study is the first to utilize PEA tubular scaffolds to investigate the effect of pulsatile perfusion, luminal flow and mechanical stimulation on vascular cell behavior in a 3D environment.

The primary limitation of this study was the lack of homogenous cell distribution throughout the tubular PEA construct even with the use of a bioreactor. Although some cellular infiltration was observed, the pore size and porosity of the tubular construct may not have been sufficient for the 10T1/2 cells to populate the construct.

### 5.3 Future work

Future work should investigate techniques to improve cellular infiltration in electrospun tubular PEA constructs such leaching (e.g. salt,<sup>155</sup> sugars<sup>156</sup> or other porogens) and sacrificial polymers.<sup>157</sup> These methods, may allow for increased cell density and homogenous cell distribution throughout the scaffold which would permit powerful *in vitro* vascular differentiation studies in a 3D environment. This study demonstrated the ability for PEAs to support 10T1/2 differentiation and future work should incorporate other stem cell sources to engineer vascular constructs which, combined with growth factors and bioreactors, may provide a 3D vascular tissue model for preclinical testing, that could also potentially be used as a suitable vascular graft. Finally, since this study focused on the differentiation of 10T1/2 cells into VSMCs, the response of the cells to vasoactive agents needs to be studied.

### 5.4 Significance

This work has demonstrated the ability of electrospun PEA scaffolds to support the differentiation of 10T1/2 cells into VSMCs. As such, this *in vitro* model of cell differentiation on electrospun PEA scaffolds could serve as a potential platform to fabricate small-diameter tissue engineered vascular grafts to address the current need for 3D vascular tissue models as testing platforms for pharmaceutical<sup>158</sup> and intravascular stent testing.<sup>159</sup>

## 6 References

1. Statistics Canada., Ranking, number and percentage of deaths for the 10 leading causes, Canada, 2000, 2010 and 2011. (2014). Available at: <http://www.statcan.gc.ca/daily-quotidien/140128/t140128b001-eng.htm>. (Accessed: 11th April 2015)
2. Kannan, R. Y., Salacinski, H. J., Butler, P. E., Hamilton, G. & Seifalian, A. M. Current status of prosthetic bypass grafts: a review. *J. Biomed. Mater. Res. B. Appl. Biomater.* **74**, 570–81 (2005).
3. Rashid, S. T., Fuller, B., Hamilton, G. & Seifalian, A. M. Tissue engineering of a hybrid bypass graft for coronary and lower limb bypass surgery. *FASEB J.* **22**, 2084–2089 (2008).
4. Shinoka, T. & Breuer, C. Tissue-engineered blood vessels in pediatric cardiac surgery. *Yale J. Biol. Med.* **81**, 161–6 (2008).
5. Rabkin, E. & Schoen, F. J. Cardiovascular tissue engineering. *Cardiovasc. Pathol.* **11**, 305–317 (2002).
6. Krawiec, J. T. & Vorp, D. A. Adult stem cell-based tissue engineered blood vessels: A review. *Biomaterials* **33**, 3388–3400 (2012).
7. Lim, S. H. *et al.* Tissue-engineered blood vessels with endothelial nitric oxide synthase activity. *J. Biomed. Mater. Res. B. Appl. Biomater.* **85**, 537–46 (2008).
8. Roh, J. D. *et al.* Construction of an autologous tissue-engineered venous conduit from bone marrow-derived vascular cells: optimization of cell harvest and seeding techniques. *J. Pediatr. Surg.* **42**, 198–202 (2007).
9. Mirensky, T. L. *et al.* Tissue-engineered vascular grafts: does cell seeding matter? *J. Pediatr. Surg.* **45**, 1299–305 (2010).

10. Higgins, S. P., Solan, A. K. & Niklason, L. E. Effects of polyglycolic acid on porcine smooth muscle cell growth and differentiation. *J. Biomed. Mater. Res. A* **67**, 295–302 (2003).
11. Srinath, D., Lin, S., Knight, D. K., Rizkalla, A. S. & Mequanint, K. Fibrous biodegradable l-alanine-based scaffolds for vascular tissue engineering. *J. Tissue Eng. Regen. Med.* **8**, 578–588 (2014).
12. Yamanouchi, D. *et al.* Biodegradable arginine-based poly(ester-amide)s as non-viral gene delivery reagents. *Biomaterials* **29**, 3269–3277 (2008).
13. Zilinskas, G. J., Soleimani, A. & Gillies, E. R. Poly(ester amide)-Poly(ethylene oxide) Graft Copolymers: Towards Micellar Drug Delivery Vehicles. *Int. J. Polym. Sci.* **2012**, 1–11 (2012).
14. Knight, D. K., Gillies, E. R. & Mequanint, K. Biomimetic L-aspartic acid-derived functional poly(ester amide)s for vascular tissue engineering. *Acta Biomater.* **10**, 3484–3496 (2014).
15. Xie, C., Ritchie, R. P., Huang, H., Zhang, J. & Chen, Y. E. Smooth Muscle Cell Differentiation In Vitro Models and Underlying Molecular Mechanisms. *Arterioscler. Thromb. Vasc. Biol.* **31**, 1485–1494 (2011).
16. Braun, F., Lorf, T. & Ringe, B. Update of current immunosuppressive drugs used in clinical organ transplantation. *Transpl. Int.* **11**, 77–81 (1998).
17. Rong, Z. *et al.* An Effective Approach to Prevent Immune Rejection of Human ESC-Derived Allografts. *Cell Stem Cell* **14**, 121–130 (2014).
18. Okano, H. *et al.* Steps Toward Safe Cell Therapy Using Induced Pluripotent Stem Cells. *Circ. Res.* **112**, 523–533 (2013).
19. Steinhoff, G. *et al.* Tissue Engineering of Pulmonary Heart Valves on Allogenic Acellular Matrix Conduits In Vivo Restoration of Valve Tissue. *Circulation* **102**, III50–III55 (2000).

20. Vesely, I. Heart Valve Tissue Engineering. *Circ. Res.* **97**, 743–755 (2005).
21. Roll, S. *et al.* Dacron vs. PTFE as bypass materials in peripheral vascular surgery--systematic review and meta-analysis. *BMC Surg.* **8**, 22 (2008).
22. Kapadia, M. R., Popowich, D. A. & Kibbe, M. R. Modified Prosthetic Vascular Conduits. *Circulation* **117**, 1873–1882 (2008).
23. Weinberg, C. B. & Bell, E. A blood vessel model constructed from collagen and cultured vascular cells. *Science* **231**, 397–400 (1986).
24. Isenberg, B. C., Williams, C. & Tranquillo, R. T. Small-Diameter Artificial Arteries Engineered In Vitro. *Circ. Res.* **98**, 25–35 (2005).
25. Sundaram, S. & Niklason, L. E. Smooth Muscle and Other Cell Sources for Human Blood Vessel Engineering. *Cells Tissues Organs* **195**, 15–25 (2012).
26. Niklason, L. E. *et al.* Functional arteries grown in vitro. *Science* **284**, 489–93 (1999).
27. Wang, C. *et al.* A small diameter elastic blood vessel wall prepared under pulsatile conditions from polyglycolic acid mesh and smooth muscle cells differentiated from adipose-derived stem cells. *Biomaterials* **31**, 621–630 (2010).
28. Patel, A., Fine, B., Sandig, M. & Mequanint, K. Elastin biosynthesis: The missing link in tissue-engineered blood vessels. *Cardiovasc. Res.* **71**, 40–49 (2006).
29. Bashur, C. A., Venkataraman, L. & Ramamurthi, A. Tissue Engineering and Regenerative Strategies to Replicate Biocomplexity of Vascular Elastic Matrix Assembly. *Tissue Eng. Part B. Rev.* **18**, 203–217 (2012).
30. Berglund, J. D. & Galis, Z. S. Designer blood vessels and therapeutic revascularization. *Br. J. Pharmacol.* **140**, 627–636 (2003).
31. Seifu, D. G., Purnama, A., Mequanint, K. & Mantovani, D. Small-diameter vascular tissue engineering. *Nat. Rev. Cardiol.* **10**, 410–421 (2013).

32. Statistics-Heart and Stroke foundation of Canada. **1**, 1–5 (2009).
33. Michaels, A. D. & Chatterjee, K. Angioplasty Versus Bypass Surgery for Coronary Artery Disease. *Circulation* **106**, e187–e190 (2002).
34. Knight, D. K., Gillies, E. R. & Mequanint, K. Vascular grafting strategies in coronary intervention. *Front. Mater. Biomater.* **1**, 1–16 (2014).
35. Slavin, L., Chhabra, A. & Tobis, J. M. Drug-eluting stents: preventing restenosis. *Cardiol. Rev.* **15**, 1–12 (2007).
36. Rzucidlo, E. M., Martin, K. A. & Powell, R. J. Regulation of vascular smooth muscle cell differentiation. *J. Vasc. Surg.* **45 Suppl A**, A25–32 (2007).
37. Shin’oka, T., Imai, Y. & Ikada, Y. Transplantation of a tissue-engineered pulmonary artery. *N. Engl. J. Med.* **344**, 532–533 (2001).
38. Patterson, J. T. *et al.* Tissue-engineered vascular grafts for use in the treatment of congenital heart disease: from the bench to the clinic and back again. *Regen. Med.* **7**, 409–419 (2012).
39. Shin’oka, T. *et al.* Midterm clinical result of tissue-engineered vascular autografts seeded with autologous bone marrow cells. *J. Thorac. Cardiovasc. Surg.* **129**, 1330–1338 (2005).
40. Hibino, N. *et al.* Late-term results of tissue-engineered vascular grafts in humans. *J. Thorac. Cardiovasc. Surg.* **139**, 431–436 (2010).
41. Curtis, J. Tissue from the lab mends a broken heart. Available at: <http://yalemedicine.yale.edu/spring2012/features/feature/121804/>. (Accessed: 25th June 2016)
42. Konig, G. *et al.* Mechanical properties of completely autologous human tissue engineered blood vessels compared to human saphenous vein and mammary artery. *Biomaterials* **30**, 1542–1550 (2009).

43. McAllister, T. N. *et al.* Effectiveness of haemodialysis access with an autologous tissue-engineered vascular graft: a multicentre cohort study. *Lancet (London, England)* **373**, 1440–6 (2009).
44. Dahl, S. L. M. *et al.* Readily available tissue-engineered vascular grafts. *Sci. Transl. Med.* **3**, 68ra9 (2011).
45. Lawrence, S. Langer startup reports data, starts pivotal trial for bioengineered blood vessel for dialysis patients. (2016). Available at: <http://www.fiercebiotech.com/medical-devices/langer-startup-reports-data-starts-pivotal-trial-for-bioengineered-blood-vessel-for>. (Accessed: 25th June 2016)
46. L'Heureux, N. & Letourneur, D. Clinical translation of tissue-engineered constructs for severe leg injuries. *Ann. Transl. Med.* **3**, 134 (2015).
47. Gibbons, M. C., Foley, M. A. & Cardinal, K. O. Thinking Inside the Box: Keeping Tissue-Engineered Constructs *In Vitro* for Use as Preclinical Models. *Tissue Eng. Part B Rev.* **19**, 14–30 (2013).
48. Beamish, J. A., He, P., Kottke-Marchant, K. & Marchant, R. E. Molecular regulation of contractile smooth muscle cell phenotype: implications for vascular tissue engineering. *Tissue Eng. Part B. Rev.* **16**, 467–91 (2010).
49. Laflamme, K. *et al.* Tissue-Engineered Human Vascular Media With a Functional Endothelin System. *Circulation* **111**, 459–464 (2005).
50. Tkacs, N. C. & Thompson, H. J. From bedside to bench and back again: research issues in animal models of human disease. *Biol. Res. Nurs.* **8**, 78–88 (2006).
51. L'Heureux, N. *et al.* Technology Insight: the evolution of tissue-engineered vascular grafts—from research to clinical practice. *Nat. Clin. Pract. Cardiovasc. Med.* **4**, 389–395 (2007).
52. Benam, K. H. *et al.* Engineered In Vitro Disease Models. *Annu. Rev. Pathol. Mech. Dis* **10**, 195–262 (2015).



53. Riha, G. M., Lin, P. H., Lumsden, A. B., Yao, Q. & Chen, C. Review: Application of Stem Cells for Vascular Tissue Engineering. *Tissue Eng.* **11**, 1535–1552 (2005).
54. Takahashi, K. & Yamanaka, S. Induction of Pluripotent Stem Cells from Mouse Embryonic and Adult Fibroblast Cultures by Defined Factors. *Cell* **126**, 663–676 (2006).
55. Levenberg, S. *et al.* Differentiation of human embryonic stem cells on three-dimensional polymer scaffolds. *Proc. Natl. Acad. Sci.* **100**, 12741–12746 (2003).
56. Xie, C. *et al.* Three-dimensional growth of iPS cell-derived smooth muscle cells on nanofibrous scaffolds. *Biomaterials* **32**, 4369–4375 (2011).
57. Bajpai, V. K., Mistriotis, P., Loh, Y.-H., Daley, G. Q. & Andreadis, S. T. Functional vascular smooth muscle cells derived from human induced pluripotent stem cells via mesenchymal stem cell intermediates. *Cardiovasc. Res.* **96**, 391–400 (2012).
58. Zhang, R. *et al.* Nuclear fusion-independent smooth muscle differentiation of human adipose-derived stem cells induced by a smooth muscle environment. *Stem Cells* **30**, 481–90 (2012).
59. National Institutes of Health (NIH). What are Adult Stem Cells? [Stem Cell Information]. (2015). Available at: <http://stemcells.nih.gov/info/basics/pages/basics4.aspx>. (Accessed: 25th June 2016)
60. Weissman, I. L. Stem Cells: Units of Development, Units of Regeneration, and Units in Evolution. *Cell* **100**, 157–168 (2000).
61. Wang, C. *et al.* Differentiation of adipose-derived stem cells into contractile smooth muscle cells induced by transforming growth factor-beta1 and bone morphogenetic protein-4. *Tissue Eng. Part A* **16**, 1201–1213 (2010).

62. Deluzio, T. G., Seifu, D. G. & Mequanint, K. 3D scaffolds in tissue engineering and regenerative medicine: beyond structural templates? *Pharm. Bioprocess.* **1**, 267–281 (2013).
63. O'Brien, F. J. Biomaterials & scaffolds for tissue engineering. *Mater. Today* **14**, 88–95 (2011).
64. Ingavle, G. C. & Leach, J. K. Advancements in electrospinning of polymeric nanofibrous scaffolds for tissue engineering. *Tissue Eng. Part B. Rev.* **20**, 277–293 (2014).
65. Boccafoschi, F., Habermehl, J., Vesentini, S. & Mantovani, D. Biological performances of collagen-based scaffolds for vascular tissue engineering. *Biomaterials* **26**, 7410–7417 (2005).
66. Swartz, D. D., Russell, J. A. & Andreadis, S. T. Engineering of fibrin-based functional and implantable small-diameter blood vessels. *Am. J. Physiol. Heart Circ. Physiol.* **288**, H1451–60 (2005).
67. McKenna, K. A. *et al.* Mechanical property characterization of electrospun recombinant human tropoelastin for vascular graft biomaterials. *Acta Biomater.* **8**, 225–233 (2012).
68. Goisis, G. *et al.* Biocompatibility studies of anionic collagen membranes with different degree of glutaraldehyde cross-linking. *Biomaterials* **20**, 27–34 (1999).
69. Jeschke, B. *et al.* RGD-peptides for tissue engineering of articular cartilage. *Biomaterials* **23**, 3455–3463 (2002).
70. Vara, D. S. *et al.* Cardiovascular tissue engineering: state of the art. *Pathol. Biol.* **53**, 599–612 (2005).
71. Speer, D. P., Chvapil, M., Eskelson, C. D. & Ulreich, J. Biological effects of residual glutaraldehyde in glutaraldehyde-tanned collagen biomaterials. *J. Biomed. Mater. Res.* **14**, 753–64 (1980).

72. Rana, D., Zreiqat, H., Benkirane-Jessel, N., Ramakrishna, S. & Ramalingam, M. Development of decellularized scaffolds for stem cell-driven tissue engineering. *J. Tissue Eng. Regen. Med.* (2015). doi:10.1002/term.2061
73. Leyh, R. . *et al.* Acellularized porcine heart valve scaffolds for heart valve tissue engineering and the risk of cross-species transmission of porcine endogenous retrovirus. *J. Thorac. Cardiovasc. Surg.* **126**, 1000–1004 (2003).
74. Alini, M. *et al.* The Potential and Limitations of a Cell-Seeded Collagen/Hyaluronan Scaffold to Engineer an Intervertebral Disc-Like Matrix. *Spine (Phila. Pa. 1976)*. **28**, 446–453 (2003).
75. Zhang, W. J., Liu, W., Cui, L. & Cao, Y. Tissue engineering of blood vessel. *J. Cell. Mol. Med.* **11**, 945–957 (2007).
76. Lichtenstein, I. L. Polyglycolic Acid (PGA) Sutures. *JAMA J. Am. Med. Assoc.* **214**, 760 (1970).
77. Gong, Z. & Niklason, L. E. Small-diameter human vessel wall engineered from bone marrow-derived mesenchymal stem cells (hMSCs). *FASEB J.* **22**, 1635–1648 (2008).
78. Knight, T. A. & Payne, R. G. Characterization of a PGA-based scaffold for use in a tissue-engineered neo-urinary conduit. *Methods Mol. Biol.* **1001**, 179–88 (2013).
79. Ito, Y., Kajihara, M. & Imanishi, Y. Materials for enhancing cell adhesion by immobilization of cell-adhesive peptide. *J. Biomed. Mater. Res.* **25**, 1325–1337 (1991).
80. Pang, X. & Chu, C.-C. Synthesis, characterization and biodegradation of functionalized amino acid-based poly(ester amide)s. *Biomaterials* **31**, 3745–3754 (2010).

81. Guo, K. & Chu, C. C. Biodegradable and injectable paclitaxel-loaded poly(ester amide)s microspheres: Fabrication and characterization. *J. Biomed. Mater. Res. Part B Appl. Biomater.* **89B**, 491–500 (2009).
82. Wamhoff, B. R., Bowles, D. K. & Owens, G. K. Excitation-Transcription Coupling in Arterial Smooth Muscle. *Circ. Res.* **98**, 868–878 (2006).
83. Zhang, L., Xiong, C. & Deng, X. Biodegradable polyester blends for biomedical application. *J. Appl. Polym. Sci.* **56**, 103–112 (1995).
84. Horwitz, J. A. *et al.* Biological performance of biodegradable amino acid-based poly(ester amide)s: Endothelial cell adhesion and inflammation in vitro. *J. Biomed. Mater. Res. Part A* **95A**, 371–380 (2010).
85. Knight, D. K., Gillies, E. R. & Mequanint, K. Strategies in functional poly(ester amide) syntheses to study human coronary artery smooth muscle cell interactions. *Biomacromolecules* **12**, 2475–2487 (2011).
86. Karimi, P., Rizkalla, A. S. & Mequanint, K. Versatile Biodegradable Poly(ester amide)s Derived from  $\alpha$ -Amino Acids for Vascular Tissue Engineering. *Materials (Basel)*. **3**, 2346–2368 (2010).
87. Rubashkin, M. G., Ou, G. & Weaver, V. M. Deconstructing Signaling in Three Dimensions. *Biochemistry* **53**, 2078–2090 (2014).
88. Lin, S., Sandig, M. & Mequanint, K. Three-Dimensional Topography of Synthetic Scaffolds Induces Elastin Synthesis by Human Coronary Artery Smooth Muscle Cells. *Tissue Eng. Part A* **17**, 1561–1571 (2011).
89. O'Brien, F. J., Harley, B. A., Yannas, I. V. & Gibson, L. Influence of freezing rate on pore structure in freeze-dried collagen-GAG scaffolds. *Biomaterials* **25**, 1077–1086 (2004).

90. Lu, T., Li, Y. & Chen, T. Techniques for fabrication and construction of three-dimensional scaffolds for tissue engineering. *Int. J. Nanomedicine* **8**, 337–350 (2013).
91. Mikos, A. G. & Temenoff, J. S. Formation of highly porous biodegradable scaffolds for tissue engineering. *Electron. J. Biotechnol.* **3**, 0–0 (2000).
92. Murphy, W. L., Dennis, R. G., Kileny, J. L. & Mooney, D. J. Salt Fusion: An Approach to Improve Pore Interconnectivity within Tissue Engineering Scaffolds. *Tissue Eng.* **8**, (2002).
93. Lu, T., Li, Y. & Chen, T. Techniques for fabrication and construction of three-dimensional scaffolds for tissue engineering. *Int. J. Nanomedicine* **8**, 337–50 (2013).
94. Soletti, L. *et al.* A bilayered elastomeric scaffold for tissue engineering of small diameter vascular grafts. *Acta Biomater.* **6**, 110–122 (2010).
95. Hasan, A. *et al.* Electrospun scaffolds for tissue engineering of vascular grafts. *Acta Biomater.* **10**, 11–25 (2014).
96. Annabi, N. *et al.* Controlling the porosity and microarchitecture of hydrogels for tissue engineering. *Tissue Eng. Part B. Rev.* **16**, 371–83 (2010).
97. Hansmann, J., Groeber, F., Kahlig, A., Kleinhans, C. & Walles, H. Bioreactors in tissue engineering - principles, applications and commercial constraints. *Biotechnol. J.* **8**, 298–307 (2013).
98. Riha, G. M., Lin, P. H., Lumsden, A. B., Yao, Q. & Chen, C. Roles of Hemodynamic Forces in Vascular Cell Differentiation. *Ann. Biomed. Eng.* **33**, 772–779 (2005).
99. Song, L. *et al.* Successful development of small diameter tissue-engineering vascular vessels by our novel integrally designed pulsatile perfusion-based bioreactor. *PLoS One* **7**, e42569 (2012).

100. Stegemann, J. P. & Nerem, R. M. Phenotype modulation in vascular tissue engineering using biochemical and mechanical stimulation. *Ann. Biomed. Eng.* **31**, 391–402 (2003).
101. Fischer, L. J. *et al.* Endothelial Differentiation of Adipose-Derived Stem Cells: Effects of Endothelial Cell Growth Supplement and Shear Force. *J. Surg. Res.* **152**, 157–166 (2009).
102. Sundaram, S., Echter, A., Sivarapatna, A., Qiu, C. & Niklason, L. Small-Diameter Vascular Graft Engineered Using Human Embryonic Stem Cell-Derived Mesenchymal Cells. *Tissue Eng. Part A* **20**, 740–750 (2014).
103. Takahashi, K. *et al.* Induction of Pluripotent Stem Cells from Adult Human Fibroblasts by Defined Factors. *Cell* **131**, 861–872 (2007).
104. Doherty, T. M. *et al.* Calcification in atherosclerosis: bone biology and chronic inflammation at the arterial crossroads. *Proc. Natl. Acad. Sci. U. S. A.* **100**, 11201–6 (2003).
105. Sundaram, S. *et al.* Tissue-engineered vascular grafts created from human induced pluripotent stem cells. *Stem Cells Transl. Med.* **3**, 1535–43 (2014).
106. Wang, Y. *et al.* Engineering vascular tissue with functional smooth muscle cells derived from human iPS cells and nanofibrous scaffolds. *Biomaterials* **35**, 8960–8969 (2014).
107. Dash, B. C. *et al.* Tissue-Engineered Vascular Rings from Human iPSC-Derived Smooth Muscle Cells. **7**, 19–28 (2016).
108. Ge, X. *et al.* Modeling supravalvular aortic stenosis syndrome with human induced pluripotent stem cells. *Circulation* **126**, 1695–704 (2012).
109. Matsumura, G., Miyagawa-Tomita, S., Shin’oka, T., Ikada, Y. & Kurosawa, H. First Evidence That Bone Marrow Cells Contribute to the Construction of Tissue-Engineered Vascular Autografts In Vivo. *Circulation* **108**, 1729–1734 (2003).

110. Cho, S.-W. *et al.* Evidence for In Vivo Growth Potential and Vascular Remodeling of Tissue-Engineered Artery. *Tissue Eng. Part A* **15**, 901–912 (2009).
111. Roh, J. D. *et al.* Tissue-engineered vascular grafts transform into mature blood vessels via an inflammation-mediated process of vascular remodeling. *Proc. Natl. Acad. Sci.* **107**, 4669–4674 (2010).
112. Park, J. S. *et al.* Mechanobiology of mesenchymal stem cells and their use in cardiovascular repair. *Front. Biosci.* **12**, 5098–116 (2007).
113. Nieponice, A. *et al.* In Vivo Assessment of a Tissue-Engineered Vascular Graft Combining a Biodegradable Elastomeric Scaffold and Muscle-Derived Stem Cells in a Rat Model. *Tissue Eng. Part A* **16**, 1215–1223 (2010).
114. Peng, H.-F., Liu, J. Y., Andreadis, S. T. & Swartz, D. D. Hair follicle-derived smooth muscle cells and small intestinal submucosa for engineering mechanically robust and vasoreactive vascular media. *Tissue Eng. Part A* **17**, 981–90 (2011).
115. Hirschi, K. K., Rohovsky, S. A. & D'Amore, P. A. PDGF, TGF- $\beta$ , and Heterotypic Cell–Cell Interactions Mediate Endothelial Cell–induced Recruitment of 10T1/2 Cells and Their Differentiation to a Smooth Muscle Fate. *J. Cell Biol.* **141**, 805–814 (1998).
116. Zhao, Y. *et al.* The development of a tissue-engineered artery using decellularized scaffold and autologous ovine mesenchymal stem cells. *Biomaterials* **31**, 296–307 (2010).
117. Hashi, C. K. *et al.* Antithrombogenic property of bone marrow mesenchymal stem cells in nanofibrous vascular grafts. *Proc. Natl. Acad. Sci.* **104**, 11915–11920 (2007).
118. Zuk, P. A. *et al.* Multilineage cells from human adipose tissue: implications for cell-based therapies. *Tissue Eng.* **7**, 211–28 (2001).

119. Strioga, M., Viswanathan, S., Darinskas, A., Slaby, O. & Michalek, J. Same or not the same? Comparison of adipose tissue-derived versus bone marrow-derived mesenchymal stem and stromal cells. *Stem Cells Dev.* **21**, 2724–2752 (2012).
120. Siddappa, R., Licht, R., van Blitterswijk, C. & de Boer, J. Donor variation and loss of multipotency during in vitro expansion of human mesenchymal stem cells for bone tissue engineering. *J. Orthop. Res.* **25**, 1029–1041 (2007).
121. Rodríguez, L. V. *et al.* Clonogenic multipotent stem cells in human adipose tissue differentiate into functional smooth muscle cells. *Proc. Natl. Acad. Sci. U. S. A.* **103**, 12167–12172 (2006).
122. Wang, C. *et al.* A small diameter elastic blood vessel wall prepared under pulsatile conditions from polyglycolic acid mesh and smooth muscle cells differentiated from adipose-derived stem cells. *Biomaterials* **31**, 621–630 (2010).
123. Harris, L. J. *et al.* Differentiation of adult stem cells into smooth muscle for vascular tissue engineering. *J. Surg. Res.* **168**, 306–314 (2011).
124. DiMuzio, P. & Tulenko, T. Tissue Engineering Applications to Vascular Bypass Graft Development: The Use of Adipose-Derived Stem Cells. *J. Vasc. Surg. Off. Publ. Soc. Vasc. Surg. [and] Int. Soc. Cardiovasc. Surgery, North Am. Chapter* **45**, 99–103 (2007).
125. Madonna, R., Geng, Y.-J. & Caterina, R. De. Adipose Tissue-Derived Stem Cells Characterization and Potential for Cardiovascular Repair. *Arterioscler. Thromb. Vasc. Biol.* **29**, 1723–1729 (2009).
126. Madonna, R. *et al.* Age-dependent impairment of number and angiogenic potential of adipose tissue-derived progenitor cells. *Eur. J. Clin. Invest.* **41**, 126–33 (2011).
127. Krawiec, J. T. *et al.* A Cautionary Tale for Autologous Vascular Tissue Engineering: Impact of Human Demographics on the Ability of Adipose-Derived Mesenchymal Stem Cells to Recruit and Differentiate into Smooth Muscle Cells. *Tissue Eng. Part A* **21**, 426–437 (2015).



128. Krawiec, J. T. *et al.* In Vivo Functional Evaluation of Tissue-Engineered Vascular Grafts Fabricated Using Human Adipose-Derived Stem Cells from High Cardiovascular Risk Populations. *Tissue Eng. Part A* **22**, 765–775 (2016).
129. Puiggali, J. *et al.* The frustrated structure of poly(l-lactide). *Polymer (Guildf)*. **41**, 8921–8930 (2000).
130. Said, S. S., Pickering, J. G. & Mequanint, K. Controlled delivery of fibroblast growth factor-9 from biodegradable poly(ester amide) fibers for building functional neovasculature. *Pharm. Res.* **31**, 3335–3347 (2014).
131. Tinevez, J.-Y. Directionality plugin for ImageJ. Available at: <<http://fiji.sc/wiki/index.php/Directionality>>. (Accessed: 13th August 2016)
132. Lin, S. & Mequanint, K. Activation of Transcription Factor *GAX* and Concomitant Downregulation of IL-1 $\beta$  and ERK1/2 Modulate Vascular Smooth Muscle Cell Phenotype in 3D Fibrous Scaffolds. *Tissue Eng. Part A* **21**, 2356–2365 (2015).
133. Wittbecker, E. L. & Morgan, P. W. Interfacial polycondensation. I. *J. Polym. Sci.* **40**, 289–297 (1959).
134. Zander, N. E., Orlicki, J. A., Rawlett, A. M. & Beebe, T. P. Electrospun polycaprolactone scaffolds with tailored porosity using two approaches for enhanced cellular infiltration. *J. Mater. Sci. Mater. Med.* **24**, 179–187 (2013).
135. Bölgen, N., Menceloğlu, Y. Z., Acatay, K., Vargel, I. & Pişkin, E. In vitro and in vivo degradation of non-woven materials made of poly(epsilon-caprolactone) nanofibers prepared by electrospinning under different conditions. *J. Biomater. Sci. Polym. Ed.* **16**, 1537–55 (2005).
136. Yang, F., Murugan, R., Wang, S. & Ramakrishna, S. Electrospinning of nano/micro scale poly(L-lactic acid) aligned fibers and their potential in neural tissue engineering. *Biomaterials* **26**, 2603–10 (2005).

137. Chen, M., Patra, P. K., Lovett, M. L., Kaplan, D. L. & Bhowmick, S. Role of electrospun fibre diameter and corresponding specific surface area (SSA) on cell attachment. *J. Tissue Eng. Regen. Med.* **3**, 269–79 (2009).
138. Dodge, J. T., Brown, B. G., Bolson, E. L. & Dodge, H. T. Lumen diameter of normal human coronary arteries. Influence of age, sex, anatomic variation, and left ventricular hypertrophy or dilation. *Circulation* **86**, 232–46 (1992).
139. Zhu, X., Cui, W., Li, X. & Jin, Y. Electrospun fibrous mats with high porosity as potential scaffolds for skin tissue engineering. *Biomacromolecules* **9**, 1795–801 (2008).
140. Jeong, K.-Y., Paik, D.-H. & Choi, S.-W. Fabrication of Tubular Scaffolds with Controllable Fiber Orientations Using Electrospinning for Tissue Engineering. *Macromol. Mater. Eng.* **299**, 1425–1429 (2014).
141. Raghavan, B. K. & Coffin, D. W. Control of Inter-fiber Fusing for Nanofiber Webs via Electrospinning. *J. Eng. Fiber. Fabr.* **6**, (2011).
142. Aviss, K.J, Gough, J.E. and Downes, S. Aligned electrospun polymer fibres for skeletal muscle regeneration. *Eur. Cells Mater.* **19**, 193–204 (2010).
143. Bashur, C. A., Dahlgren, L. A. & Goldstein, A. S. Effect of fiber diameter and orientation on fibroblast morphology and proliferation on electrospun poly(d,l-lactic-co-glycolic acid) meshes. *Biomaterials* **27**, 5681–5688 (2006).
144. Liu, C. *et al.* The effect of the fibre orientation of electrospun scaffolds on the matrix production of rabbit annulus fibrosus-derived stem cells. *Bone Res.* **3**, 15012 (2015).
145. Yin, Z. *et al.* The regulation of tendon stem cell differentiation by the alignment of nanofibers. *Biomaterials* **31**, 2163–2175 (2010).
146. Ng, K. W., Leong, D. T. W. & Hutmacher, D. W. The challenge to measure cell proliferation in two and three dimensions. *Tissue Eng.* **11**, 182–191 (2005).

147. Xie, Y. *et al.* Three-dimensional flow perfusion culture system for stem cell proliferation inside the critical-size beta-tricalcium phosphate scaffold. *Tissue Eng.* **12**, 3535–43 (2006).
148. Zhao, F. & Ma, T. Perfusion bioreactor system for human mesenchymal stem cell tissue engineering: dynamic cell seeding and construct development. *Biotechnol. Bioeng.* **91**, 482–93 (2005).
149. Nam, J., Huang, Y., Agarwal, S. & Lannutti, J. Improved cellular infiltration in electrospun fiber via engineered porosity. *Tissue Eng.* **13**, 2249–57 (2007).
150. Baker, B. M. *et al.* The potential to improve cell infiltration in composite fiber-aligned electrospun scaffolds by the selective removal of sacrificial fibers. *Biomaterials* **29**, 2348–2358 (2008).
151. Zheng, X. *et al.* Proteomic analysis for the assessment of different lots of fetal bovine serum as a raw material for cell culture. Part IV. Application of proteomics to the manufacture of biological drugs. *Biotechnol. Prog.* **22**, 1294–300 (2006).
152. Hirschi, K. K., Rohovsky, S. A. & D'Amore, P. A. PDGF, TGF- $\beta$ , and Heterotypic Cell–Cell Interactions Mediate Endothelial Cell–induced Recruitment of 10T1/2 Cells and Their Differentiation to a Smooth Muscle Fate. *J. Cell Biol.* **141**, 805–814 (1998).
153. Wang, Z., Wang, D.-Z., Pipes, G. C. T. & Olson, E. N. Myocardin is a master regulator of smooth muscle gene expression. *Proc. Natl. Acad. Sci.* **100**, 7129–7134 (2003).
154. Knight, D. K. *et al.* Focal Contact Formation of Vascular Smooth Muscle Cells on Langmuir–Blodgett and Solvent-Cast Films of Biodegradable Poly(ester amide)s. *ACS Appl. Mater. Interfaces* **4**, 1303–1312 (2012).
155. Kim, T. G., Chung, H. J. & Park, T. G. Macroporous and nanofibrous hyaluronic acid/collagen hybrid scaffold fabricated by concurrent electrospinning and deposition/leaching of salt particles. *Acta Biomater.* **4**, 1611–1619 (2008).

156. Smith, I. O., Liu, X. H., Smith, L. A. & Ma, P. X. Nanostructured polymer scaffolds for tissue engineering and regenerative medicine. *Wiley Interdiscip. Rev. Nanomedicine Nanobiotechnology* **1**, 226–236 (2009).
157. Baker, B. M. *et al.* Sacrificial nanofibrous composites provide instruction without impediment and enable functional tissue formation. doi:10.1073/pnas.1206962109
158. Laflamme, K. *et al.* Adventitia contribution in vascular tone: insights from adventitia-derived cells in a tissue-engineered human blood vessel. *FASEB J.* **20**, 1245–1247 (2006).
159. Cardinal, K. O. & Williams, S. K. Assessment of the intimal response to a protein-modified stent in a tissue-engineered blood vessel mimic. *Tissue Eng. Part A* **15**, 3869–76 (2009).
160. Waterhouse, A., Wise, S. G., Ng, M. K. C. & Weiss, A. S. Elastin as a nonthrombogenic biomaterial. *Tissue Eng. Part B. Rev.* **17**, 93–99 (2011).
161. Sill, T. J. & von Recum, H. A. Electrospinning: Applications in drug delivery and tissue engineering. *Biomaterials* **29**, 1989–2006 (2008).

## 7 Copyright permissions

**Ballen, Karen**  
To: Sarah Kiros  
RE: copyright permission

Today at 1:32 PM

BK

Dear Sarah:

Copyright permission is granted for use of this figure in your dissertation, as long as it is not for commercial purposes.

Kind regards,

Karen Ballen  
Manager, Reprints, Permissions and Open Access

---

**From:** Sarah Kiros [redacted]  
**Sent:** Friday, August 26, 2016 12:26 PM  
**To:** Ballen, Karen  
**Subject:** copyright permission

Hello,

I would like to use the a figure from the following publication for use in my dissertation, and I would like to know if I could get copyright permission.

"Elastin as a nonthrombogenic biomaterial  
[Anna Waterhouse, Steven G. Wise, Martin K.C. Ng and Anthony S. Weiss](#)  
[Tissue Engineering, Part B: Reviews](#). 17.2 (Apr. 2011): p93.

Figure 2

Kind regards,  
Sarah Kiros

8/26/2016

Copyright Clearance Center



**Confirmation Number: 11586025**  
**Order Date: 08/21/2016**

**Customer Information**



**This is not an invoice**

**Order Details**

**Regenerative medicine**

Billing Status:  
**N/A**

**Order detail ID:** 70025512  
**ISSN:** 1746-0751  
**Publication Type:** Journal  
**Volume:**  
**Issue:**  
**Start page:**  
**Publisher:** FUTURE MEDICINE LTD

**Permission Status:** **Granted**  
**Permission type:** Republish or display content  
**Type of use:** Thesis/Dissertation  
**Job Ticket:** 501170585  
**Order License Id:** 3934211036273

**Requestor type:** Academic institution  
**Format:** Print, Electronic  
**Portion:** chart/graph/table/figure  
**Number of charts/graphs/tables/figures:** 1  
**Title or numeric reference of the portion(s):** Figure 1, Tissue-engineered vascular graft as... the modified Fontan operation  
**Title of the article or chapter the portion is from:** Tissue-engineered vascular grafts for use in the treatment of congenital heart disease: from the bench to the clinic and back again  
**Editor of portion(s):** N/A  
**Author of portion(s):** Patterson, Joseph T ; et al  
**Volume of serial or monograph:** 7  
**Issue, if republishing an article from a serial:** 3  
**Page range of portion:** 14  
**Publication date of portion:** May 1, 2012  
**Rights for:** Main product  
**Duration of use:** Current edition and up to 5 years  
**Creation of copies for the disabled:** no

<https://www.copyright.com/printOrder.do?id=11586025>

1/2

8/26/2016

RightsLink - Your Account

## ELSEVIER LICENSE TERMS AND CONDITIONS

Aug 26, 2016

This Agreement between Sarah Kiros ("You") and Elsevier ("Elsevier") consists of your license details and the terms and conditions provided by Elsevier and Copyright Clearance Center.

|                                              |                                                                                         |
|----------------------------------------------|-----------------------------------------------------------------------------------------|
| License Number                               | 3931680638230                                                                           |
| License date                                 | Aug 17, 2016                                                                            |
| Licensed Content Publisher                   | Elsevier                                                                                |
| Licensed Content Publication                 | Biomaterials                                                                            |
| Licensed Content Title                       | Electrospinning: Applications in drug delivery and tissue engineering                   |
| Licensed Content Author                      | Travis J. Sill, Horst A. von Recum                                                      |
| Licensed Content Date                        | May 2008                                                                                |
| Licensed Content Volume Number               | 29                                                                                      |
| Licensed Content Issue Number                | 13                                                                                      |
| Licensed Content Pages                       | 18                                                                                      |
| Start Page                                   | 1989                                                                                    |
| End Page                                     | 2006                                                                                    |
| Type of Use                                  | reuse in a thesis/dissertation                                                          |
| Portion                                      | figures/tables/illustrations                                                            |
| Number of figures/tables/illustrations       | 1                                                                                       |
| Format                                       | both print and electronic                                                               |
| Are you the author of this Elsevier article? | No                                                                                      |
| Will you be translating?                     | No                                                                                      |
| Order reference number                       |                                                                                         |
| Original figure numbers                      | Figure 1                                                                                |
| Title of your thesis/dissertation            | 10T1/2 cell interactions with electrospun PEA fibers: an in vitro differentiation model |
| Expected completion date                     | Aug 2016                                                                                |
| Estimated size (number of pages)             | 70                                                                                      |
| Elsevier VAT number                          | GB 494 6272 12                                                                          |

## 8 Curriculum Vitae

## Sarah Kiros

### EDUCATION

---

- 2014-2016                      **Master of Engineering Science, Biomedical Engineering**
- The University of Western Ontario,  
London, Ontario
- Thesis title: *Electrospinning of poly (ester amide) fibres for mesenchymal progenitor cell differentiation*
- Supervisor: Dr. Kibret Mequanint
- 2008- 2013                      **Bachelor of Engineering, Biomedical Engineering**
- Department of Electrical and Computer Engineering,  
Ryerson University,  
Toronto, Ontario

### PROFESSIONAL AFFILIATIONS, CERTIFICATIONS AND HONOURS

---

- 2014-present                      **Student member, Professional Engineers Ontario (PEO)**
- Engineering Intern (EIT)
- 2014                                      **Teaching Assistant Training Program Certificate**
- The University of Western Ontario
- 2014-2016                      **Western Graduate Research Scholarship**
- The University of Western Ontario
- 2012-2013                      **Dean's List, Faculty of Engineering and Architectural Science, Ryerson University**
- 2008                                      **Ryerson University Entrance Scholarship (\$1000)**



## **EMPLOYMENT AND SELECTED VOLUNTEERING EXPERIENCE**

---

- September-December 2015 **Graduate Teaching Assistant, Tissue Engineering (CBE4423)**
- Nov 2013-Jan 2014 **Sunnybrook Health Sciences Centre**  
 Volunteer, Biomedical Engineering Department  
 Toronto, Ontario
- October 2013 **St. Paul's Hospital**  
 Volunteer, Addis Ababa, Ethiopia
- July-August 2012 **Ministry of Health and Long-Term Care**  
 Office Assistant, Health Boards Secretariat (Full-Time)  
 Toronto, Ontario
- May-September 2011 **ServiceOntario, Ministry of Government Services**  
 Project and Communications Assistant (Full-Time)  
 Toronto, Ontario

## **ACADEMIC COMMUNITY INVOLVEMENT**

---

- September 2014 **BME Graduate representative**, Society of Graduate Students University of Western Ontario
- August 2014 **See the Line Symposium- Research Symposium**  
 Conference Volunteer